Charles University

Faculty of Social Sciences
Institute of Economic Studies

MASTER'S THESIS

Analysis of Term Structures in High Frequencies

Author: **Bc. Adam Nedvěd**

Supervisor: **doc. PhDr. Jozef Baruník, Ph.D.**

Academic Year: **2017/2018**

Declaration of Authorship

The author hereby declares that he compiled this thesis independently, using only the listed resources and literature, and the thesis has not been used to obtain a different or the same degree.

The author grants to Charles University permission to reproduce and to distribute copies of this thesis document in whole or in part.

Prague, July 30, 2018

Signature

Acknowledgments

I would like to express gratitude to my supervisor doc. PhDr. Jozef Baruník, Ph.D. for his patient guidance and support that allowed this thesis to come to life.

Abstract

This thesis represents an in-depth empirical study of the dependence structures within the term structure of interest rates. Firstly, a comprehensive overview of term structure modelling literature and methods is provided together with a summary of theoretical notions regarding the use of high-frequency data and spectral analysis. Contrary to most studies, the frequency-domain approach is employed, with a special focus on dependency across various quantiles of the joint distribution of the term structure. The main results are obtained using the quantile cross-spectral analysis, a new robust and non-parametric method allowing to uncover dependence structures in quantiles of the joint distribution of multivariate time series. The results are estimated using a dataset consisting of 15 years worth of high-frequency tick-by-tick time series of US Treasury futures. Complex dependence structures are revealed showing signs of both cyclicity and dependence in various parts of the joint distribution of the term structure in the frequency domain.

JEL Classification	C49, C55, C58, E43, G12, G13
Keywords	term structure of interest rates, yield curves, high-frequency analysis, spectral analysis, interest rate futures

Author's e-mail	`adam.nedved@fsv.cuni.cz`
Supervisor's e-mail	`barunik@fsv.cuni.cz`

Abstrakt

Tato diplomová práce představuje podrobnou empirickou studii závislostních struktur obsažených v časové struktuře úrokových sazeb. Nejdříve je představen přehled literatury a metod týkajících se modelování časové struktury úrokových sazeb. Teoretické aspekty použití vysokofrekvenčních dat a spektrální analýzy jsou představeny posléze. Narozdíl od většiny obdobných studií je tato práce postavena na analýze ve frekvenční doméně se zvýšenou pozorností věnovanou závislostem mezi kvantily společného rozdělení v různých částech časové struktury úrokových sazeb. Hlavní závěry jsou získány aplikací kvantilové křížové spektrální analýzy, nové robustní neparametrické metody, která umožňuje odhalení závislostních struktur v kvantilech společného rozdělení časových řad

o více proměnných. Výsledky jsou odhadnuty na datech, která se skládají z 15 let vysokofrekvenčních časových řad amerických futurit zaznamenaných po jednotlivých transakcích. Komplexní závislostní struktury vykazující známky cykličnosti i propojenosti v různých částech společného rozdělení časové struktury úrokových sazeb jsou odhaleny ve frekvenční doméně.

Klasifikace JEL	C49, C55, C58, E43, G12, G13
Klíčová slova	časová struktura úrokových sazeb, výnosové křivky, vysokofrekvenční analýza, spektrální analýza, úrokové futurity

E-mail autora	`adam.nedved@fsv.cuni.cz`
E-mail vedoucího práce	`barunik@fsv.cuni.cz`

Contents

List of Tables

List of Figures

Acronyms

CBOT Chicago Board of Trade

CME Chicago Mercantile Exchange

DNSM Dynamic Nelson-Siegel Model

GDP Gross Domestic Product

OLS Ordinary Least Squares

PCA Principal Component Analysis

RV Realised Variance

Master's Thesis Proposal

Author	Bc. Adam Nedvěd
Supervisor	doc. PhDr. Jozef Baruník, Ph.D.
Proposed topic	Analysis of Term Structures in High Frequencies

Motivation The term structure of interest rates is of a central importance to the research of the market activity. It reveals how market participants value future nominal payments with varying time to maturity. Studies focusing on the information contained in the term structure yielded important contributions to the research of monetary policy, risk management and theory of business cycles.

Much of past decade's economic research focusing on the term structures has diverged from the classical models, highlighting violations of their assumptions such as the linearity of its dependence (Junker, Szimayer and Wagner, 2006), Gaussian distribution (Righi, Schlender and Ceretta, 2015) or constant dependence (Dennis 2010). The novel method of quantile cross-spectral analysis (Baruník and Kley, 2015) allows for uncovering general dependence structures in time series while being robust to the aforementioned issues often found in the financial data. These properties make quantile cross-spectral analysis a perfect candidate for a method suitable for studying the dependences in term structures. Moreover, the availability of a novel dataset of high-frequency tick data from US Treasury market spanning over 19 years' period (first used by Cieslak and Povala, 2016) presents a unique opportunity to study the properties of the term structure with an increased precision.

Firstly, the thesis aims to study properties of the high frequency term structure of US Treasury bonds and its volatility. The goal is to uncover and describe possible dependencies across the frequency spectrum (short-term and long-term relationship), across the quantiles of its distribution (low-yields and high-yields relationship) and across the periods of varying volatility (relationship between periods of low volatility and periods of high volatility).

Secondly, the thesis would like to add to the plentiful research of the connectedness of the term structures and the real market activity. The term structures have been repeatedly found to be strongly related with the turning points of the business

cycle, proving to be an especially reliable tool for predicting economic recessions. The method of quantile cross-spectral analysis could shed more light on the nature of the connectedness of the term structures and the real business cycles, especially with regard to the relationship between low and high quantiles of their respective distributions. The nature of the method makes it suitable notably for the asymmetric nature of the business cycle dynamics.

Lastly, a significant portion of the research of the term structures has been devoted to finding determinants of the factors of the term structures. More specifically, the term structure of US Treasury bonds has been found to be sensitive to changes of monetary policy. By means of the quantile cross-spectral coherency, this thesis would like to add to the existing research by analysing the degree of connectedness of the term structures with regard to the employed monetary policy.

Hypotheses

Hypothesis #1: Term structures exhibit common cyclical behaviour across different quantiles

Hypothesis #2: Volatility of term structures is connected with stock markets volatility

Hypothesis #3: Connectedness of term structures depends on the employed monetary policy

Methodology High-frequency tick by tick data from the US Treasury market spanning from January 1992 to December 2010 will be used to construct the high frequency term structures through conversion of the bond data to the equivalent zero-coupon yields. A method of quantile cross-spectral analysis will be employed to study the general dependence structures in quantiles of the joint distribution of the term structures, its volatilities and exogenous economic time series of interest in the frequency domain. The quantile cross-spectral analysis is an entirely model-free and non-parametric method robust to distributional assumptions that hinder the performance of classical models. Unlike the classical covariance-based approaches, quantile cross-spectral analysis does take into account quantiles of the entire distribution of the analysed time series, revealing dependencies that remain hidden when employing just the averaged information.

Expected Contribution This thesis aims to contribute to the research of the term structures by employing a new methodology of quantile cross-spectral analysis. The goal of the study is to analyse the term structure and its volatility within the frequency domain with focus on the quantiles of its distribution. This novel approach

is robust to the shortcomings of the classical approach mentioned in the recent literature. Moreover, it has a potential to uncover dependencies that remained hidden to this day.

In the first part, the thesis aims to describe the nature of the dependencies in the term structure across the frequency spectrum, quantiles of its distribution and its differing volatilities. New findings in this part could benefit the theory of the bond portfolio risk management. In the second part of the thesis, the asymmetric nature of the business cycles dynamics and its relationship with the term structure will be assessed with possible new findings regarding the varying nature of connectedness of term structures and business cycles, especially in the "good times" and the "bad times". In its last part, the thesis will analyse the nature of connectedness of the monetary policy and term structures with possible implications on the efficiency of the monetary policy.

The analysis of the term structures will also benefit from the availability of the novel dataset of tick-by-tick high frequency data of US Treasury bonds that further increase the relevancy of the expected outcomes.

Outline

1. Introduction
2. Literature Review
3. Term Structure Overview
4. Data, Descriptive Statistics and Methodology
5. Analysis of Connectedness of Term Structures in High Frequencies
6. Analysis of Connectedness of Term Structures and Market Activity
7. Conclusion

Core bibliography

Baruník, J., & Kley, T. (2015). Quantile Cross-Spectral Measures of Dependence between Economic Variables (October 23, 2015).

Cieslak, A., & Povala, P. (2016). Information in the Term Structure of Yield Curve Volatility. The Journal of Finance, 71(3), 1393–1436.

Deibold, F. X., Rudebusch, G. D., & Aruoba, S. B. (2006). The macroeconomy and the yield curve: a dynamic latent factor approach Francis. Journal of Econometrics, 131, 309–338.

Estrella, A., & Hardouvelis, G. A. (1991). The Term Structure as a Predictor of Real Economic Activity. Journal of Finance, 46(2), 555–576.

Fama, E. F. (1990). Term-structure forecasts of interest rates, inflation and real returns. Journal of Monetary Economics, 25(1), 59–76.

Junker, M., Szimayer, A., & Wagner, N. (2006). Nonlinear term structure dependence: Copula functions, empirics, and risk implications. Journal of Banking and Finance, 30(4), 1171–1199.

Philip, Dennis, Estimation of Factors for Term Structures with Dependence Clusters (May 14, 2010).

Righi, M. B., Schlender, S. G., & Ceretta, P. S. (2015). Pair copula constructions to determine the dependence structure of Treasury bond yields. IIMB Management Review, 27(4), 216–227.

Author

Supervisor

Chapter 1

Introduction

Term structure of interest rates has been a focal point of economic research for decades. The relatively simple representation of the relationship between interest rates and terms to maturity contains information crucial to a wide variety of economic agents. At each point in time, the term structure reveals how economic agents aggregately value cash flows with respect to different time horizons. This information is carefully analysed by central bankers when adjusting monetary policy, governments as term structures can predict future path of the economy and other institutions that are simply trying to hedge against adverse interest rate movements. It is no wonder that both researchers and practitioners find the understanding of the complex dynamics within the term structure to be key for their work. However, analyses of term structures often rely on low-frequency quote data and techniques that disregard important properties of financial time series such as their heavy-tailed non-Gaussian distributions.

This thesis represents an in-depth empirical study of the dependence structures contained within the term structure. Its contribution relies on a combination of several novelty approaches. Firstly, we compute a high-frequency representation of the term structure using a unique dataset of 15 years worth of tick-by-tick interest rate futures trade data. Not only are the trade data often more accurate than traditionally used quote data, but the dataset also allows us to analyse intraday volatility within the term structure. Secondly, the analysis is carried out in the frequency-domain contrary to the more traditional time-domain approaches. This allow us to interpret variation and dependence in different parts of the term structure in terms of cycles of various frequencies. Finally, we use a novel method of quantile cross-spectral analysis in order

to study dependence structures between quantiles of the joint distribution of the term structure in the frequency domain. Using this robust and model-free technique, we test whether is the dependence between various parts of the term structure constant or whether it differs across different parts of the joint distribution.

The chapters of this thesis are organised as follows. Chapter 2 represents a review of the most important contributions to the term structure modelling literature as well as a review of spectral analysis, interest rate futures and high-frequency estimation literature with a focus on term structures. Theoretical foundations behind the methods used in this thesis are laid in Chapter 3. This chapter provides a comprehensive overview of the term structure modelling approaches, methods using high-frequency data and (cross-)spectral analysis methods. Chapter 4 is dedicated to the description of the raw interest rate futures dataset and all subsequent transformations applied to it in order to achieve dataset suitable for subsequent analyses. Chapter 5 offers a detailed discussion of the results of spectral analysis of the term structure in three parts: first part focuses on univariate spectral representations of various parts of the term structure, second part deals with cross-spectral dependence in the term structure using common techniques and the third part uncovers the dependence structure in detail using the quantile cross-spectral analysis. Chapter 6 concludes.

Chapter 2

Literature Review

This chapter provides an overview of the relevant literature concerning term structure modelling with a special attention paid to spectral analysis and high-frequency estimation. Overviews of contemporary nonparametric modelling approaches and interest rate futures are also covered in respective sections.

For a complete and in-depth overview of the term structure modelling literature see Gibson *et al.* (2010) and Filipovic (2009) or Bjork (2009) for a more rigorous approach.

2.1 Models of Term Structure

Much of the interest in term structures revolves around the central question: Why do we observe a mismatch between the equilibrium forward rates and the future spot rates? With no uncertainty involved, we'd expect the two rates to coincide but observations of various shapes of yield curves hint at a prominent role of term premia. Naturally, multiple modelling approaches have emerged as a result of attempts to solve the puzzle.

First term structure models were heavily inspired by the derivative pricing models succeeding the famous stock option pricing model by Black & Scholes (1973). For example Merton (1973) uses government bonds as the underlying assets instead of stocks. But despite solving a related problem, the term structure estimation literature evolved separately from the rest of the derivative pricing literature due to peculiarities specific to the bonds.

The Merton (1973) model is one of the first models that used one-factor approach with a time invariant process. Models by Vasicek (1977) and Cox *et al.* (1985) were developed on the same basis while Hull & White (1990)

introduced time-variability of the short rate process driving the term structure. Although a majority of total variance in a term structure can be explained by a single dependent variable, we often observe humped-shaped yield curves with dynamics that are not attainable by means of any single factor. Naturally, the extension of models into multivariate settings allowed for a significantly better fit at a cost of losing analytical tractability. Models by Cox *et al.* (1985) and Duffie & Kan (1996) are notable examples of the multivariate approach. Finally, Ho & Lee (1986) and Heath *et al.* (1992) proposed models with only one state variable of infinite dimension - the term structure itself.

Empirical studies of the aforementioned models confirm that analytical tractability of term structure models usually comes at a cost of sub-par goodness of fit. Chan *et al.* (1992) compare eight models using a generalised method of moments and conclude that popular models like Vasicek (1977) and Cox *et al.* (1985) perform poorly and hint at an important role of relationship between volatility of interest rate and the risk-less rate. Survey by Boero & Torricelli (1996) concludes with similar results adding that no model clearly outperforms no other. Ait-Sahalia (1996) rejects specifications of most popular models by comparing implied parametric densities with the estimated non-parametric counterparts.

Employing purely statistical methods to estimate the term structure represents a completely different and mostly successful approach. Litterman & Scheinkman (1991) find that over 90% of total variance of excess returns over risk-free rate can be explained by the first three principal components. The effectiveness of statistical methods like principal component analysis has been well documented Barber & Copper (2012). A great success has been achieved by means of curve fitting. McCulluch (1971) used cubic splines and Vasicek & Fong (1982) later proposed using exponential splines to easily reproduce empirically-sound yield curve shapes. The parametric model proposed by Nelson & Siegel (1987) and its derivatives are very simple yet efficient when fitting the entire range of observable yield curves. For this reason, the Nelson-Siegel family of models remains favourite among practitioners as documented in the survey among central bankers Bank for International Settlements (2005).

2.2 Spectral Analysis of Term Structure

Following the famous description of the spectral representation of a typical economic time series Granger (1966), a term structure of interest rates has

been covered in a similar fashion in Granger & Rees (1968). Presenting the spectra of yields on securities of British Government between 1924 and 1962, the conclusion is that the term structure adheres to the "typical shape of economic variable" and that observed interest rates follow a random walk model. With largely inconclusive results, Sargent (1971) uses the spectral approach to study phase shifts among yields of different maturities in order to test the expectation hypothesis. Similarly, Assenmacher-Wesche & Gerlach (2008) test the expectation hypothesis using the spectral decomposition and conclude that the expectation hypothesis cannot be rejected for maturities ranging from 6 months to 4 years.

Among the more recent publications, Hallett & Richter (2004) analyse parameter changes of a term structure model before, during and after structural shocks using data from the USA, UK and Germany. As a result, the authors were able to distinguish parameter responses relative to a given frequency range. Using Japanese yield curve data, Tsuji (2006) finds almost no cyclical components in the yield curve slope, which could provide an explanation for the limited predictive power that Japanese slope curve has with respect to the real GDP.

2.3 Modern Term Structure Analysis

The long-history of research aimed at the term structure makes it an attractive subject to test new estimation techniques on. With each new technique, there is a chance to uncover new dependence structure that has so far remained hidden. The contribution of the new approaches is usually based on the ability to loosen assumptions such as normality of distributions, symmetry or linearity of the dependence structures.

Kiermeier (2014) uses the wavelet analysis to test significance of the five-factor Nelson-Siegel model on various time scales using European zero-coupon curves estimated by ICAP. Copula based estimation techniques represent another popular contemporary approach to term structure estimation. Junker *et al.* (2006) study nonlinear dependence structures of US Treasury yields using copulas and reveal an upper tail dependence in yield innovations. Similarly, the dependence structure in US Treasury yields is estimated using pair copula in the article by Righi *et al.* (2015). The authors find a strong dependence of yields and their past values together with decreasing yield variability with increasing time to maturity of a bond. Noureldin (2014) uses copulas to study

time-varying dependence structures among the factors in the Dynamic Nelson-Siegel model. Finally, Kuriyama (2016) uses quantile regression to find evidence of cointegration in the US term structure data with a mixed evidence of contintegration across all quantiles but a strong evidence in the central part of respective distributions.

2.4 Interest Rate Futures

A large portion of the term structure of interest rates research employs either quote or trade data of government bonds with varying maturities. However, these datasets can be vulnerable to errors, especially when using quote data that are scarcely precise for "off-the-run" bonds. One way to avoid this problem is to use interest rate derivatives transaction data.

Björk & Landén (2000) present a detailed general framework to interest rate futures and forward pricing. Similarly, Jegadeesh & Pennacchi (1996) use Eurodollar futures data in construction of a two-factor term structure of interest rates model. Futures data are commonly used in studies of commodity markets. Bessembinder *et al.* (1995) test investors' expectations about mean reversion in spot asset prices using futures prices from eleven different markets and conclude that there is a significant evidence of mean reversion in commodity futures markets but a very weak evidence in the US Treasure futures market.

Another branch of literature focuses on the pricing specifics of futures contracts. Using the Eurodollar futures data, Sandaresan (1991) suggests that the differences between implied forward prices and the futures prices are only in minor part caused by the marking-to-market mechanism, contrary to what Cox *et al.* (1980) suggest.

2.5 Term Structure in High Frequencies

Even though computing power is increasingly more affordable and high-frequency datasets more available, the high-frequency term structure literature remains relatively scarce. A recent study by Cieslak & Povala (2016) explores information content in high-frequency US Treasury market data. The authors estimate a no-arbitrage term structure model with stochastic covariance and as a result, they propose a decomposition of conditional interest rate volatility into components of term premia, short-term expectations and their conditional covariance.

The study by Shin & Zhong (2017) concludes that augmenting the Dynamic Nelson-Siegel model with realised volatility serving as a volatility measure can improve bond yield density forecasts.

One popular way to utilise high-frequency data is to analyse the impact of policy announcements. Fleming & Remolona (1999) document significant shocks resulting from macroeconomic policy announcements on medium term interest rates while the effect on short rates being comparatively modest. Similarly, the model introduced by Piazzesi (2005) utilises a high-frequency policy rule based on the decisions by the Federal Reserve and improves the fit of the latent three-factor term structure model at its short end. Among other results, the author documents a snake shape of a volatility curve.

Chapter 3

Theoretical Review

The most important theoretical notions employed in this thesis are covered in the subsequent sections. Firstly, economic theories of term structure and zero coupon bonds are introduced followed by a comprehensive summary of the most important modelling approaches. Secondly, concepts surrounding the analysis and use of high-frequency data are introduced. Following is an introduction into spectral, cross-spectral and quantile cross-spectral methods. And finally, the chapter is concluded with a brief overview of the interest rate futures.

3.1 Zero Coupon Bonds

A *zero coupon bond* constitutes a claim with no coupon payments during the entire holding period that pays its full face value at the time of the maturity. A real world government bonds usually pay its holders fixed coupons with a known frequency until the date of the bond's maturity. But to vastly simplify the analytical tractability of the problem, we will make use of the fact that any coupon-bearing bond can be equivalently reproduced with a portfolio of zero coupon bonds with maturities and face values mimicking the coupon payments at their respective due dates. The following sections introduce the basic concepts associated with the term structure following the text by Gibson *et al.* (2010).

Let us consider a zero coupon bond with a face value equal to 1. The *log-holding period return* $hpr(t, t+n, T)$ of a zero coupon bond with a *time of maturity* T that is bought at the time t and which is being held until the time

$t + n$ is denoted by:

$$hpr(t, t + n, T) = p(t + n, T) - p(t, T)$$

where $p(t, T)$ is the natural logarithm of the price of the zero coupon bond at the time t with time of maturity T and $t + n \leq T$. In the case when $t + n = T$, the return of the bond is equal to the face value and the per-period holding period return is equal to the *yield to maturity* $R(t, T)$:

$$R(t, T) = \frac{hpr(t, T, T)}{T} = -\frac{p(t, T)}{T}.$$

The *short rate* $r(t)$ (or instantaneous risk-free interest rate) is a yield on the currently maturing bond, i.e.,

$$r(t) = \lim_{T \to t^+} R(t, T).$$

The *forward rate* $f(t, T_1, T_2)$ is the rate of a risk-free loan beginning at the time T_1 which is ending at the time T_2, therefore:

$$f(t, T_1, T_2) = \frac{p(t, T_1) - p(t, T_2)}{T_2 - T_1}.$$

Finally the rate at the time t for which one can obtain a loan for an instantaneous period of time $f(t, T) \coloneqq (f, T, T)$ is called the *instantaneous forward rate*.

Zero coupon bonds with identical time to maturity and face values may in practice offer different yields due to the presence of default, credit, liquidity or other risks. When modelling the term structure of interest rates, we will be interested in the varying levels of bond yields resulting from variations in their respective time to maturity. Other associated risks will be considered fixed throughout the thesis.

3.2 Term Structure

Market participants usually value future cash flows with respect to the length of investment horizon. If we obtained, at any given time, yields of identical bonds differing solely in their maturities while holding all other factors fixed, we could observe the current market's valuation of money with respect to the

investment horizon. We construct the *term structure of interest rates* as a function $R(t,T)$ that for a fixed time t maps a continuous time parameter T to real values of the bond yields. The graphical representation of this function is called the *yield curve*.

The vast body of research devoted to the drivers of the term structure has been inspired by the fact that the today's term structure contains information about the market participants' views about the future path of the economy. After accounting for related risks, expected values of the average future short yields constitute the yields of long maturity bonds. An accurate interpretation of the shape of the term structure is therefore highly useful when making an investment or policy decisions.

The theory explaining variability in shapes of term structure has branched into three main directions: the expectation hypothesis, the liquidity preference and the preferred habitat theory.

3.2.1 The Expectation Hypothesis

The most straight-forward explanation is given be the expectation hypothesis which puts the emphasis on the investor's expectations of the future spot rates. The forward rate is therefore an unbiased estimator of future spot rates and the term structure is given by:

$$R(t,T) = \frac{1}{T-t}\int_t^T \mathbb{E}_t\big(r(s)\big)ds$$

where $R(t,T)$ is the yield to maturity, t denotes the current time, T denotes the time of maturity of the bond and $r(t)$ is the short term rate.

3.2.2 The Liquidity Preference Theory

If we assumed that the investors are risk-averse and that they prefer receiving the same nominal payments sooner rather than later, keeping other factors fixed, then the investors demand a premium $L(s,T)$ for buying a security with a longer maturity to compensate for the additional risk. Borrowers are willing to pay this premium as they prefer borrowing long term over short term. Under the liquidity preference theory, the term structure is given by:

$$R(t,T) = \frac{1}{T-t}\Big(\int_t^T \mathbb{E}_t\big(r(s)\big)ds + \int_t^T L(s,T)ds\Big)$$

where $L(t,T) > 0$ denotes the term premium at time t for a bond with time of maturity T.

3.2.3 The Preferred Habitat Theory

Empirically, the slope of the term structure is not always positive as the expectation hypothesis and the liquidity preference theories would suggest. Since the lenders and the borrowers might have different preferences relative to the investment horizon, the resulting premium $L(t,T)$ might be any real number depending on the intersection of the supply and demand at the time t. The term structure is given by:

$$R(t,T) = \frac{1}{T-t}\Big(\int_t^T \mathbb{E}_t\big(r(s)\big)ds + \int_t^T L(s,T)ds\Big)$$

where $L(t,T) \in \mathbb{R}$.

3.3 Models of the Zero Coupon Term Structure

The term structure of interest rates is a continuous function and as such consists of an infinite number of individual zero coupon yields. As demonstrated in the previous sections, zero coupon yields can also be derived from the short-term rates $r(t)$ for $t \in [t,T]$. However a collection of the entire range of short rates is usually not readily available for analysis and therefore the shape of the term structure or its features have to be estimated from the available data.

Several techniques have been proposed in order to model and forecast the term structure accurately while keeping the model complexity reasonably low. The most common approaches to modelling of the term structure are summarised below following a detailed overview of the term structure modelling literature by Gibson *et al.* (2010).

3.3.1 General Equilibrium Models

The early models of term structure are based on the assumption that exogenously specified markets are efficient in reaching of their equilibria. The term structure of interest rates is modelled using utility functions of the investors on the market that has reached its equilibrium. These models are usually affine-class, single-factor and time-invariant.

Single-factor models assume that term structures can be completely specified using a single explaining factor, usually the short rate $r(t)$. The use of a single factor implies that changes in the interest rates are perfectly correlated along the term structure which contradicts the real world observations. The specification of these models usually starts with a definition of a stochastic process driving the short rates from which the form of the term structure is derived.

Time-invariant models imply that the short-rate dynamics govern an endogenous term-structure. In practice this means that we cannot use the model to fit time-varying shapes of the term structure. On the other hand, specifying the term structure models using only time-varying parameters usually leads to an undesired over-parametrisation and over-fitting of the term structure.

Finally, in the affine-class models, the term structure is an affine function of the short rate, ie.:

$$R(t,T) = \frac{-a(t,T)}{T-t} r(t) + \frac{b(t,T)}{T-t}$$

where $a(t,T)$ and $b(t,T)$ are deterministic functions. These models are usually derived from the specification of the stochastic process driving the spot rates.

A famous example of such models is the model proposed by Vasicek (1977). The author defines the short-term rate process as a mean-reverting random walk process with a drift, ie.:

$$dr(t) = \kappa(\theta - r(t))dt + \sigma dW(t)$$

where κ, θ and σ are all positive and constant and $W(t)$ is a standard Wiener process. The θ is a long-term value of $r(t)$ while κ governs the adjustment speed of the mean-reverting process.

The explicit solution for the short-term rate is:

$$r(t) = \theta + (r(s) - \theta)exp(-\kappa(t-s)) + \sigma_r \int_s^t exp(-\kappa(t-s))dW(u)$$

where $r(t)$ follows a normal distribution which can result in negative interest rates. This undesirable property was addressed in later models like the one by Cox *et al.* (1985).

Their term structure is given by:

$$R(t,T) = R(t,\infty) + \frac{1 - exp(-(T-t)\kappa)}{(T-t)\kappa}(r(t) - R(t,\infty)) + \frac{\sigma_r^2}{4(T-t)\kappa^3}(1 - exp(-(T-t)\kappa))$$

which allows for both positively and negatively sloped as well as for humped-shaped yield curves.

Large amount of general equilibrium models have since been proposed. Some authors propose improvements to specifications of the short-term rate process, utility functions or other market characteristics (Cox *et al.* 1985), some allow for a time variation of model parameters (Hull & White 1993) and others introduce additional exogenous factors to drive the term structure (Jamshidian 1995).

Despite being popular for their analytical tractability, the general equilibrium models have not been widely adopted by practitioners. It has been well documented that the forecasting performance of such models is rather poor (Chan *et al.* 1992) and that under certain conditions it can perform even poorer than random walk models (Duffee 2002). Moreover these models have no mechanism allowing for calibration of the fit using the contemporaneously observable cross-sections of data.

3.3.2 No Arbitrage Models

A different approach to the term structure modelling is represented by an idea that the entire term structure is in fact given exogenously by a cross-section of zero coupon yields at a given point in time t_0. Subsequently, the dynamics of the entire term structure for $t > t_0$ are modelled based on the assumption that no arbitrage opportunities are present on the market. Compared to the general equilibrium models, the no arbitrage models employ cross-sectional characteristics of interest rates rather than relying on the time series dynamics of the interest rates.

The first such model was introduced by Ho & Lee (1986) in a form of a discrete recombining binomial tree. In their model, the time is divided into equidistant periods where the term structure at t_0 is set according to the observed data. In each subsequent time period $t > t_0$, the previous term structure is multiplied by a period-dependent perturbation function $h(\tau)$ with probability

π or by a function $h^*(\tau)$ with probability $(1-\pi)$ where

$$\pi h(t) + (1-\pi)h^*(t) = 1.$$

Given the probability measure π and a parameter δ, the perturbation functions can be expressed as

$$h(\tau) = \frac{1}{\pi + (1-\pi)\delta^\tau}, h^*(\tau) = \frac{\delta^\tau}{\pi + (1-\pi)\delta^\tau}$$

and the corresponding bond prices as

$$B(t,T) = h(T-t)\frac{B(t-1,T)}{B(t-1,t)}$$

or

$$B(t,T) = h^*(T-t)\frac{B(t-1,T)}{B(t-1,t)}.$$

Following the derivations in Gibson *et al.* (2010), we arrive at the following functional form of the interest rate

$$\begin{aligned} r(t) = r(t-1) + (f(0,t) - f(0,t-1)) + \log(\frac{\pi + (1-\pi)\delta^\tau}{\pi + (1-\pi)\delta^{\tau-1}}) \\ - (1-\pi)\log(\delta) + \epsilon_t \end{aligned}$$

where ϵ_t is an i.i.d. random noise term with $\mathbb{E}(\epsilon_t) = 0$.

Besides the previous-period interest rate, the slope of the term structure and a time-dependent constant also influence the contemporaneous interest rate. The parameters π and δ have to be estimated from the data.

Similarly to the Vasicek model, Ho and Lee model also allows for negative interest rates which implies that it is not a necessarily arbitrage-free model. Also, the lack of built-in mean reversion mechanism means that in extreme cases, the interest rates can drift to infinity. Finally, the single-factor approach implies that bonds across all maturities are perfectly correlated which does not correspond to observed data. However, arbitrage free models generally fit the data better than general equilibrium models since they use cross-sectional data to make an initial fit of the term structure. Like general equilibrium models, no arbitrage models are popular for their analytical tractability.

Many extensions of the Ho and Lee model were proposed including the famous Heath, Jarrow and Morton model Heath *et al.* (1992) model which extends the original discrete single factor model into multiple factor continuous

time model. Moreover, the Heath, Jarrow and Morton model imposes exogenous stochastic structure upon forward rates instead of the zero coupon bond prices. The resulting model is not only dealing with some drawbacks of the previous arbitrage fee models, but it also represents a general framework that is fully compatible with general equilibrium class models.

3.3.3 Smoothing Splines

Spline methods are based on fitting of the term structure with a piecewise polynomial called a spline function. For a closed maturity interval, we can estimate the term structure (or any continuously differentiable function) with a suitable polynomial function to a predefined degree of precision. The precision of the fit increases with the increasing order of the polynomial used to fit the term structure over some interval. Higher order polynomials however produce curves that are not smooth enough to resemble empirical yield curves. One solution is to use a sequence of lower order polynomials to create a piecewise polynomial joined smoothly at so called knot points. The spline functions used to fit term structures usually rely on quadratic or cubic polynomials.

The approach using splines was first introduced by McCulluch (1971) who parametrised the function of present value of future coupon payments using a cubic splines:

$$\delta(m) = 1 + \sum_{i=1}^{k} a_i f_i(m)$$

where $\delta(m)$ is a continuous discount k-parameter spline function and $f_i's$ are polynomial functions. The linearity of the model allows for estimation of the term structure using the ordinary least squares. Important shortcoming of this method is that its results are largely sensitive to the value of k and the precise placement of the knot points (Fernandez-Rodriguez 2006).

As a reaction to the poor fit of equilibrium models to the observed data, Vasicek & Fong (1982) proposed a method of exponential splines fitting. Exponential splines deal with some shortcomings of polynomial splines including the fact that polynomials are not strictly decay functions. Shea (1984) shows that spline methods can provide local flexibility to approximate very complex shapes of term structure. At the same time, these methods are sensitive to anomalies in data and parameter selection that can result in completely unrealistic estimates.

3.3.4 Principal Component Analysis

Principal Component Analysis (PCA) is a statistical method based on a decomposition of the covariance matrix that allows for a reduction of dimensionality of multidimensional datasets while retaining as much of their original variance as possible. By applying the PCA on the covariance matrix of zero-coupon rate changes, we obtain a set of orthogonal eigenvectors (factors) accounting for most variability in the zero-coupon rate.

Following Filipovic (2009), the principal components analysis relies on the spectral decomposition theorem, ie.:

$$Q = ALA^T$$

where $L = \text{diag}(\lambda_1, \ldots, \lambda_n)$ is the diagonal matrix of eigenvalues of Q and A is an orthogonal matrix with columns $a_1, \ldots, a_n$ are the normalised eigenvectors of Q. Each eigenvector is associated with an eigenvalue whose magnitude represents the amount of variation of the original data explained by the corresponding eigenvector.

Litterman & Scheinkman (1991) used the principal component analysis on term structure data to find that the three factors with the highest eigenvalues explain a minimum of 96% of variance in the data. Moreover, the resulting factors are easily interpretable as the first factor is associated with parallel changes in the yields, the second factor is generally associated to the steepness of the curve and the third factor represents its curvature. Interestingly, the interpretation of the factors obtained through the PCA along with their loadings are very similar to the factors and loadings obtained using the Dynamic Nelson-Siegel model described in Section 3.3.5.

3.3.5 Parametric Methods

Parametric estimation of the term structure of interest rates relies on a specification of a class of continuous real functions defined over the entire maturity domain, usually consisting of exponential components. Contrary to the general equilibrium and no arbitrage models, parametric models do not assume any functional relationships arising from the underlying economic theory. But unlike purely statistical methods like PCA, parametric methods impose a predefined structure on the term structure. The proposed functional specification

must be flexible enough to replicate empirically observable shapes of the term structure while remaining parsimonious.

Nelson-Siegel Model Arguably, the most popular parametric method was introduced by Nelson & Siegel (1987) who, adhering to the expectation hypothesis, expressed as a condition

$$R(t,T) = \frac{1}{T-t}\int_0^{T-t} f(s)ds,$$

assumed the following instantaneous forward rate function:

$$f(\tau) = \beta_0 + \beta_1 \exp\Big(-\frac{\tau}{u}\Big) + \beta_2\left(\frac{\tau}{u}\exp\Big(-\frac{\tau}{u}\Big)\right)$$

where $\tau := T - t$ is the time to maturity, β_0, β_1 and β_2 are factors to be estimated and u is a time constant. The suggested term structure is obtained by integrating $f(\cdot)$ from zero to τ and rearranging:

$$R(t,T) = R(\tau) = \beta_0 + (\beta_1 + \beta_2)\frac{1-\exp\big(-\frac{\tau}{u}\big)}{\frac{\tau}{u}} - \beta_2\exp\Big(-\frac{\tau}{u}\Big).$$

Even though the estimated factors are highly related to the factors obtained using PCA, the Nelson-Siegel approach is different because it imposes a predefined structure on the factors.

Dynamic Nelson-Siegel Model (DNSM) An alternative factorisation of the Nelson-Siegel model was introduced by Diebold & Li (2006) who interpret the Nelson-Siegel model parameters β_0, β_1 and β_2 as three latent dynamic factors:

$$R(t,\tau) = \beta_{0t} + \beta_{1t}\frac{1-\exp(-\lambda_t\tau)}{\lambda_t\tau} + \beta_{2t}\Big(\frac{1-\exp(-\lambda_t\tau)}{\lambda_t\tau} - \exp(-\lambda_t\tau)\Big),$$

where β_{0t} represents a long-term factor which can also be viewed as a factor governing the level of the yield curve. β_{1t} represents a short-term factor which is related to the general slope of yield curve. and β_{2t} governs the middle section of the yield curve and is closely related to its curvature. The dynamic parameter λ_t represents the exponential decay rate of the curve. Large values of λ_t result in fast decay and generally better fit at short maturities. Analogically, small values of λ_t lead to a slow decay and a better fit at long maturities.

Svensson Model The Nelson-Siegel model was later extended by Svensson (1994) who proposed the following functional form of the forward rate:

$$f(\tau) = \beta_0 + \beta_1 \exp\Big(-\frac{\tau}{u}\Big) + \beta_2\left(\frac{\tau}{u}\exp\Big(-\frac{\tau}{u}\Big)\right) + \beta_3\left(\frac{\tau}{v}\exp\Big(-\frac{\tau}{v}\Big)\right)$$

which introduces a fourth term with a new factor β_3 which allows for a double humped shape of the term structure and a second constant v. After integration and rearrangement, we obtain the following term structure curve:

$$R(t,T) = R(\tau) = \beta_0 + (\beta_1 + \beta_2)\frac{1-\exp\big(-\frac{\tau}{u}\big)}{\frac{\tau}{u}} - \beta_2\exp\Big(-\frac{\tau}{u}\Big) + \\ + \beta_3\Big(\frac{1-\exp\big(-\frac{\tau}{v}\big)}{\frac{\tau}{v}} - \exp\big(-\frac{\tau}{v}\big)\Big)$$

The parametric methods of modelling of the term structure gained substantial popularity due to their flexibility and ease of estimation. A survey among central banks by Bank for International Settlements (2005) has revealed that 9 out of 13 participating banks used Nelson-Siegel or Svensson model for estimation of the term structure of interest rates.

3.4 High-Frequency Data

The ever-increasing computing power and data storage capacities combined with ever-decreasing storing and computing costs have allowed for recording of financial time series at tick-by-tick basis with highly granular timestamps. The resulting information-rich datasets provide new opportunities for the researchers while posing new challenges related to the data-handling, modelling and correct estimation. Some of these challenges are related to an irregular spacing of time between observations, bid-ask bounce or serial dependence. A more in-depth discussion of such issues can be found in Goodhart & O'Hara (1997).

3.4.1 Data Synchronisation

Tick-by-tick datasets are obtained through sampling of individual transactions on the markets. Each tick observation includes a highly granular timestamp recording the transaction time as well as other variables of interest such as price or type of the contract. Tick datasets are rich in information but do not

allow for a direct multivariate analysis due to inherent asynchronicity of the observations.

More formally, we observe prices $P_i(t)$ for each bond $i \in 1, ..., I$ sampled at transaction times $t_{i,1}, \ldots, t_{i,n_i}$ during a given time period $[t, T]$ such that $t_{i,1} \geq t$ and $t_{i,n_i} \leq T$. However, we usually observe different transaction times for different bonds so $t_{i,m} \neq t_{j,m}$ for some bond $j \in 1, ..., I, j \neq i$ and some $m \in \{1, \ldots, \min\{n_i, n_j\}\}$. In fact, we cannot even guarantee that $n_i = n_j$ so we might encounter different number of observations for each bond. To obtain an $I \times N$ matrix required for a multivariate analysis, we first need to synchronise the time series to obtain N observations in the given time period $[t, T]$ sampled at identical times for each bond.

Previous Tick One of the easiest approaches to data synchronisation is to use a previous tick estimator Zhang (2011). First, the sampling frequency has to be defined as a number N of equally spaced times $t_1, \ldots, t_N$ within the period $[t, T]$ such that $t_1 > t$ and $t_N = T$. Then for each bond i, we pick the previous tick times:

$$t'_{i,r} = \max\{t_{i,l} \leq t_r, l = 1, \ldots, n_i\}, \quad r = 1, \ldots, N.$$

The synchronised dataset is simply obtained by selecting the bond prices at the previous pick times $P_i(t_r) = P_i(t'_{i,r}), r = 1, \ldots, m$. An obvious drawback of this method is that we ignore all but one observation between our equally spaced sampling times which decreases the efficiency. Moreover, the method creates new data points where observations are missing which produces a bias.

Refresh Time An alternative synchronisation scheme proposed by Barndorff-Nielsen *et al.* (2011) is different in construction from the previous tick in that each sampling period includes at least one tick of each bond and that the resulting sampling times don't have to be equally spaced. Formally, let us write the number of transactions of a bond i up to the time t as a counting process $N_i(t)$ and the respective transaction times as $t_{i,1}, \ldots, t_{i,n_i}$. The first refresh time is defined as:

$$t'_1 = \max(t_{1,1}, \ldots, t_{I,1})$$

and each subsequent refresh time is defined recursively as:

$$t'_{r+1} = \max(t_{1,N_1(t'_r)+1}, \ldots, t_{I,N_I(t'_r)+1}).$$

Once we have the new sampling times $t'_1, \ldots, t'_{r_{\max}}$, we obtain the synchronised dataset by resampling prices of each bond $P_i(t'_r)$ for all $r = 1, \ldots, r_{\max}$. The problem of this approach is that the most illiquid asset is the one responsible for the selection of the highest number of the sampling times.

Generalised Sampling Time The method proposed by Aït-Sahalia *et al.* (2010) is more general than previous tick and refresh time. The generalised sampling time is defined as a sequence of points $\{t_1, \ldots, t_N\}$ for a collection of I assets satisfying the following conditions. Firstly, $t = t_1 < \cdots < t_{N-1} < t_N = T$. Secondly, at least one observation for each bond i must exist between the consecutive points in time t_r, t_{r+1}. Finally, the time intervals $\left\{\Delta_r = t_{r+1} - t_r, r \in \{1, \ldots, N-1\}\right\}$ converge in probability to zero. The synchronised dataset is obtained as $P_i(t'_r) = P_i(t'_{r,i})$ by selecting an arbitrary observation at the time $t'_{r,i} \in (t_r, r_{r+1}]$ for each asset i and each time interval $r = 1, \ldots, N-1$.

It can be seen that both previous tick and refresh time are in fact special cases of the generalised sampling time scheme. If we select $t'_{r,i}$ to be the time of the last transaction in each time interval, then we replicate the previous tick scheme. Similarly, we will arrive at refresh time scheme if we follow the scheme's recursive definition of t'_r. The advantage stemming from random drawing of the points from the time intervals is the robustness against the data misplacement error.

3.4.2 Realised Variance

Realised variance (RV) is a nonparametric volatility estimator capable of utilising the information contained in the high-frequency data. This ex-post measure is useful in contexts that require modelling of volatility dynamics. It allows for estimation of the cumulative price variation over a given period using the tick data.

Let us consider a continuous stochastic process of logarithm of asset prices

$p(t)$ given by the diffusion process:

$$p(t) = \int_0^t \mu(s)ds + \int_0^t \sigma(s)dW(s)$$

where $\mu(t)$ is a continuous drift process with finite variance, $\sigma(t)$ is a strictly positive volatility process, W is a standard Brownian motion and time $t \in [0, T]$.

We are interested in estimation of the integrated variance:

$$\mathrm{IV}(t) = \int_{t-\Delta}^t \sigma^2(s)ds$$

which gives us the amount of variance accumulated over the time period of $[t - \Delta, t]$.

Now suppose that we observe $n+1$ prices $p(0), \ldots, p(n)$ on an equally spaced interval $[0, T]$. The sum of squared returns:

$$\mathrm{RV}(n) = \sum_{i=1}^{n} \Big(p(i) - p(i-1)\Big)^2$$

is an estimator of the integrated variance IV called realised variance. In fact realised variance converges almost surely to the integrated variance as $n \to \infty$ (or equivalently $\Delta \to 0$) as shown in Andersen *et al.* (2003).

3.5 Spectral Analysis of Economic Time Series

Classical time series analysis is concerned with uncovering information hidden in the autocovariance structure of the data in the time domain. Alternatively, we can move away from the time domain to the frequency domain and study the information hidden in the "frequency content" of the data. Under such transformation, the information content remains exactly the same (Nerlove 1964), but the new point of view allows for uncovering relationships that are otherwise difficult to reveal.

We can think of economic time series as of a combination of trends, noise and cycles. Since there are usually multiple cyclical components of various lengths present in the data generating process, the classical time series analysis mainly concerned with autocovariance structures becomes largely ineffective when analysing the influence of cyclical patterns hidden in the data.

The basic idea behind the spectral analysis is that any stochastic time series can be decomposed into an infinite number of sine and cosine waves (Nerlove 1964). This allow us to view an economic time series as a sum of cyclical components with various amplitudes, frequencies and phases (i.e., the origin in time of the time series). Subsequently, this will allow us analyse the *spectrum of the time series*, which can be thought of as a decomposition of the variance of the series attributed to different frequencies.

This section represents a brief summary of some of the most important notions in theory of spectral analysis following a brilliant textbook by Granger & Hatanaka (1964). Throughout, we will be considering a stationary, complex data generating process $\{X_t\}$. This process has first and second moments that are not functions of time t and autocovariance μ that is dependent on the distance between time periods t and s, i.e.,

$$\begin{aligned}\mathbb{E}(X_t) &= 0\\ \mathbb{E}(X_t\bar{X}_t) &= \sigma^2\\ \mathbb{E}(X_t\bar{X}_s) &= \mu(t-s) = \mu_\tau, \quad \tau = t-s\end{aligned}$$

for all t, s where $\bar{X}$ is the complex conjugate of X.

3.5.1 Power Spectrum

Let us consider the following generating process X_t:

$$X_t = \sum_{j=1}^{k} a_j \exp(it\omega_j)$$

where $(\omega_j, j = 1, \ldots, k)$ is a set of real numbers with $|\omega_j| \leq \pi$ and $(a_j, j = 1, \ldots, k)$ is a set of independent, complex random variables where for all j $\mathbb{E}(a_j) = 0$, $\mathbb{E}(a_j\bar{a}_j) = \sigma_j^2$ and $\mathbb{E}(a_j\bar{a}_k) = 0$, $j \neq k$. Each term of X_t is a periodic function:

$$a_j \exp(i\omega_j t) = a_j(\cos(t\omega_j) + i\sin(t\omega_j))$$

with period $\frac{\omega_j}{2\pi}$ and angular frequency ω_j.

The sequence of autocovariances μ_t of (any) stationary process X_t satisfies:

$$\mu_t = \int_{-\pi}^{\pi} \exp(it\omega) dF(\omega)$$

where $F(\omega)$ is a step function with steps of size σ_j^2 at $\omega = \omega_j, j = 1, \ldots, k$. $F(\omega)$ is thus monotonically increasing function with extremes at $F(-\pi) = 0$ and $F(\pi) = \sum_{j=1}^{k} \sigma_j^2$, where $F(\pi)$ is the variance of the generating process X_t. This equation is called *the spectral representation of the covariance function* and $F(\omega)$ is called *the power spectral distribution function.*

Moreover (any) stationary process X_t can be written in the form called *Cramér representation of a stationary process*:

$$X_t = \int_{-\pi}^{\pi} \exp(it\omega) dz(\omega)$$

where $z(\omega)$ is a complex, random function termed a *process of non-correlated increments* such that:

$$\begin{aligned} \mathbb{E}(dz(\omega_1)\overline{dz(\omega_2)}) &= 0, \quad \omega_1 \neq \omega_2, \\ &= dF(\omega), \quad \omega_1 = \omega_2 = \omega. \end{aligned}$$

Since $F(\omega)$ is a monotonically increasing function, it can be decomposed into three components:

$$F(\omega) = F_1(\omega) + F_2(\omega) + F_3(\omega)$$

where $F_1(\omega)$ is a non-decreasing, absolutely continuous function, $F_2(\omega)$ is a non-decreasing, step-function and $F_3(\omega)$ is a non-decreasing singular function which is assumed to be zero in economic applications. Any stationary process X_t can be thus decomposed into two uncorrelated components X_1 and X_2:

$$X_t = X_1(t) + X_2(t).$$

$X_1(t)$ is a member of the class of non-deterministic processes with an absolutely continuous power spectral distribution function and thus its sequence of autocovariances follows:

$$\mu_t = \mathbb{E}(X_1(t)\overline{X_1(t-\tau)}) = \int_{-\pi}^{\pi} \exp(it\omega) f(\omega) d\omega.$$

$X_2(t)$ represents a deterministic component corresponding to a linear cyclic

process in a form of:

$$X_2(t) = \sum_{j=1}^{\infty} a_j \exp(it\omega_j), \quad |\omega_j| \leq \pi \text{ for all } j.$$

Finally, let us consider a real generating process X_t producing infinitely long, discrete and trend-free time series and its Cramér's representation:

$$X_t = \int_0^{\pi} \cos(t\omega)du(\omega) + \int_0^{\pi} \sin(t\omega)dv(\omega).$$

If we take one sample series x_t of a finite length generated by such process, then we can fit it exactly by a finite Fourier series:

$$x_t(n) = \sum_{j=0}^{n} a_j \cos(t\omega_j) + \sum_{j=1}^{n} b_j \sin(t\omega_j),$$

where $\omega_j = \frac{2\pi j}{n}$ and a_j's and b_j's are such that $x_t(n) = x_t$ at $t = 1, \ldots, n$. Allowing for increasing sample lengths $n \to \infty$, the interval between adjacent frequencies shrinks $\omega_{j+1} - \omega_j \to 0$ and the above representation turns into an addition of integrals:

$$x_t = \int_0^{\pi} a(\omega) \cos(t\omega)d\omega + \int_0^{\pi} b(\omega) \sin(t\omega)d\omega.$$

This means that an infinitely long sample series $(x_t, t = 1, \ldots, \infty)$ can be fitted exactly if we choose $a(\omega)$ and $b(\omega)$ properly. If $\{x_t\}$ contains a periodic element of frequency $\omega_1 = \frac{2\pi}{m}$, then both $a(\omega)$ and $b(\omega)$ will have sharp spikes at $\omega = \omega_1$ but if the series $\{x_t\}$ contains no periodic elements, both functions will be smooth.

We are interested in the periodic regularities that are characteristic to the generating process X_t. These regularities are associated with the relative importance of particular periodic terms that generate observable cycles in the sample series. The relative importance of a particular periodic term can be thought of as a resulting decrease of variance of the series when this particular term is removed. If we define the function $F(\omega)$ as:

$$F(\omega) = F(\omega_2) - F(\omega_1) = \int_{\omega_1}^{\omega_2} (a^2(\omega) + b^2(\omega))d\omega,$$

then $F(\omega)$ corresponds to the amount of total variance that is attributable to

the frequency band (ω_1, ω_2). This function is called the *power spectral distribution function* which appears as $z(\omega)$ in the Cramér's representation of a stationary process.

3.5.2 Cross-Spectral Analysis

Apart from being able to analyse the power spectrum of one stationary process, it is often useful to extend the spectral approach to be able to explore relationships between two stationary processes and their respective components. In order to achieve this, we generalise the univariate case into a bivariate setting with a stationary random generating process $\{X_t, Y_t\}$ with a Cramér's representation:

$$X_t = \int_{-\pi}^{\pi} \exp(it\omega) dz_x(\omega)$$
$$Y_t = \int_{-\pi}^{\pi} \exp(it\omega) dz_y(\omega),$$

satisfying

$$\begin{aligned} \mathbb{E}(dz_x(\omega_1) dz_y(\omega_2)) &= 0, \quad \omega_1 \neq \omega_2 \\ &= Cr(\omega), \quad \omega_1 = \omega_2 = \omega, \end{aligned}$$

where $Cr(\omega)$ is known as the *power cross-spectrum between* $\{X_t\}$ *and* $\{Y_t\}$ which can be further decomposed following:

$$Cr(\omega) = c(\omega) + iq(\omega),$$

where $c(\omega)$ is an odd function known as the *co-spectrum* and $q(\omega)$ is an even function known as the *quadrature spectrum*. Both functions are subject to the *coherence-inequality*:

$$c^2(\omega) + q^2\omega \leq f_x(\omega) f_y(\omega).$$

When $\{X_t\}$ and $\{Y_t\}$ are both real, stationary processes, we can use the Cramér's representation:

$$X_t = \int_0^{\pi} \cos(t\omega) du_x(\omega) + \int_0^{\pi} \sin(t\omega) dv_x(\omega)$$

and

$$Y_t = \int_0^{\pi} \cos(t\omega) du_y(\omega) + \int_0^{\pi} \sin(t\omega) dv_y(\omega).$$

It is possible to interpret the co-spectrum and the quadrature spectrum in a way that each of the processes $\{X_t\}$ and $\{Y_t\}$ can be represented by an integral over all frequencies ω in $[0, \pi]$ and that each frequency ω can be decomposed into two separate components that are $\frac{\pi}{2}$ out of phase with each other. Each of the components having a random amplitude $du_x(\omega)$, $dv_x(\omega)$ and $du_y(\omega)$, $dv_y(\omega)$ and for each process, the amplitudes are uncorrelated both between the components for any frequency as well as with the random amplitudes of the components for other frequencies. This means that we are interested only in the relationships between identical frequencies in both processes, i.e. between:

$$\cos(t\omega)du_x(\omega) + \sin(t\omega)dv_x(\omega)$$

and

$$\cos(t\omega)du_y(\omega) + \sin(t\omega)dv_y(\omega).$$

Moreover, the following relationships hold:

$$\mathbb{E}(du_x(\omega)du_y(\omega)) = \mathbb{E}(dv_x(\omega)dv_y(\omega)) = 2c(\omega)d\omega,$$

meaning that twice the co-spectral density gives the covariance between the in-phase components. And furthermore, we have:

$$\begin{aligned}\mathbb{E}(du_x(\omega)dv_y(\omega)) &= 2q(\omega)d\omega \\ \mathbb{E}(du_y(\omega)dv_x(\omega)) &= -2q(\omega)d\omega,\end{aligned}$$

meaning that twice the quadrature spectral density gives the covariance between the components $\frac{\pi}{2}$ out of phase.

Finally, we will introduce crucial quantities allowing us to analyse relationship between corresponding components of two stationary processes. *Coherence at* ω, $C(\omega)$ provides us with a measure of correlation between the corresponding frequency components of two processes:

$$C(\omega) = \frac{c^2(\omega) + q^2(\omega)}{f_x(\omega)f_y(\omega)} \in [0, 1]$$

and its plot against the frequency $\omega \in [0, \pi]$ is called the *coherence diagram*. Coherence is in fact analogous in both definition and interpretation to the square of the correlation coefficient between two samples.

A measure of phase difference between the corresponding frequency com-

ponents of two processes is given by

$$\psi(\omega) = \tan^{-1} \frac{q(\omega)}{c(\omega)}$$

and its plot against the frequency $\omega \in (0, \pi)$ is called the *phase diagram*.

3.6 Quantile Cross-Spectral Analysis

The classical cross-spectral analysis introduced quantities like coherence that allow us to analyse the joint-distribution of two processes in frequency domain. But like covariance-based measures, coherency is quantifying dependence by averaging with respect to the joint distribution of the two processes. The process of averaging leads to a potential loss of information that is contained in specific parts of the joint distribution. Since the information within the tails of distributions of economic time series is often of a special interest, a new class of cross-spectral densities that characterises the dependence in quantiles of joint-distribution of processes across frequencies was proposed by Baruník & Kley (2015) whose text we will follow to introduce the concept.

Let us consider a d-variate, strictly stationary process $(\mathbf{X}_t)_{t\in\mathbb{Z}}$ with components $X_{t,j}, j = 1, \ldots, d$, a marginal distribution function of $X_{t,j}$ denoted by F_j and $q_j(\tau) \coloneqq F_j^{-1}(\tau) \coloneqq \inf\{q \in \mathbb{R} : \tau \leq F_j(q)\}, \tau \in [0, 1]$ denotes the corresponding quantile function. The *matrix of quantile cross-covariance kernels* $\Gamma_k(\tau_1, \tau_2)$ represents a measure for the serial and cross-dependency structure of $(\mathbf{X}_t)_{t\in\mathbb{Z}}$:

$$\Gamma_k(\tau_1, \tau_2) \coloneqq \left(\gamma_k^{j_1,j_2}(\tau_1, \tau_2)\right)_{j_1,j_2=1,\ldots,d}$$

where

$$\gamma_k^{j_1,j_2}(\tau_1, \tau_2) \coloneqq \mathrm{Cov}\Big(\mathrm{I}\{X_{t+k,j_1} \leq q_{j_1}(\tau_1)\},\, \mathrm{I}\{X_{t,j_2} \leq q_{j_2}(\tau_2)\}\Big),$$

$j_1, j_2 \in \{1, \ldots, d\}, k \in \mathbb{Z}, \tau_1, \tau_2 \in [0, 1]$ and $\mathrm{I}(A)$ denotes the indicator function of the event A. Note that these functions are dependent on two quantiles τ_1, τ_2 which makes them richer in information than their traditional counterparts. Moving to the frequency domain, we obtain the *matrix of quantile cross-spectral density kernels* $\mathfrak{f}(\omega; \tau_1, \tau_2)$:

$$\mathfrak{f}(\omega; \tau_1, \tau_2) \coloneqq \left(\mathfrak{f}^{j_1,j_2}(\omega; \tau_1, \tau_2)\right)_{j_1,j_2=1,\ldots,d},$$

where

$$\mathfrak{f}^{j_1,j_2}(\omega;\tau_1,\tau_2) := (2\pi)^{-1}\sum_{k=-\infty}^{\infty}\gamma_k^{j_1,j_2}(\tau_1,\tau_2)\exp(ik\omega),$$

$j_1, j_2 \in \{1,\dots,d\}, \omega \in \mathbb{R}, \tau_1, \tau_2 \in [0,1]$.

For fixed values of τ_1, τ_2, the quantile cross-spectral density kernel $\mathfrak{f}(\omega)$ is exactly the classical cross-spectral density of the bivariate, binary process $\big(\mathrm{I}\{X_{t,j_1} \le q_{j_1}(\tau_1)\}, \mathrm{I}\{X_{t,j_2} \le q_{j_2}(\tau_2)\}\big)_{t\in\mathbb{Z}}$ which indicates whether the values of the components j_1 and j_2 of $(\mathbf{X}_t)_{t\in\mathbb{Z}}$ are below the respective marginal distribution's τ_1 and τ_2 quantile.

Following this setting, there exists a right continuous orthogonal increment process $\{Z_j^T(\omega) : -\pi \le \omega \le \pi\}$ for all $j \in \{1,\dots,d\}$ and $\tau \in [0,1]$, such that the following Cramér representation:

$$\mathrm{I}\{X_{t,j} \le q_j(\tau)\} = \int_{-\pi}^{\pi}\exp(it\omega)dZ_j^t(\omega)$$

and the following relation

$$\int_{\omega_1}^{\omega_2}\mathfrak{f}^{j_1,j_2}(\omega;\tau_1,\tau_2)d\omega = \mathrm{Cov}(Z_{j_1}^{\tau_1}(\omega_2) - Z_{j_1}^{\tau_1}(\omega_1), Z_{j_2}^{\tau_2}(\omega_2) - Z_{j_2}^{\tau_2}(\omega_1))$$

where $-\pi \le \omega_1 \le \omega_2 \le \pi$ hold.

Analogously to the classical spectral quantities, we can decompose the complex-valued quantity $\mathfrak{f}^{j_1,j_2}(\omega;\tau_1,\tau_2)$ into its real part called the *quantile co-spectrum* and its imaginary part called the *quantile quadrature spectrum*. Furthermore, we consider the correlation between $dZ_{j_1}^{\tau_1}(\omega)$ and $dZ_{j_2}^{\tau_2}(\omega)$:

$$\mathfrak{R}^{j_1,j_2}(\omega;\tau_1,\tau_2) := \mathrm{Corr}(dZ_{j_1}^{\tau_1}(\omega), dZ_{j_2}^{\tau_2}(\omega)) = \frac{\mathfrak{f}^{j_1,j_2}(\omega;\tau_1,\tau_2)}{\big(\mathfrak{f}^{j_1,j_1}(\omega;\tau_1,\tau_1)\mathfrak{f}^{j_2,j_2}(\omega;\tau_2,\tau_2)\big)^{\frac{1}{2}}},$$

$(\tau_1,\tau_2) \in (0,1)^2$ termed the *quantile coherency*, with values $\mathfrak{R}^{j_1,j_2}(\omega;\tau_1,\tau_2) \in \{z \in \mathbb{C} : |z| \le 1\}$.

3.7 Interest Rate Futures

Futures contracts are legal agreements between two parties about a delivery of an underlying asset at certain pre-specified time in the future for a pre-specified price fixed at the time of the contract's inception (Kolb & Overdahl 2003). Financial futures are standardised contracts traded at centralised finan-

cial exchanges that allow for a wide range of financial instruments or indices to serve as its underlying assets. Futures contracts are usually very liquid, partly as a result of contract standardisation which allows market participants to safely trade otherwise illiquid assets. Moreover, the party who holds a short position is not obliged to physically deliver the underlying asset as the contract can be sold any time before it's maturity (Filipovic 2009).

One distinct feature of futures contracts is that the holder of the contract continuously pays or receives payments that result from an immediate depreciation or appreciation of the contract's value. This mechanism is called the *marking to market*. Each party is obliged to maintain a certain minimum balance on their account called *safety margin* to mitigate the possibility of a default on obligations.

Futures that use debt instruments like US Treasury Bills and US Treasury Bonds as an underlying asset are called *interest rate futures*. A specification of such contract either permits cash settlement or requires a certain class of debt instrument to be delivered at the contract's maturity. Because interest rate futures usually specify a broad range of contracts deliverable upon maturity, a *conversion factor invoicing system* is employed to make deliverable contract prices comparable. The conversion factor is computed so that the principle invoice amount paid from long to short is adjusted to reflect a reference yield-to-maturity.

There are two trading regimes associated with financial futures. When trading through *open outcry*, the traders are physically present in the "trading pit" where they "cry out" their bids. This auction-like process mitigates inefficiency and information asymmetry between the traders. The opening hours for physical futures exchanges are usually limited to several hours every weekday.

In the recent years, the trading pits have been mostly replaced by electronic trading systems which offer nearly 24-hour opening hours and greatly reduced transaction costs as opposed to the physical trading. Since each electronic trade is processed through a centralised trading system, the electronic trading systems offer a great opportunity for collection of high frequency tick-by-tick trading data with very granular time measurements.

Chapter 4

Data and Methodology

This chapter describes the raw dataset, discusses transformations made to the data in order to obtain a dataset suitable for estimation and comments on the methodology behind computational steps. An overview of the most important features of the estimated term structure of interest rates futures is presented and compared to five stylised facts about term structures of interest rates in the time domain.

Following sections focus on the estimation methodology and results. The explanation of employed theoretical concepts can be found in Chapter 3.

4.1 US Treasury Futures Data

The dataset used for construction of the term structure consist of four distinct high frequency tick-by-tick time series of interest rate futures trade data. The underlying contracts are US Treasury Notes and US Treasury Bonds with times to maturity ranging from 1 year and 9 months to 25 years.

All the recorded transactions were traded at the Chicago Mercantile Exchange and Chicago Board of Trade (CBOT/CME Group) futures exchange. The trading hours for the listed futures have been evolving over the time, starting with limited hours during weekdays to a nearly non-stop operation of electronic trading platform Globex. The covered futures contracts are traded quarterly with settlement dates in March, June, September and December. For more details about interest rate futures contracts traded at CBOT/CME see Johnson *et al.* (2017).

A wide range of underlying US Treasury bond contracts are eligible for delivery upon settlement. In order to make all eligible contracts directly com-

parable, CBOT/CME Group uses a conversion factor invoicing system. The invoice price IP at the settlement is calculated in the following way:

$$IP = P \times CF \times CtF + AI.$$

The daily futures settlement price P is the price of the futures contract at the settlement date expressed in points and fractions of points with a par on the basis of 100 points. CF is the conversion factor; that is the price at which a \$1 par of an underlying security would trade if it had a 6% yield-to-maturity. The conversion factor thus takes into account different coupons and remaining time to maturity of the wide range of Treasuries eligible for delivery. The CtF is the contract factor, in this case a 1/100 fraction of the underlying's face value at maturity. Finally, the seller of the contract is compensated for the interest accrued between the semi-annual coupon payment dates AI.

The parameters of each of the futures contract included in the dataset are described below.

Short-Term US Treasury Note Futures (2-Year) The deliverable securities are fixed-principal US Treasury Notes with fixed semi-annual coupon payments and the original term to maturity shorter than five years and three months (CBOT/CME Group 2018d). The remaining time to maturity of a delivered contract must be longer than one year and nine months from the first day of the delivery month and shorter than two years from the last day of the delivery month. The trading unit is represented by a multiple of US Treasury Notes with a \$200,000 face value at maturity. The minimum price fluctuation is 1/4th of 1/32nd of one point, that is \$15.625 per contract. This futures contract is traded under ticker symbol TU (Bloomberg) or ZT (Globex).

Medium-Term US Treasury Note Futures (5-Year) The deliverable securities are fixed-principal US Treasury Notes with fixed semi-annual coupon payments and the original term to maturity shorter than five years and three months (CBOT/CME Group 2018c). The remaining time to maturity of a delivered contract must be longer than four years and two months from the first day of the delivery. The trading unit is represented by a multiple of US Treasury Notes with a \$100,000 face value at maturity. The minimum price fluctuation is 1/4th of 1/32nd of one point, that is \$7.8125 per contract. This futures contract is traded under ticker symbol FV (Bloomberg) or ZF (Globex).

Long-Term US Treasury Futures (6 and half to 10-Year) The deliverable securities are fixed-principal US Treasury Notes with fixed semi-annual coupon payments and the original term to maturity shorter than 10 years (CBOT/CME Group 2018b). The remaining time to maturity of a delivered contract must be longer than six years and six months from the first day of the delivery. The trading unit is represented by a multiple of US Treasury Notes with a $100,000 face value at maturity. The minimum price fluctuation is 1/2 of 1/32nd of one point, that is $15.625 per contract. This futures contract is traded under ticker symbol TY (Bloomberg) or ZN (Globex).

US Treasury Bond Futures The deliverable securities are both callable and non-callable fixed-principal US Treasury Bonds with fixed semi-annual coupon payments. For non-callable contracts, the remaining time to maturity of must be longer than 15 years and shorter than 25 years. The deliverable callable contracts must not be callable for at least 15 years and have remaining time to maturity less than 25 years (CBOT/CME Group 2018a). The trading unit is represented by a multiple of US Treasury Bonds with a $100,000 face value at maturity. The minimum price fluctuation is 1/32nd of one point, that is $31.25 per contract. This futures contract is traded under ticker symbol US (Bloomberg) or ZB (Globex).

4.2 Data Transformations

This section provides detail on all steps of data transformation process that resulted with the dataset used for subsequent computations[1].

4.2.1 Synchronisation and Subsetting

The raw dataset consists of four tick-by-tick trade data time series of closing prices with precise timestamps. To be able to perform most of the analysis, equidistant observations synchronised across all time series were required. The previous-tick synchronisation scheme was chosen as it represents the most common approach among the practitioners. In our case, all time series were syn-

[1]All data transformations and computations were done using Python programming language. Spectral and Cross-spectral estimates were obtained using R programming language. Quantile Cross-Spectral Coherency estimates were computed using quantspec package for R (Kley 2016). All data visualisations are original and were created using ggplot2 package for R (Wickham 2016). All source codes are publicly available at `https://github.com/nedvedad/mastersthesis`.

chronised at 5-minute intervals in order to be able to obtain 5-minute realised variance estimates in subsequent steps.

Variability in trading regimes posed another issue. Trading hours for open outcry regime have changed several times within the observed period while the introduction of Globex platform resulted in nearly non-stop electronic trading. The dataset combines data from both open outcry and Globex regimes. Only observations on the intersection of all observed trading regimes were considered to maintain a constistent dataset. As a result, all trades concluded outside weekdays between 07:20 and 14:00 Central Time were discarded. Similarly, US federal holidays and dates where at least one of the time series had no recorded observation were excluded.

Finally, beginning with March 2000 contracts, the board of directors of CBOT has decided to lower the nominal coupon used in the construction of conversion factors from 8% to 6% for all Treasury futures. This change resulted in a substantial shift of futures prices and dynamics around the November 1999 period. As a consequence, only a subset of observations recorded after January 1, 2000 were kept in the final dataset to mitigate estimation errors resulting from possible inconsistencies in the data.

4.2.2 Yield to Maturity

Closing prices were used to compute yields to maturity using the following formula:

$$y_t(m) = \sqrt[m]{\frac{FV}{P_t \times CF \times CtF}} - 1,$$

where m is the contract's maturity in years, FV is the face value, P_t is the closing price observed at time t, CF is the conversion factor and CtF is the contract factor. Since the properties of relevant cheapest-to-deliver contracts are unknown, the following assumptions were made to compute the yields. Firstly, the maturities were assumed to be 2, 5, 10 and 25 years for the respective futures contracts. Secondly, the conversion factors were obtained using the published lookup tables (CBOT/CME Group 2018e) assuming zero coupon in each case.

4.2.3 Dynamic Nelson-Siegel Model Estimation

The entire term structure was estimated from the four time series of yields using the Dynamic Nelson-Siegel Model. For each observation at time t, the

Nelson-Sigel parameters were obtained via ordinary least squares estimation of the following equation:

$$\begin{bmatrix} y_t(2) \\ y_t(5) \\ y_t(10) \\ y_t(25) \end{bmatrix} = \begin{bmatrix} 1 & \frac{1-\exp(-2\lambda)}{2\lambda} & \frac{1-\exp(-2\lambda)}{2\lambda} - \exp(-2\lambda) \\ 1 & \frac{1-\exp(-5\lambda)}{5\lambda} & \frac{1-\exp(-5\lambda)}{5\lambda} - \exp(-5\lambda) \\ 1 & \frac{1-\exp(-10\lambda)}{10\lambda} & \frac{1-\exp(-10\lambda)}{10\lambda} - \exp(-10\lambda) \\ 1 & \frac{1-\exp(-25\lambda)}{25\lambda} & \frac{1-\exp(-25\lambda)}{25\lambda} - \exp(-25\lambda) \end{bmatrix} \begin{bmatrix} \beta_{0t} \\ \beta_{1t} \\ \beta_{2t} \end{bmatrix} + \begin{bmatrix} \epsilon_t(2) \\ \epsilon_t(5) \\ \epsilon_t(10) \\ \epsilon_t(25) \end{bmatrix}.$$

Exponential Decay Parameter Lambda The original Dynamic Nelson-Siegel Model allows for time-varying decay parameter λ_t. However, the improvement to goodness of fit allowed by time-varying λ_t parameter have been questioned (Hautsch & Ou 2008). Moreover, given that only four points along the yield curve are observed for each point in time, the increase in goodness of fit resulting from the estimation of dynamic λ_t would likely come at expense of instability and possibility of overfitting of the curve. For these reasons, a constant lambda was used as in the original estimation of the dynamic model by Diebold & Li (2006).

The choice of lambda is extremely important for the resulting fit. Apart from governing the exponential decay of the yield curve, the λ parameter determines where the model's curvature term attains its maximum. In Diebold & Li (2006), the authors set lambda constant at 0.7173[2] which is the value that maximises curvature term at 2 years and 6 months.

In order to determine the lambda value to be used for estimation of the yield curve, lambdas $\bar{\lambda_i}$ maximising the curvature term for maturities τ_i between 1 and 10 years with steps of 1 month were calculated, following:

$$\bar{\lambda_i} = \arg\max_{\lambda \in \Theta} \left(\frac{1-\exp(-\lambda\tau_i)}{\lambda\tau_i} - \exp(-\lambda\tau_i)\right), \quad \tau_i = \frac{12}{12}, \frac{13}{12}, \ldots, \frac{120}{12}.$$

Using each $\bar{\lambda_i}$, the Dynamic Nelson-Siegel model was fitted and mean squared error MSE_i was computed:

$$MSE_i = \frac{1}{n}\sum_{j=1}^{n}(Y_j - \hat{Y}_{i,j})^2,$$

[2]The value presented in the article is in fact 0.0609 which corresponds to maturities denoted in months as opposed to yearly maturities used in this thesis.

where n is the number of observations in the dataset, Y_j is an observed value and $\hat{Y}_{i,j}$ is a predicted value using $\bar{\lambda}_i$. Finally, the lowest MSE_i was achieved with lambda value of 0.6329 which maximises the curvature term at 2 years and 10 months, a value reasonably close to the one used in Diebold & Li (2006). Loadings of each of the Nelson-Siegel factors with respect to time to maturity are plotted in Figure A.1. Apart from showing the maximum of the curvature factor loading, it is interesting to note that the slope factor loading is dominating the curvature factor in short and medium-term maturities of up to 10 years.

4.2.4 Realised Variance

In order to mitigate the amount of microstructure noise in high-frequency datasets, intraday observations are usually integrated into daily measurements for financial analysis. The "daily last observation" approach was used to obtain daily data on yields, closing prices and beta coefficients from the Dynamic Nelson Siegel Model. Next, 5-minute realised variance of yields and beta coefficients were computed. Many high-frequency volatility estimators have been proposed over recent years, but 5-minute RV has gained the most recognition by practitioners. This is demonstrated in a study by Liu *et al.* (2015) where 400 different estimators were compared using 31 different financial asset time series including interest rates. The authors have concluded that the 5-minute RV is very difficult to beat in practice.

4.3 Resulting Dataset

After carrying all transformations described above, the resulting dataset consists of 3,775 daily observations of closing prices, yields, Dynamic Nelson-Siegel Model factors and realised variances. Period covered in the dataset spans from January 4th, 2000 to March 9th, 2015. This allows estimation of cycles two years long as the rule of thumb proposed by Granger & Hatanaka (1964) requires us to have at least seven observations of a cycle for reasonably precise estimation. The evolution of the number of intraday observations for each time series is plotted in Figure A.2. The increasing number of recorded transactions is apparent with the upward trend being attributed to increasing popularity of electronic trading platforms such as the Globex.

4.3.1 Yields and Closing Prices

The daily closing prices of each series are plotted in Figure A.3 and presented along with summary statistics in Table B.1. A tendency of variance of closing prices to increase as term to maturity increases can be clearly documented. The opposite holds for the computed yields which are plotted in Figure A.4: the volatility of yields decreases with increasing time to maturity while the overall level of yields increases with increasing time to maturity. This is supported by the summary statistics disclosed in Table B.2.

4.3.2 Nelson-Siegel Factors and Goodness of Fit

Estimated Dynamic Nelson-Siegel factors are plotted in Figure A.5. The level factor is consistently the largest and the most stable factor over the entire period. The slope factor is more volatile than level factor but still relatively stable with mostly slightly negative values. Curvature is the most unstable of all factors with especially volatile period coinciding with the financial crisis. This means that most of the yield curve dynamics can be captured by the changes to curve's curvature while the level of the yield remains mostly constant. Large shifts to yield curve's slope are not as common as shifts to curvature but in both cases these shifts are persistent.

The goodness of fit of the Dynamic Nelson-Siegel Model can be assessed from the residual plot for each series in Figure A.6 where the period of financial crisis causes an apparent shift in the estimated interest rate dynamics. The estimated yield curve fits the observed series quite well as shown in Figure A.7 where the fitted yield curve is plotted against the observed yields for a selection of sixteen different dates from the dataset. At times, there are occurrences of somewhat unrealistically U-shaped short ends of the estimated yield curves visible at maturities between 0 and 2 years. This anomaly stems from the fact that there are only 4 observations along the curve for each day and maturity of 2 years is the shortest available one. However the missing data on the short end of the yield curve should not significantly affect the estimation at longer maturities.

4.3.3 Realised Variance

Realised variance of all four yield is plotted in Figure A.8. Three findings are apparent from the plot. Firstly, the overall level of yields' volatility decreases

with increasing time to maturity. Secondly, the realised variance of each series has significantly increased around the beginning of financial crisis. And lastly, the pre-crisis period was more volatile for all four time series than the post-crisis period.

4.4 Stylised Facts About Term Structure

Term structure of interest rate has been a central topic of economic research for several decades. Numerous empirical studies were concluded and as a consequence, several recurring empirical properties of term structures were termed as "stylised facts". We will consider whether the term structure constructed from interest rate futures data confronts to these stylised facts before committing to the spectral analysis.

The following five observations about shape, volatility and dynamics of yield curves were originally summarised in Diebold & Li (2006).

Average Shape The average yield curve shape should be concave and increasing. The plot of the estimated term structure for each date included in the dataset is presented in Figure A.9 along with mean and median term structure. Even though individual yield curves take various shapes, most of them are indeed concave and increasing. The estimated average and median yield curve shapes are too concave and increasing.

Variety of Shapes Yield curves assume several different shapes over time. There are four most commonly observed types: upward-sloping, downward sloping, humped and inverted humped. The evolution of the estimated yield curve over the observed period is plotted in Figure A.10. We can see that even though the average shape is upward and concave, there are periods of negatively sloped curves and periods of flat curves. These observations can also be seen in the "cuts" of the term structure as shown in Figure A.7. A hump shape is sometimes present in the short end of the yield curve but this is to be attributed to the lack of observations with maturities shorter than 2 years as discussed in Section 4.3.2.

Yield and Spread Dynamics Dynamics of yields should be persistent and dynamics of spread should be significantly less persistent. Diebold & Li (2006) link strong persistence of yield dynamics to strong persistence of the model's

level factor. Similarly, weak persistence of spread dynamics should be linked to weak persistence of the model's slope factor. All factors are plotted in Figure A.5 where persistence in factors is evident. Supplementary Augmented Dickey-Fuller test in Table B.3 fails to reject unit-root for all factor series even at 10% significance level. Looking at autocorrelation functions of the series of factors in Figure A.11 however shows no significant difference between persistence in slope and level factors.

Volatility of Short and Long Ends The short end of the term structure is documented to be more volatile than its long end. This is easily observable from the plot of realised variances of yields in Figure A.8 where the volatility clearly decreases with increasing term to maturity. The Dynamic Nelson Siegel Model factor loadings in Figure A.1 reveal that the long end of the yield curve is predominantly governed by the level factor. If we consider the realised variance of model factors in Figure A.12, it is clear that the level factor is the least volatile one and thus the long end is less volatile than the short end as well.

Persistence of Short and Long Rates Long rates are expected to be more persistent than short rates. Using argument from the previous paragraph and looking at the autocorrelation functions of model factors in Figure A.11, the level factor seems to be the most persistent along with the slope factor which could hint at high persistence of long rates. The persistence of yield series A.4 is very high for each of the series and autocorrelation function shows to be inconclusive as each of the series contains a unit-root process.

Estimated yield curves have shown to have concave and upward-sloping shape on average while also attaining flat and downward sloping shapes during certain periods. Yields' volatility appears to be a decreasing function of time to maturity. Dynamics of yields are highly persistent, however so are the spread dynamics. Similarly, both short and long rates exhibit persistence of a very high degree.

Chapter 5

Spectral Analysis of Term Structure

Following sections present empirical findings obtained by application of multiple spectral analysis techniques to the term structure data. Firstly, power spectra of individual time series will be estimated and discussed. Then, the cross-dependence in frequency domain within different parts of term structure will be analysed using cross-spectral analysis. Finally, using the quantile cross-spectral analysis, we will carry out an in-depth analysis of dependence structures within the joint distributions of various parts of the term structure in frequency domain.

5.1 Spectral Analysis

Periodograms were used to obtain non-parametric estimates of spectral densities. Despite their convenience, periodograms are known to produce highly fluctuating spectral density estimates with large variances. Although periodograms are asymptotically unbiased, it can be shown that their variance does not converge to zero with increasing sample sizes. In another words, periodogram is not a consistent estimator of spectral density (Nerlove 1964). In order to obtain a consistent estimator, local averaging of raw periodograms using Daniell kernel was employed as proposed in Bloomfield (2004).

Yields Estimated power spectra of all yield series with 95% confidence intervals are presented in Figures A.13, A.14, A.15 and A.16. In all spectral plots, frequencies corresponding to periods of 1 week, 1 month and 1 year were

highlighted with dashed vertical lines. All spectra follow what Granger calls "a typical spectral shape of economic variable" with peaks around frequencies corresponding to one year, which also corresponds to empirical findings by Granger & Rees (1968). A typical spectrum of economic variable contains highly dominant low frequency components that can be a consequence of a trend in mean, unit-root, strong cyclic components with low frequencies or leakage of power around neighbouring frequencies. Power in such spectral densities steadily decreases as the frequency increases. The amount of variance explained by high frequency components generally decreases with increasing time to maturity, meaning that short rates are better explained by high-frequency cycles than long rates.

First-Differenced Yields Results of Dickey-Fuller test in Table B.4 hint at presence of unit root in three out of four series of yields. To deal with the problem of non-stationarity, which is especially crucial for estimation of quantile cross-spectral coherency in later sections, all series of yields were first-differenced. Their spectra are shown in Figures A.17, A.18, A.19 and A.20. As expected, the first-differencing has flattened the spectra of yields. This is due to the fact that first-differencing is equal to application of high-pass filter to a time series.

If the first-differenced yield series followed a random walk process, we'd see completely flat power spectra with equal contributions of each frequency to the spectral density. However, all four spectral density plots of yields show significant peaks at frequencies around 0.83. This finding suggests that there might be cyclical components in yields corresponding to 2.4 days (or roughly a half-week) long periods.

Spectograms of Yields Power spectra of non-stationary time series can also be represented by spectograms in order to deal with non-stationarity of time series. Firstly, the data are sliced into many overlapping windows of equal length, moving both the beginning and the end of each window by a single observation at a time. Spectral density is then estimated for each window and plotted in time-frequency domain. The advantage of this approach is that it allows us to observe the evolution of the spectral density series over time. Spectrograms for yield series are plotted in Figures A.21, A.22, A.23 and A.24. It is important to keep in mind that we need at least seven observations for each cycle to get a reasonable estimate of the power spectrum. The window

length of 125 observations that was used in construction of these spectograms thus allows us to analyse only frequencies that are large than 0.11.

It is clear from the figures that the spectra of yields are not constant in time. The period between 2005 and 2007 has relatively little variance explained by high frequencies in all series. Yields with 2-year maturity have the highest amount of variance explained by high frequencies together with the 5-year yield series. However, during the period between 2012 and 2013, we observe extremely low density estimates in high frequencies of the 2-year yield series. Peaks around the frequency 0.83 observed in previous plots are not apparent in the spectogram representations of yields.

Realised Variances of Yields Power spectra of realised variance of yield series (shown in Figure A.8) can be found in Figures A.25, A.26, A.27 and A.28. All series have mostly flat spectra with a large spike at frequencies corresponding to yearly cycles, indicating strong seasonal behaviour of volatility of the yields. Moreover, all spectra show significant peaks around weekly frequencies, suggesting a weekly cyclical movements in volatility of interest rate futures yields. There are few other supplemental peaks that present especially in the series with maturities of 2 and 5 years which are the most volatile series.

Dynamic Nelson-Siegel Factors Spectra of first-differenced series of Dynamic Nelson-Siegel Model factors from Figure A.5 are shown in Figures A.29, A.30 and A.31. We are not only using the convenience of dimension-reduction of the Nelson-Siegel model here but we are also taking advantage of the fact that the model factors are interpretable as level, slope and curvature of yield curve, allowing us to focus on different aspects of the term structure.

The low-frequency bands of spectra are apparently suppressed by the use of the first-differencing filter but there are signs of long-term cycles around frequencies corresponding to 4 months in each spectrum. Moreover, the spectrum of the level factor has a relatively low contribution of frequencies around 0.5. Cycles longer than a month have relatively little influence in all series.

Realised Variances of Dynamic Nelson-Siegel Factors If we look at realised variances of the factors in Figures A.32, A.33 and A.34, we find similar spectral shapes to those of realised variances of yields with significant yearly seasonal component and apparent peaks at frequencies corresponding to week-long cy-

cles, meaning that both realised variances of yields and of DNSM factors are possibly cyclical with weekly periods.

5.2 Cross-Spectral Analysis

Cross-spectral analysis allows us to measure the extent of interrelatedness between two time series and reveals information about their common lag structure. For the first part, coherence diagrams are used which, as mentioned in Section 3.5.2, essentially translate to correlation coefficients between corresponding frequencies of time series. For the second part, phase diagrams are used to analyse possible phase shifts between the two series.

The interpretation of phase diagrams is much more peculiar. As Granger & Hatanaka (1964) put it, we are looking for parts of the phase diagram where the values "lie about a straight line". If, at the same time, the coherence between the two series is "reasonably high" within the frequency range where phase lies about a straight line, then this can indicate a simple time-lag between corresponding frequency components of the two series. The degree of the time-lag is indicated by the slope of the straight line, about which the phase values lie.

Yields Firstly, the average coherence was computed over three distinct frequency ranges for series of first-differenced yields following the analysis in Granger & Rees (1968). The long-run range is defined as frequencies corresponding to periods of over three years. The medium-run spans from one year to three years and the short-run corresponds to periods between six months and one year. All estimates are displayed in Table B.5.

Granger and Rees found that, generally, as the frequency increased the coherency between components decreased. Contrary to this result, we find that coherency remains relatively stable across frequency ranges using our dataset. The degree of dependence between series is decreasing with increasing time to maturity. The highest degree of dependence was found between 5Y and 10Y first-differenced yields series, which can be seen in detail in Figure A.35. The coherency is relatively stable across all frequencies while phase is consistently close to zero. The lowest average coherency is between 2Y and 25Y series, which can be seen in Figure A.36. The coherency diagram is much more erratic between 2-years and 25-years maturities. Moreover, we observe small peaks in

phase around 1 week and 1 month periods in all yields cross-spectra, hinting at possible lag structure between yield series for the respective periods.

Realised Variances of Yields The cross-spectra of realised variances of yields are generally flat with dependence between series being uniformly distributed across the entire frequency domain. Squared coherencies between all pairs of series of realised variances of yields are plotted in Figure A.37. The degree of dependence between realised variances of yields increases with decreasing time to maturity with the highest values at the long-term part of the term structure. Phase for all combinations of realised variances of yields is close to zero, revealing no significant lag structure between any pair of series over any frequency range.

Dynamic Nelson-Siegel Factors Squared coherencies between pairs of Dynamic Nelson-Siegel Model factors are plotted in Figure A.38. The dependence between level and slope factor seems to be higher between frequencies corresponding to 1 week and 1 year while dependence between level and curvature is low across the whole spectrum with possible peak around frequencies corresponding to 3 days. Dependence between slope and curvature factor is much higher and is increasing with increasing frequency. No significant lag structure has been found between the factor estimates of the Dynamic Nelson-Siegel Model.

Realised Variances of Dynamic Nelson-Siegel Factors The cross-spectral plots of realised variances between Dynamic Nelson-Siegel Model factors are displayed in Figures A.39, A.40 and A.41. The dependence structure between volatility of term structure slope and curvature factors is generally very high and uniformly distributed across the entire frequency domain. However, dependences between volatilities of level and slope factors and between volatilities level and curvature factors share both positive and negative peaks. Squared coherency is significantly lower for these series for frequencies between 1 week and 1 year range. Moreover, realised volatilities between level and slope and between level and curvature of the term structure are seemingly positively connected in 1-week long cycles. Finally, we document peaks in squared coherency around half-week long cycles between these series. This frequency corresponds to a frequency at which yield series showed significant cyclical components as

documented in Section 5.1. No significant lag structure was found between realised variances of DNSM factors.

Dynamic Nelson-Siegel Factors and Yields Finally, Figure A.42 presents squared coherencies between series of first-differenced DNSM factors and first-differenced yields of interest rate futures. This series of plots reveals, how are yields with different maturities connected with level, slope and curvature factors of the term structure across the frequency domain. The level factor has flat dependence structure with all yield series where the overall dependence level increases with increasing time to maturity of yield series. All series show spikes around half-week long cycles. The dependence between slope factor and first-differenced yields seem to be low, erratic and flat with several significant spikes. Given the highly erratic dependence structure, the spikes are expected to be a consequence of imperfect smoothing rather than evidence of several highly contributing frequencies. The curvature factor is most highly connected with all series of first-differenced yields. The dependence structure with the 2 years short-rate is highest for long cycles and steadily decreases with increasing frequency. The dependence with both 5 and 10 year yields is relatively higher with similar decreasing profile. Squared coherence between first-differences of curvature factor and 25 year yields is flat and just below 0.5 level. All pairs including the first-differenced curvature factor seem to be highly connected in the high frequency range. Phase diagrams show no significant lag structure any of the aforementioned pairs of time series.

5.3 Quantile Cross-Spectral Analysis

Spectral analysis allowed us to project the variance of parts of term structure onto frequency domain and analyse contribution of cycles of various lengths to their overall variance. Move to the cross-spectral analysis made it possible to analyse the degree of connectedness of pairs of times series in frequency domain. In another words, we could see how are cycles of different frequencies on average connected with each other across different parts of the term structure.

Using the quantile cross-spectral analysis described in Section 3.6 gets us one step further. The average degree of connectedness between cycles of time series expressed by squared coherency will further be decomposed across quantiles of the joint distribution. The degree of connectedness between quantiles

of various parts of the term structure will be presented by means of squared quantile coherency in frequency domain.

Yields Squared quantile cross-spectral coherency between yields with two years maturity and the remaining yield series across five different quantile levels is plotted in Figure A.43. Values of τ_1 on the vertical axis give us the quantile of the marginal distribution of the two-years series while values of τ_2 on the horizontal axis give us quantiles of the marginal distributions of complementary series that together with two-years series constitute a pair for which the quantile coherency is computed.

There are a couple of findings standing out. Firstly, the dependence structure between yields is not uniform across the joint distribution, which is impossible to reveal using ordinary coherency measures. Secondly, most of the dependency between yield series occurs at the main diagonal, that is in the parts of the joint distribution where $\tau_1 = \tau_2$. Nevertheless, there are also spikes in quantile coherency in other parts of the joint distribution, for example around frequency 0.6 for $\tau_1 = 0.5, \tau_2 = 0.95$. Thirdly, the dependence in low frequencies often occurs at tails of the joint distribution of the series. Notably, between two-year and five-year series we can see for $\tau_1 = 0.95, \tau_2 = 0.05$ that the dependence in frequencies between 1 month and 1 year is relatively high despite the two series being otherwise independent in this particular part of the joint distribution.

We find similar results looking at quantile coherency plots of the first-differenced series of yields with 25 years maturity in Figure A.44. Notice, that the degree of dependence, as measured by the squared quantile coherency, is expectedly increasing with a decreasing distance between respective maturities of the analysed yields. However, the offset is not constant. For example looking at the tail of joint distribution where $\tau_1 = \tau_2 = 0.05$, we see a clear spike in quantile coherency between 25Y series and 10Y series, suggesting that the dependence is strong in weekly cycles at the tail of the joint distribution of these two series. The quantile coherency for the other two series show no significant increase within this frequency range.

Realised Variances of Yields Dependence between realised variances of yields of interest rate futures was already analysed in Section 5.2. Using classical coherency measures, the results were mostly flat plots with varying degree of overall dependence and its volatility. To analyse the relationships between

volatility of yields within the term structure in more detail, we plot the quantile coherency for all combinations of realised volatility series in Figures A.45, A.46, A.47 and A.48.

Analysis of the degree of dependence within volatilities of different parts of the term structure in various parts of the joint distribution reveals considerably more detail. Similarly to the case of first-differenced yields, we observe that all series are most significantly connected at main diagonals where $\tau_1 = \tau_2$, except for the low-frequency range between 1 month and 1 year, for which the series are connected across almost all parts of their joint distribution. In most cases, we observe higher quantile coherency for weekly frequencies in different parts of the joint distribution, mainly but not exclusively where $\tau_1 = \tau_2$. We also observe several supplementary peaks in quantile coherency. For example in Figure A.46 for $\tau_1 = \tau_2 = 0.25$, the coherency is a notably stronger for half-week cycles. In the same figure, there are also apparent peaks in coherency for frequency 0.6 between volatility of 5-year and 10-year yields at the tail of the joint distribution where $\tau_1 = \tau_2 = 0.05$.

Dynamic Nelson-Siegel Factors Quantile coherency plots for first-differenced series of Dynamic Nelson-Siegel Model factors are available in Figures A.49, A.50 and A.51. The level factor is generally the least connected one with all other factors while the slope and curvature factors share more complex dependence structure. Figure A.51 shows that slope and curvature of the term structure are more connected for those parts of their joint distribution where $\tau_1 = 1-\tau_2$, ie.: on the diagonal with "opposite quantiles" of respective marginal distributions. Moreover, for the first-differenced slope and curvature factors, there are multiple peaks of quantile coherency in different parts of the frequency range and joint distribution. For example looking at the parts where $\tau_1 = 0.75, \tau_2 = 0.5$ or $\tau_1 = 0.75, \tau_2 = 0.25$, we document a peak of quantile coherency for frequencies around 0.75. While looking at the tail of the joint distribution, where $\tau_1 = 0.05, \tau_2 = 0.95$, we see an increase of quantile coherency at the very end of the high-frequency range. Clearly, quantile cross-spectral analysis reveals more detail about the general dependence structure than ordinary cross-spectral measures.

Realised Variances of Dynamic Nelson-Siegel Factors Degree of connectedness across frequencies between volatility of level, slope and curvature of the terms structure is shown in Figures A.52, A.53 and A.54. Generally, the

volatility of term structure factors is highest on the diagonal where $\tau_1 = \tau_2$ with especially strong week-long cycles appearing at various parts of the joint distribution of all analysed pairs of time series.

Dynamic Nelson-Siegel Factors and Yields Finally, quantile coherency between first-differenced DNSM factors and first-differenced series of yields was computed with results available in Figures A.55, A.56 and A.57. The dependence between the level of the term structure and individual yields and between the curvature of the term structure and individual yields are the strongest with highest coherency appearing on the diagonal where $\tau_1 = \tau_2$. The slope factor, on the other hand shows very little coherency overall with highest value on the opposite diagonal where $\tau_1 = 1 - \tau_2$. Most of the cross-spectra are flat, with signs of positive peaks in the tails of the joint distribution.

Chapter 6

Conclusion

Term structures are among the most attractive topics in economic research. They do not merely reveal market participants' valuation of money in time, but they also share a deep connection with monetary policy and risk management. For these reasons, decades of research have been dedicated to the understanding of drivers and dependencies within term structures. The most important directions and approaches to term structure modelling were summarised in Section 3.2.

Advances in computing technology allow us to obtain, store and analyse huge amount of data recorded with ever-increasing precision. A novelty dataset of tick-by-tick trade data recorded at an interest rate futures exchange provided us with an opportunity to construct a high-frequency term structure dataset with an unprecedented amount of information and detail. Theory behind usage of tick-by-tick high-frequency data was introduced in Section 3.4, overview of interest rate futures and construction of term structures was covered in Sections 3.1, 3.2 and 3.7. Finally, the entire Chapter 4 was dedicated to the process of construction of the dataset suitable for subsequent analyses.

While not entirely new, the (cross-)spectral analysis is not nearly as popular approach as the classical time-domain analysis of economic time series. This also applies to empirical term structure literature, despite the advantages that analysis of time series in frequency domain brings. We find the spectral decomposition especially suitable for term structures as their complex dynamics is susceptible to cyclical behaviour. The methods of spectral analysis were introduced in Section 3.5.

General dependence structure within term structures are quite complex as there are multiple exogenous and endogenous factors affecting its dynamics.

Quantile cross-spectral analysis was employed in order to analyse information hidden in the various parts of the joint distribution of the term structure in frequency domain, revealing remarkable degree of insight about the dynamics within the term structure. Moreover, combination of large and information-rich high-frequency dataset and the robust and non-parametric estimation technique presented a great opportunity to study the term structure with unprecedented detail.

The results of the analysis of high-frequency term structure in frequency domain were presented in Chapter 5. Firstly, the univariate analyses of power spectra were carried out, introducing spectral density of various parts of the term structure and revealing cycles in yields and weekly cyclical behaviour of volatility. Secondly, dependence structures within the term structure were analysed using classical cross-spectral coherency measures, uncovering more detail about how are different parts and aspects of the term structure connected in the frequency domain. Finally, the quantile cross-spectral analysis was employed, revealing details of the dependence structure in quantiles of the joint distribution of different parts of term structure.

We found that the dependence structure significantly varies across different parts of the joint distribution. In some cases, we found stronger dependency in tails of joint distributions, in other cases we documented dependency across completely different quantiles of marginal distributions and in most cases, we found large discrepancies between connectedness of high-frequency and low-frequency components of the term structure. Most of these findings are supported by empirical literature about financial time series but would be impossible to reveal using classical cross-spectral analysis.

We believe that the aforementioned findings have important implications not only for the understanding of the dynamics of the term structure itself, but also for fields like risk management and monetary policy that often rely on various assumptions regarding the joint distribution of the term structure. Since term structure has been found to be highly connected with real economic activity, we believe that using quantile cross-spectral analysis to study the dependence between the term structure and indicators of economic activity like GDP or stock indices across quantiles of their joint distribution is the logical next step in the frequency-domain analysis of term structures. We also believe that using this approach could bring new valuable insights applicable in both research and practice.

Bibliography

Ait-Sahalia, Y. (1996): "Testing Continuous-Time Models of the Spot Interest Rate." *Review of Financial studies* **9(2)**: pp. 385–426.

Aït-Sahalia, Y., J. Fan, & D. Xiu (2010): "High-Frequency Covariance Estimates With Noisy and Asynchronous Financial Data." *Journal of the American Statistical Association* **105(492)**: pp. 1504–1517.

Andersen, T. G., T. Bollerslev, F. X. Diebold, & P. Labys (2003): "Modeling and Forecasting Realized Volatility." *Econometrica* **71**: pp. 529–626.

Assenmacher-Wesche, K. & S. Gerlach (2008): "The Term Structure of Interest Rates Across Frequencies." *ECB Working Paper* **976**.

Bank for International Settlements (2005): "Zero-coupon yield curves : technical documentation." *Technical Report 25*, Bank for International Settlements, Basel, Switzerland.

Barber, J. R. & M. L. Copper (2012): "Principal component analysis of yield curve movements." *Journal of Economics and Finance* **36(3)**: pp. 750–765.

Barndorff-Nielsen, O. E., P. R. Hansen, A. Lunde, & N. Shephard (2011): "Multivariate realised kernels: Consistent positive semi-definite estimators of the covariation of equity prices with noise and non-synchronous trading." *Journal of Econometrics* **162(2)**: pp. 149–169.

Baruník, J. & T. Kley (2015): "Quantile Cross-Spectral Measures of Dependence between Economic Variables." *Unpublished* .

Bessembinder, H., J. F. Coughenour, & P. J. Seguin (1995): "Mean Reversion in Equilibrium Asset Prices : Evidence from the Futures Term Structure." *The Journal of Finance* **50(1)**: pp. 361–375.

Bjork, T. (2009): "An Overview of Interest Rate Theory." *Handbook of Financial Time Series* pp. 615–651.

Björk, T. & C. Landén (2000): "On the Term Structure of Futures and Forward Prices." *Technical report*, EFI - The Economic Research Institute, Stockholm School of Economics Suggested, Stockholm.

Black, F. & M. Scholes (1973): "The Pricing of Options and Corporate Liabilities." *The Journal of Political Economy* **81(3)**: pp. 637–654.

Bloomfield, P. (2004): *Fourier Analysis of Time Series: An Introduction.* John Wiley & Sons.

Boero, G. & C. Torricelli (1996): "A comparative evaluation of alternative models of the term structure of interest rates." *European Journal of Operational Research* **93(1)**: pp. 205–223.

CBOT/CME Group (2018a): "CBOT Rulebook, Chapter 18: U.S. Treasury Bond Futures." *Technical report*, CBOT/CME Group.

CBOT/CME Group (2018b): "CBOT Rulebook, Chapter 19: Long-Term U.S. Treasury Note Futures." *Technical report*, CBOT/CME Group.

CBOT/CME Group (2018c): "CBOT Rulebook, Chapter 20: Medium-Term U.S. Treasury Note Futures." *Technical report*, CBOT/CME Group.

CBOT/CME Group (2018d): "CBOT Rulebook, Chapter 21: Short-Term U.S. Treasury Note Futures." *Technical report*, CBOT/CME Group.

CBOT/CME Group (2018e): "U.S. Treasury Futures Conversion Factor Look-Up Tables." *Technical report*, CBOT/CME Group.

Chan, K. C. C., G. A. Karolyi, F. A. Longstaff, & A. B. Sanders (1992): "An empirical comparison of alternative models of the short-term interest rate." *The journal of finance* **47(3)**: pp. 1209–1227.

Cieslak, A. & P. Povala (2016): "Information in the Term Structure of Yield Curve Volatility." *Journal of Finance* **71(3)**: pp. 1393–1436.

Cox, J., J. Ingersoll, & S. Ross (1980): "The Relationship between Forward Prices and Future Prices." *Journal of Financial Economics* **9**: p. 26.

Cox, J., J. Ingersoll Jr, & S. Ross (1985): "A Theory of the Term Structure of Interest Rates." *Econometrica* **53(2)**: pp. 385–407.

Diebold, F. X. & C. Li (2006): "Forecasting the term structure of government bond yields." *Journal of Econometrics* **130(2)**: pp. 337–364.

Duffee, G. R. (2002): "Term Premia and Interest Rate Forecasts in Affine Models." *The Journal of Finance* **LVII(1)**: pp. 405–443.

Duffie, D. & R. Kan (1996): "A Yield-Factor of Interest Rates." *Mathematical Finance* **6(4)**: pp. 379–406.

Fernandez-Rodriguez, F. (2006): "Interest Rate Term Structure Modeling Using Free-Knot Splines." *Journal of Business* **79(6)**: pp. 3083–3099.

Filipovic, D. (2009): *Term-Structure Models*. Berlin, Heidelberg: Springer Berlin Heidelberg.

Fleming, M. J. & E. M. Remolona (1999): "The Term Structure of Announcement Effects." *Technical Report 71*, Bank for International Settlements, Basel, Switzerland.

Gibson, R., F. Lhabitant, & D. Talay (2010): "Modeling the Term Structure of Interest Rates." *Foundations and Trends in Finance* **5(1-2)**.

Goodhart, C. A. & M. O'Hara (1997): "High frequency data in financial markets: Issues and applications." *Journal of Empirical Finance* **4(2-3)**: pp. 73–114.

Granger, C. W. J. (1966): "The Typical Spectral Shape of an Economic Variable." *Econometrica* **34(1)**: pp. 150–161.

Granger, C. W. J. & M. Hatanaka (1964): *Spectral Analysis of Economic Time Series*. Princeton University Press.

Granger, C. W. J. & H. Rees (1968): "Spectral analysis of the term structure of interest rates." *The Review of Economic Studies* **35(1)**: pp. 67–76.

Hallett, A. H. & C. R. Richter (2004): "Spectral Analysis as a Tool for Financial Policy: An Analysis of the Short-End of the British Term Structure." *Computational Economics* **23(3)**: pp. 271–288.

Hautsch, N. & Y. Ou (2008): "Yield Curve Factors, Factor Volatilities, and the Predictability of Bond Excess Returns." *SSRN Electronic Journal* .

Heath, D., R. A. Jarrow, & A. J. Morton (1992): "Bond Pricing and the Term Structure of Interest Rates: A New Methodology for Contingent Claims Valuation." *Econometrica* **60(1)**: pp. 77–105.

Ho, T. S. & S.-B. Lee (1986): "Term Structure Movements and Pricing Interest Rate Contingent Claims." *The Journal of Finance* **41(5)**: pp. 1011–1029.

Hull, J. & A. White (1990): "Pricing Interest-Rate-Derivative Securities." *Review of Financial Studies, Society for Financial Studies* **3(4)**: pp. 573–592.

Hull, J. & A. White (1993): "One-Factor Interest-Rate Models and the Valuation of Interest-Rate Derivative Securities." *The Journal of Financial and Quantitative Analysis* **28(2)**: pp. 235 –254.

Jamshidian, F. (1995): "A simple class of square-root interest-rate models." *Applied Mathematical Finance* **2(1)**: pp. 61–72.

Jegadeesh, N. & G. G. Pennacchi (1996): "The Behavior of Interest Rates Implied by the Term Structure of Eurodollar Futures." *Journal of Money, Credit & Banking (Ohio State University Press)* **28(3)**: pp. 426–446.

Johnson, N., J. Kerpel, & J. Kronstein (2017): "Understanding Treasury Futures." *Technical report*, CME Group.

Junker, M., A. Szimayer, & N. Wagner (2006): "Nonlinear term structure dependence: Copula functions, empirics, and risk implications." *Journal of Banking and Finance* **30(4)**: pp. 1171–1199.

Kiermeier, M. M. (2014): "Essay on Wavelet analysis and the European term structure of interest rates." *Business and Economic Horizons* **9(4)**: pp. 18–26.

Kley, T. (2016): "Quantile-based spectral analysis in an object-oriented framework and a reference implementation in r: The quantspec package." *Journal of Statistical Software* **70(3)**: pp. 1–27.

Kolb, R. & J. Overdahl (2003): *Financial Derivatives*. Hoboken, New Jersey: John Wiley & Sons, Inc., third edition.

Kuriyama, N. (2016): "Testing cointegration in quantile regressions with an application to the term structure of interest rates." *Studies in Nonlinear Dynamics and Econometrics* **20(2)**: pp. 107–121.

Litterman, R. B. & J. Scheinkman (1991): "Common Factors Affecting Bond Returns." *The Journal of Fixed Income* **1(1)**: pp. 54–61.

Liu, L. Y., A. J. Patton, & K. Sheppard (2015): "Does anything beat 5-minute RV? A comparison of realized measures across multiple asset classes." *Journal of Econometrics* **187(1)**: pp. 293–311.

McCulluch, H. J. (1971): "Measuring the term structure of interest rates." *The Journal of Business* **44(1)**: pp. 19–31.

Merton, R. C. (1973): "Theory of rational option pricing." *Bell Journal of Economics and Management Science* **4(1)**: pp. 141–183.

Nelson, C. R. & A. F. Siegel (1987): "Parsimonious Modeling of Yield Curves." *The Journal of Business* **60(4)**: pp. 473–489.

Nerlove, M. (1964): "Spectral Analysis of Seasonal Adjustment Procedures." *Econometrica* **32(3)**: pp. 241–286.

Noureldin, D. (2014): "Time-varying Dependence in the Term Structure of Interest Rates: A Copula-based Apporach." In "Econometric Methods and Their Applications in Finance, Macro and Related Fields," p. 80. World Scientific.

Piazzesi, M. (2005): "Bond Yields and the Federal Reserve." *Journal of Political Economy* **113(2)**: pp. 311–344.

Righi, M. B., S. G. Schlender, & P. S. Ceretta (2015): "Pair copula constructions to determine the dependence structure of Treasury bond yields." *IIMB Management Review* **27(4)**: pp. 216–227.

Sandaresan, S. (1991): "Futures Prices on Yields , Forward Prices , and Implied Forward Prices from Term Structure." *The Journal of Financial and Quantitative Analysis* **26(3)**: pp. 409–424.

Sargent, T. (1971): "Expectations at the Short End of the Yield Curve: An Application of Macaulay's Test." *Essays on Interest Rates* **2**: pp. 391–412.

Shea, G. S. (1984): "Pitfalls in Smoothing Interest Rate Term Structure Data: Equilibrium Models and Spline Approximations." *The Journal of Financial and Quantitative Analysis* **19(3)**: p. 253.

Shin, M. & M. Zhong (2017): "Does realized volatility help bond yield density prediction?" *International Journal of Forecasting* **33(2)**: pp. 373–389.

Svensson, L. E. O. (1994): "Estimating and Interpreting Forward Interest Rates: Sweden 1992-1994." *Technical report*, National Bureau of Economic Research, Cambridge, Massachusetts.

Tsuji, C. (2006): "Does the term structure predict real economic activity in Japan?" *Applied Financial Economics Letters* **1(4)**: pp. 249–257.

Vasicek, O. (1977): "An Equilibrium Characterization of the Term Structure." *Journal of Financial Economics* **5**: pp. 177–188.

Vasicek, O. & H. G. Fong (1982): "Term Structure Modeling Using Exponential Splines." *Journal of Finance* **37(2)**: pp. 339–348.

Wickham, H. (2016): *ggplot2: Elegant Graphics for Data Analysis*. Springer-Verlag New York.

Zhang, L. (2011): "Estimating covariation: Epps effect, microstructure noise." *Journal of Econometrics* **160(1)**: pp. 33–47.

Appendix A

Figures

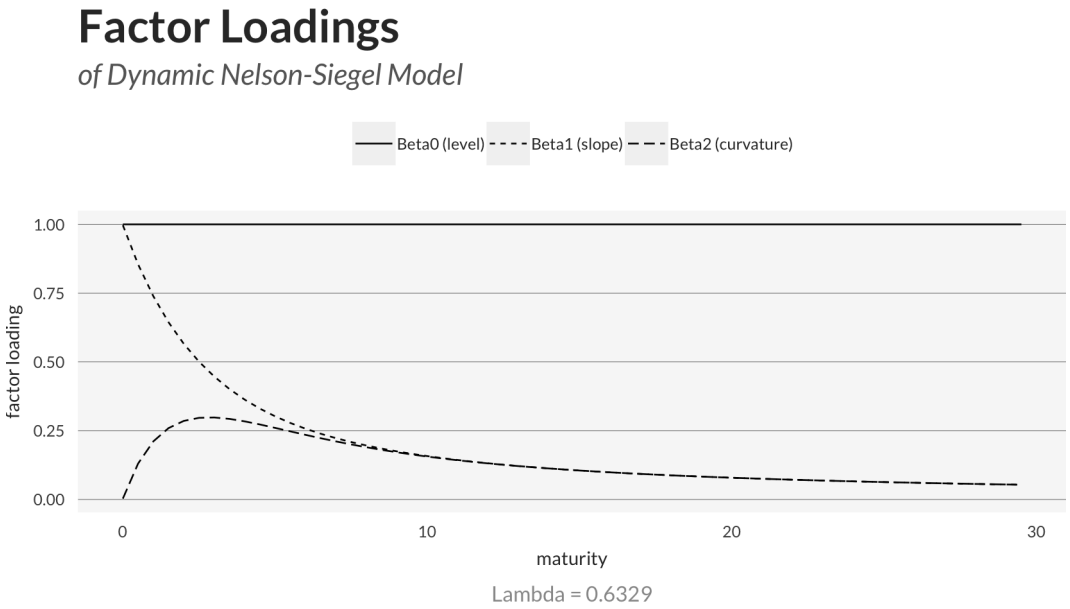

Figure A.1: Dynamic Nelson-Siegel Model factor loadings

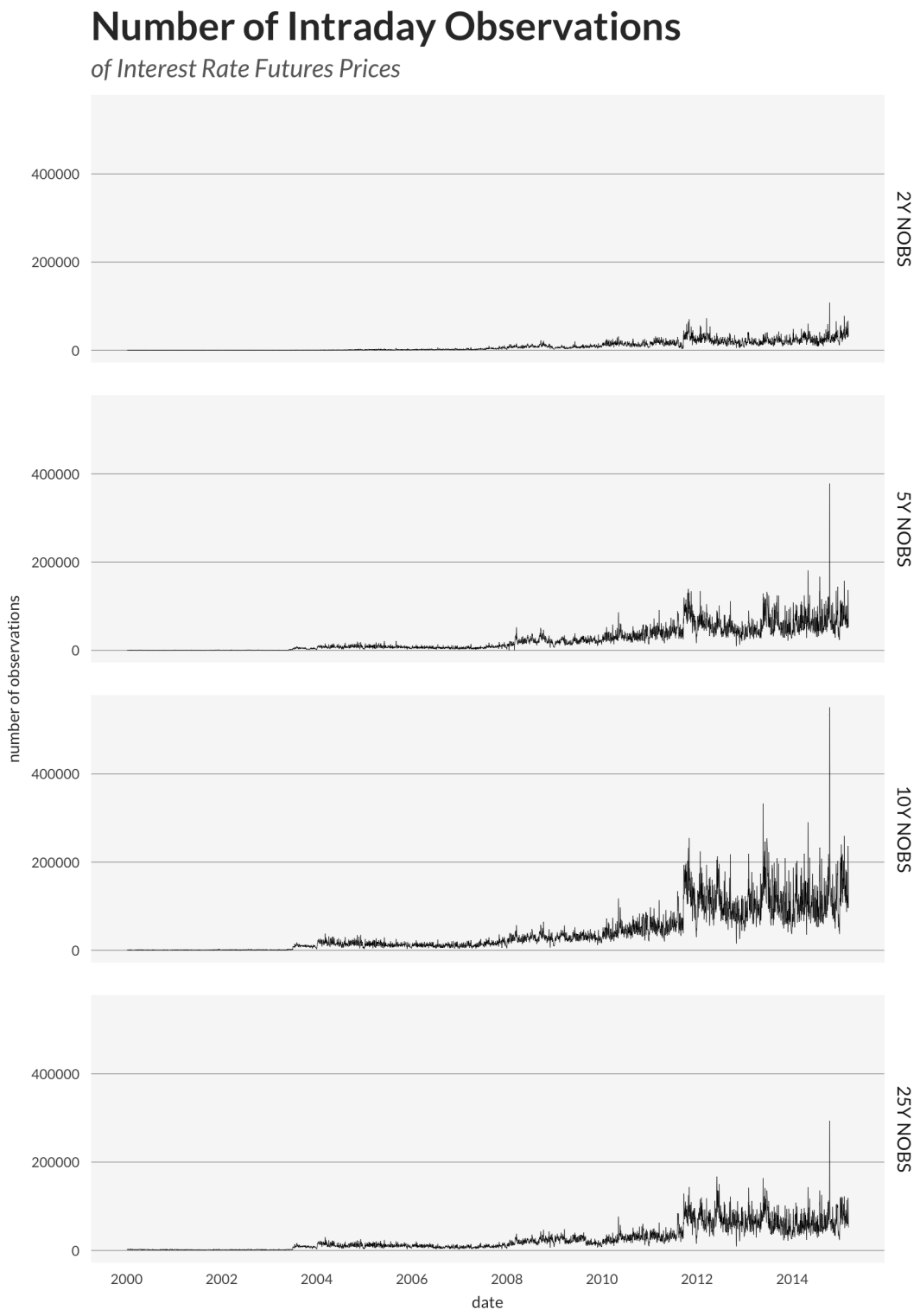

Figure A.2: Number of intraday observations

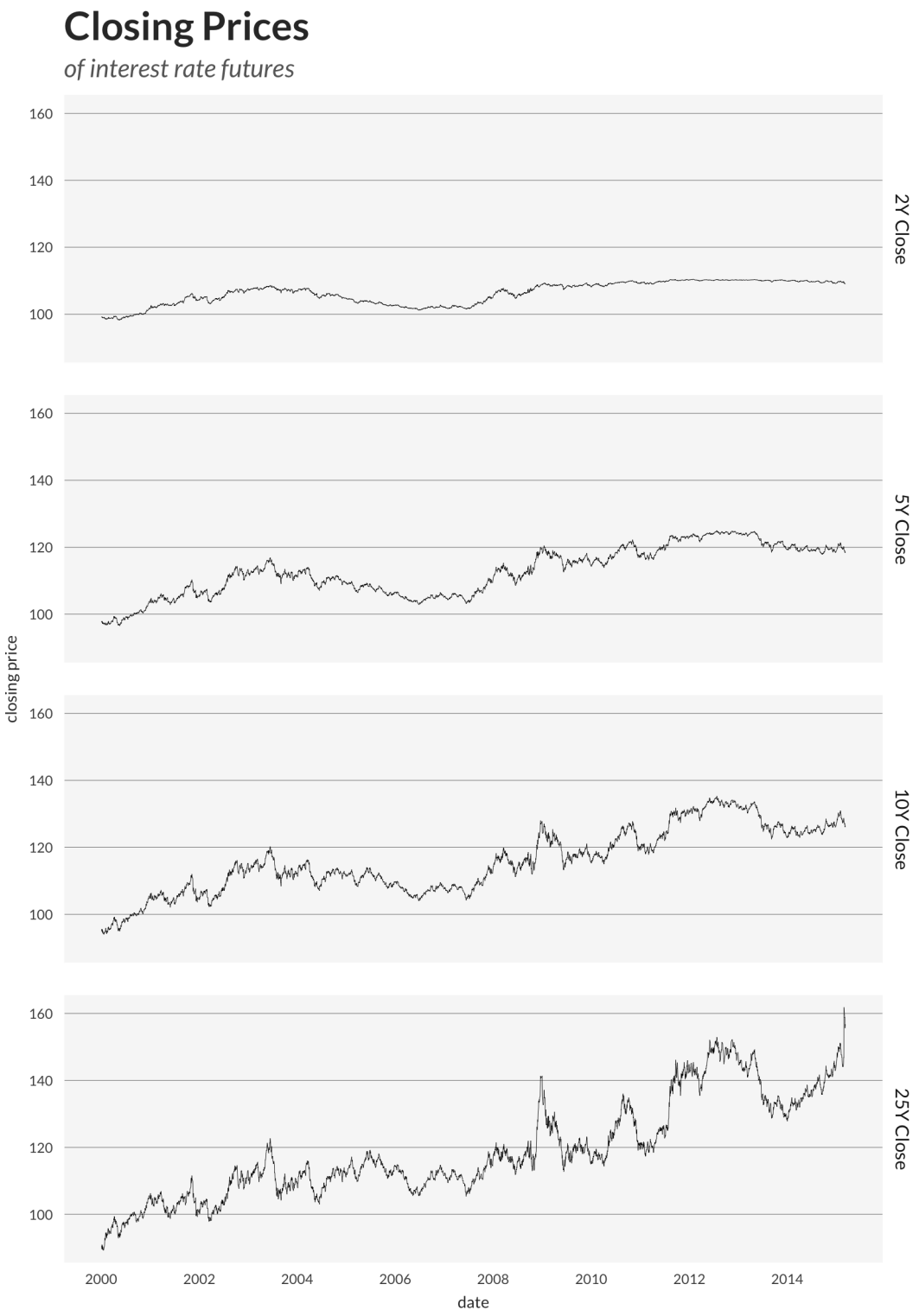

Figure A.3: Daily closing prices

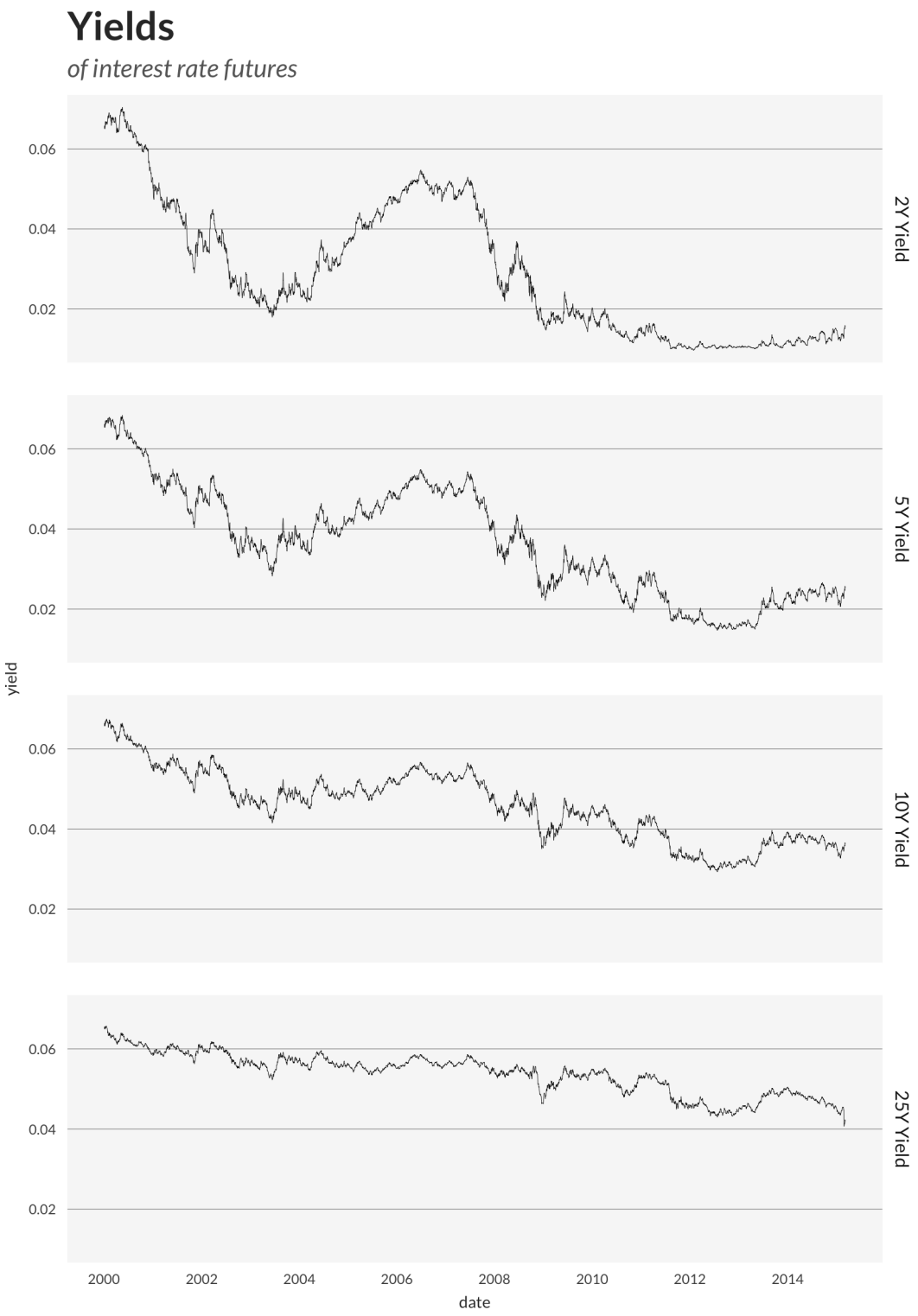

Figure A.4: Yields

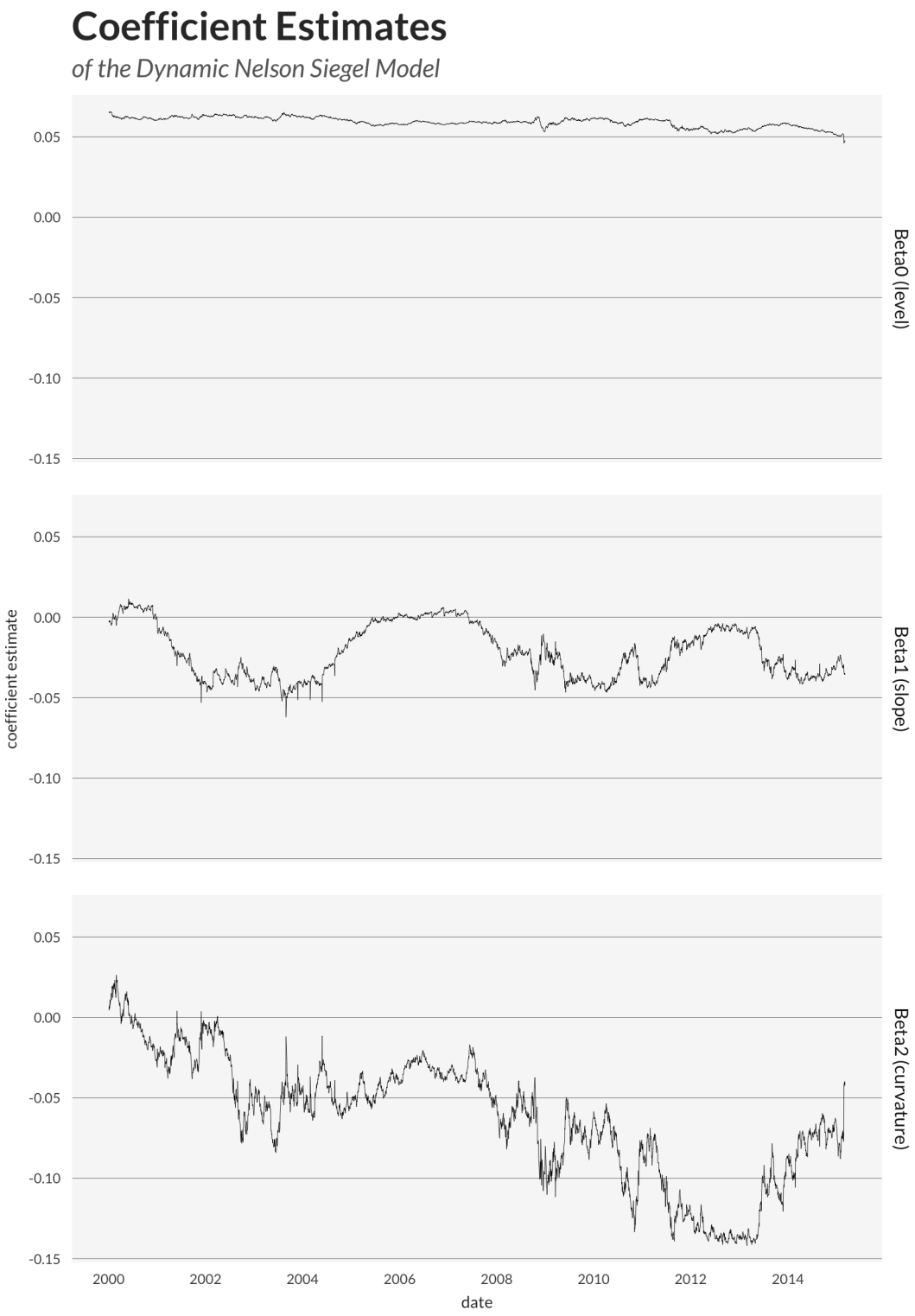

Figure A.5: DNSM coefficient estimates

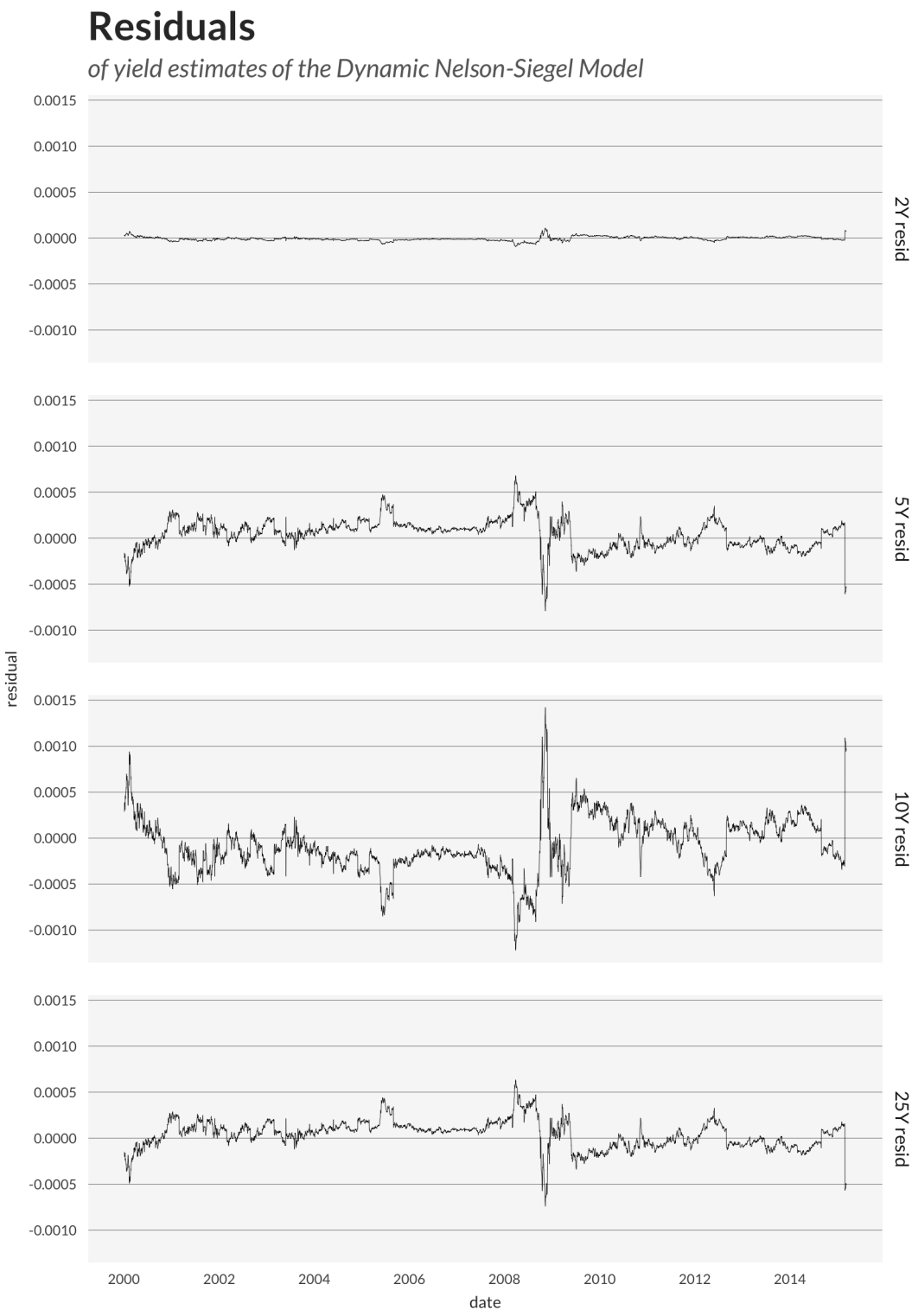

Figure A.6: Residuals from the estimation of the DNSM

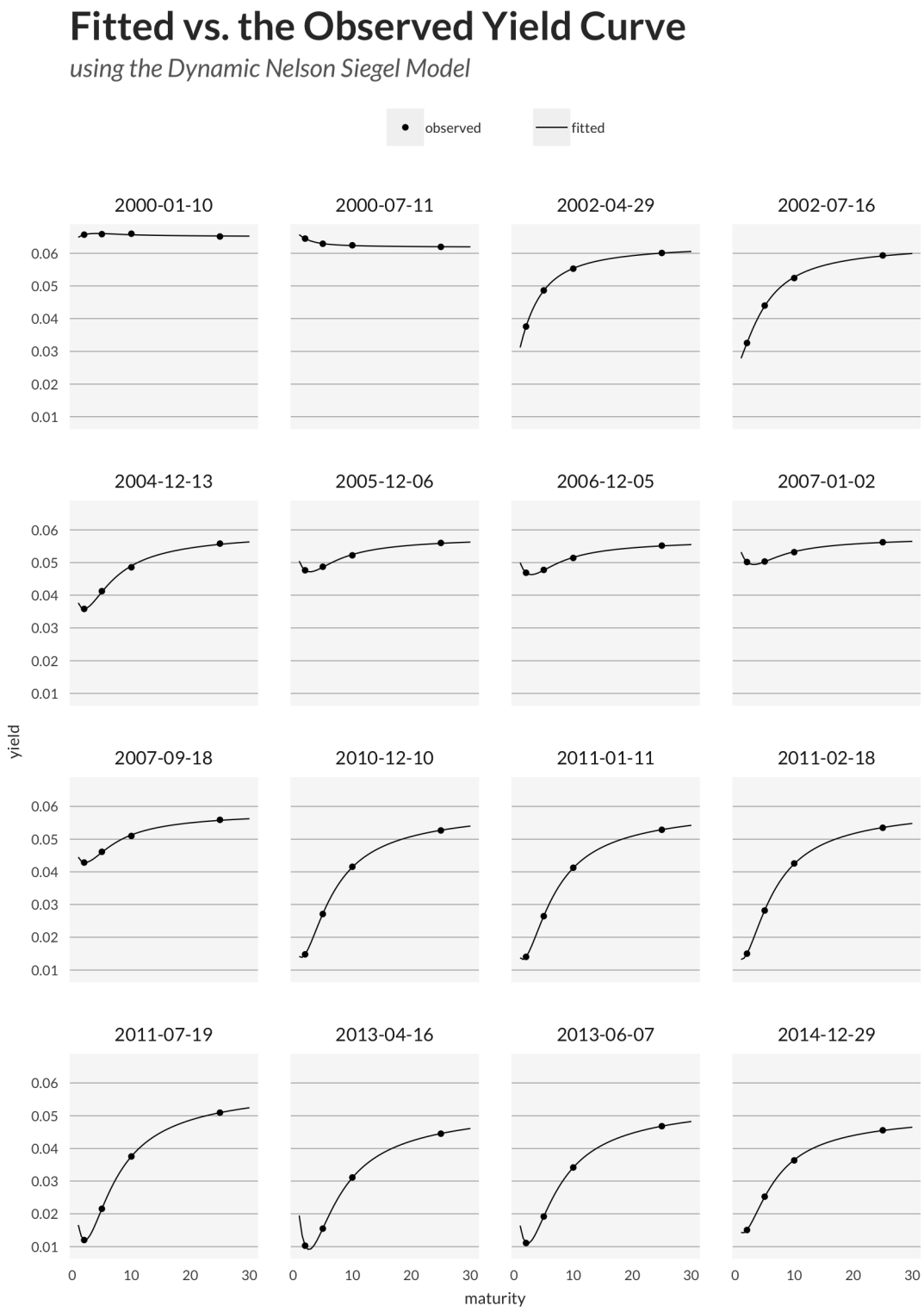

Figure A.7: Fitted vs. observed yield curve

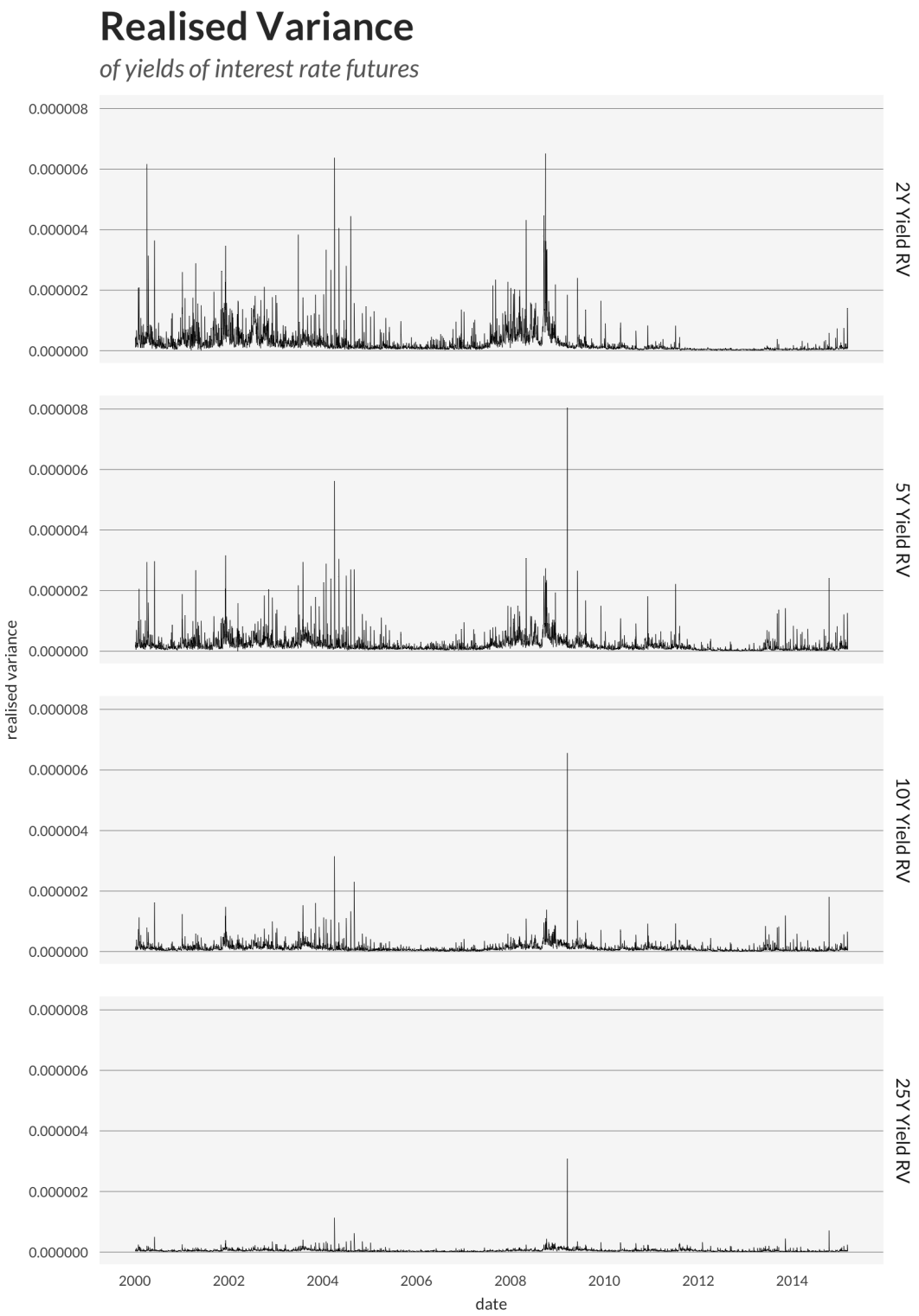

Figure A.8: Realised variance of yields

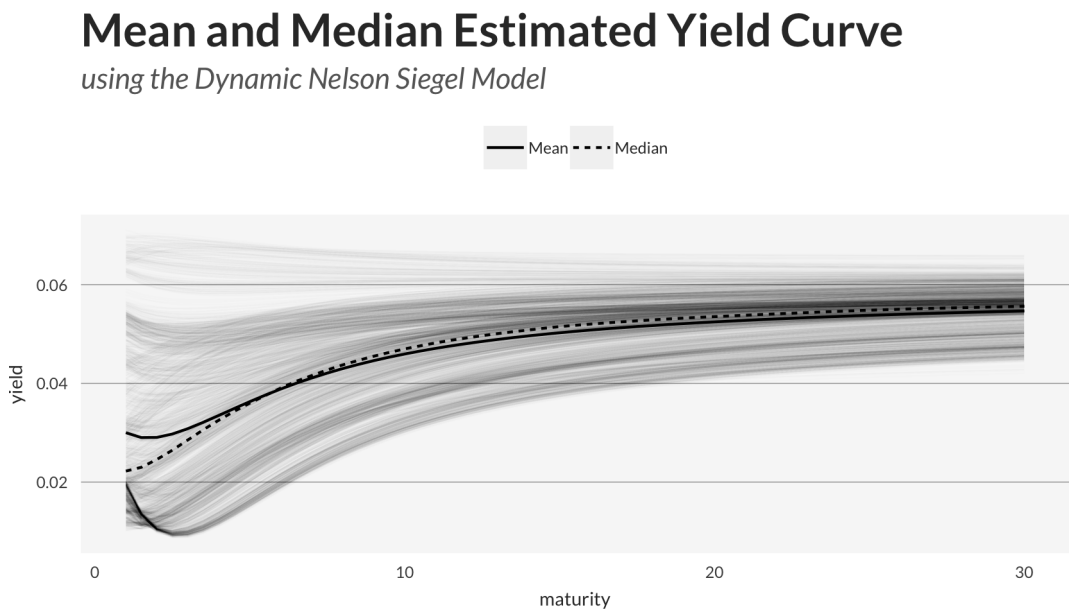

Figure A.9: Mean and median estimated term structure

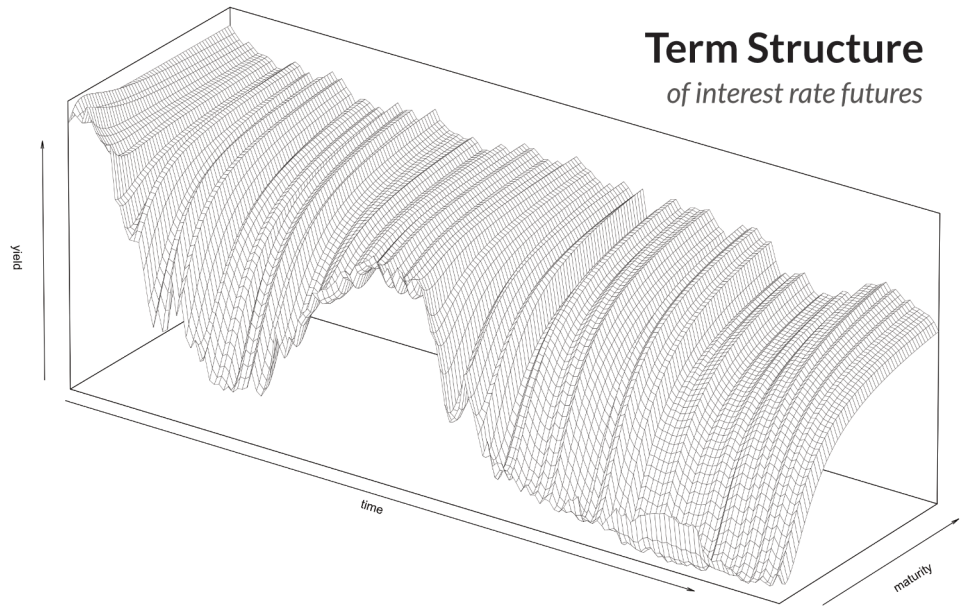

Figure A.10: Term structure

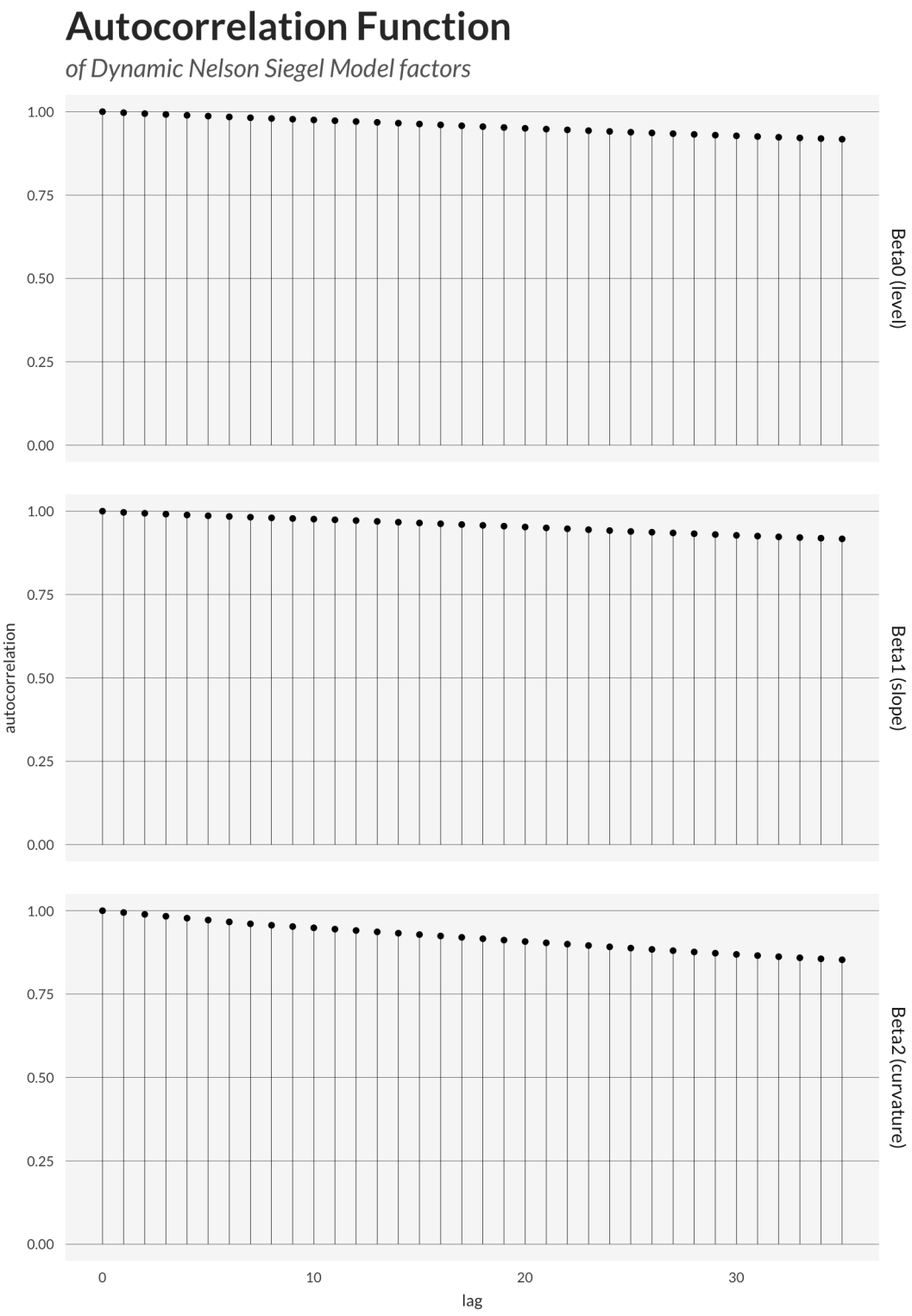

Figure A.11: Autocorrelation functions of DNSM factors

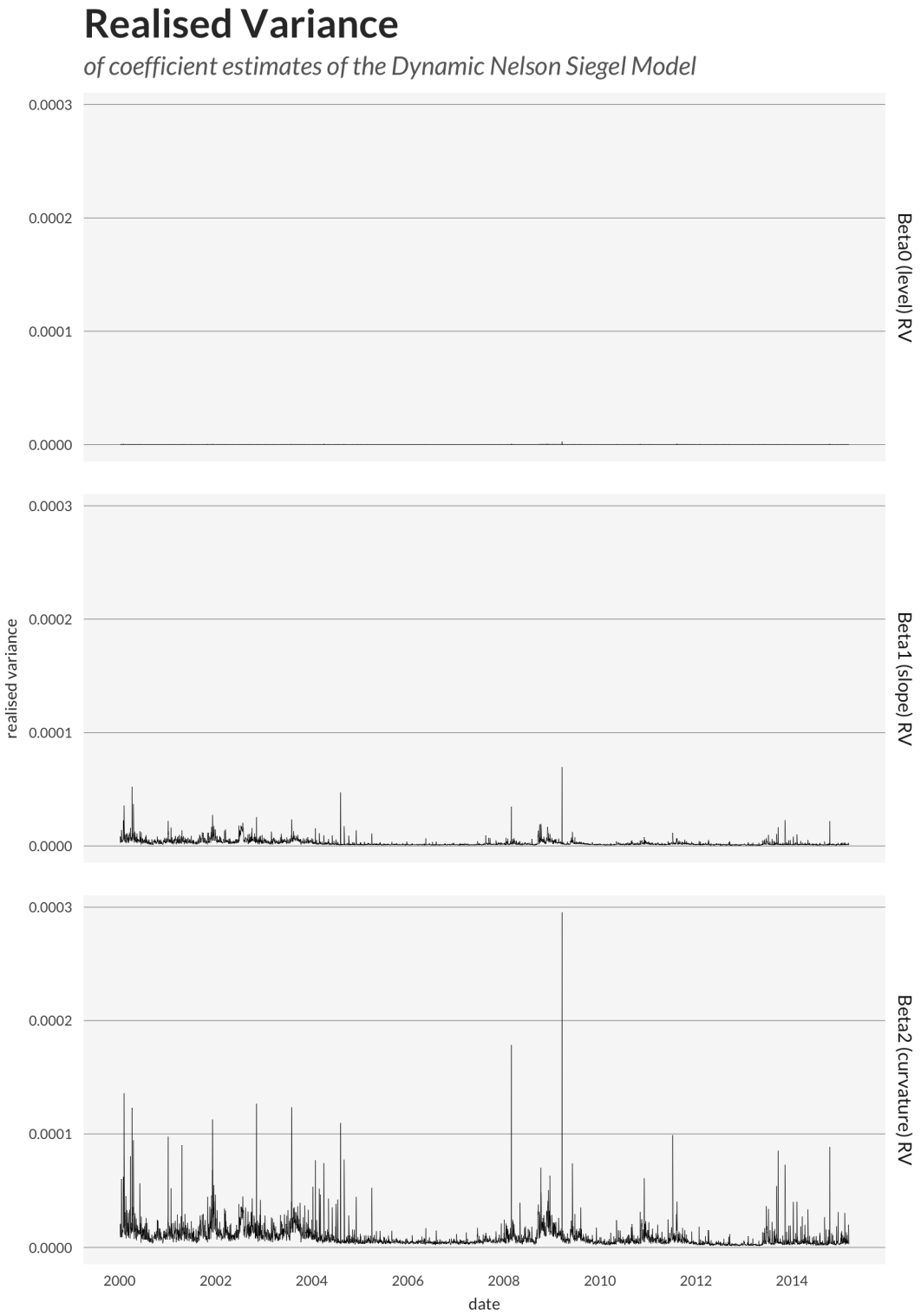

Figure A.12: Realised variance of Dynamic Nelson-Siegel Model factors

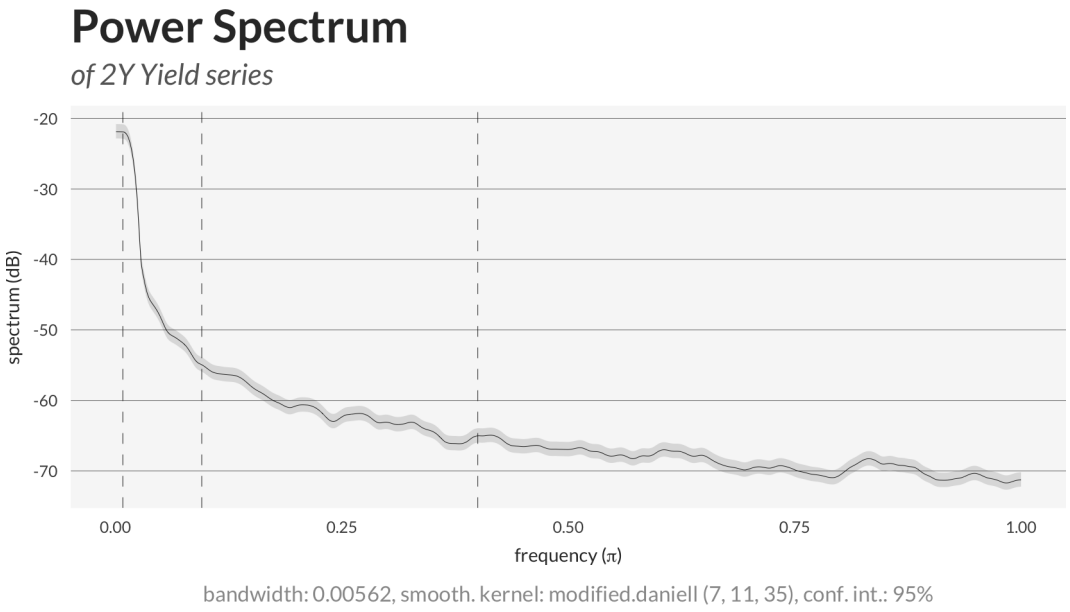

Figure A.13: Spectrum of 2Y yields

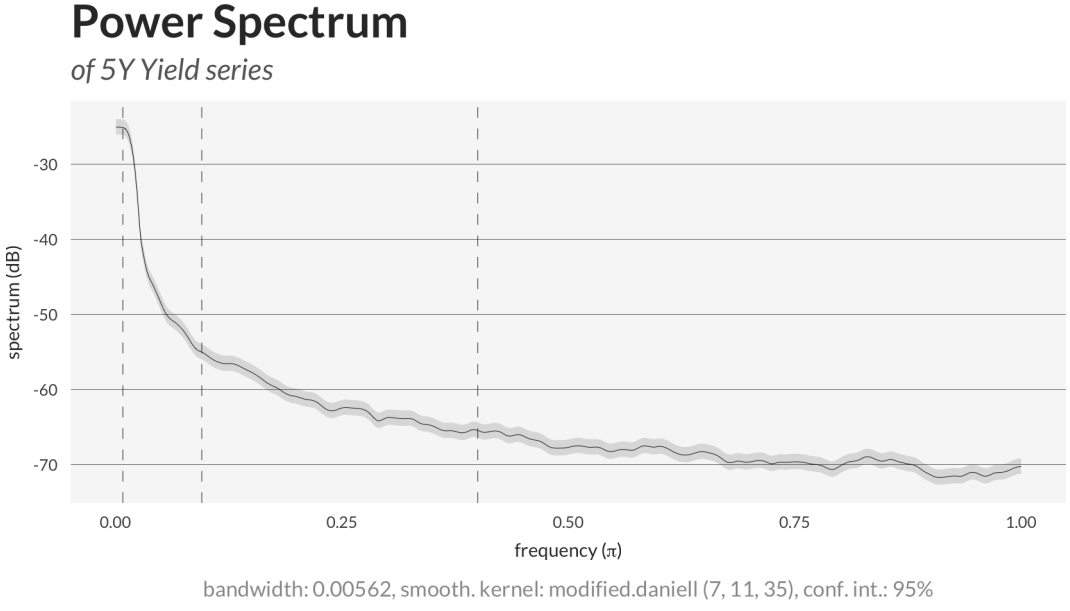

Figure A.14: Spectrum of 5Y yields

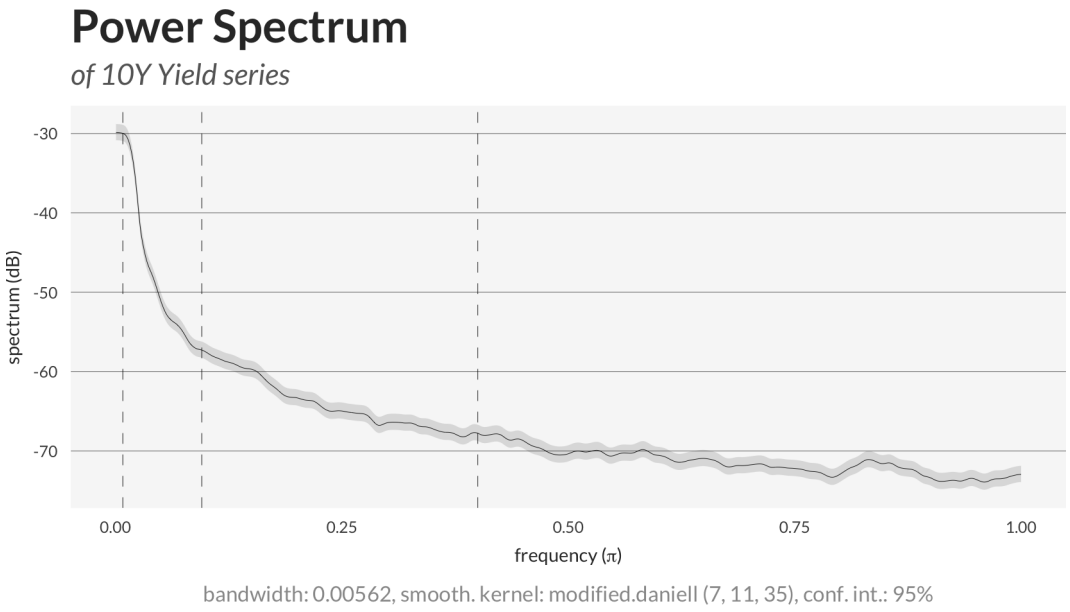

Figure A.15: Spectrum of 10Y yields

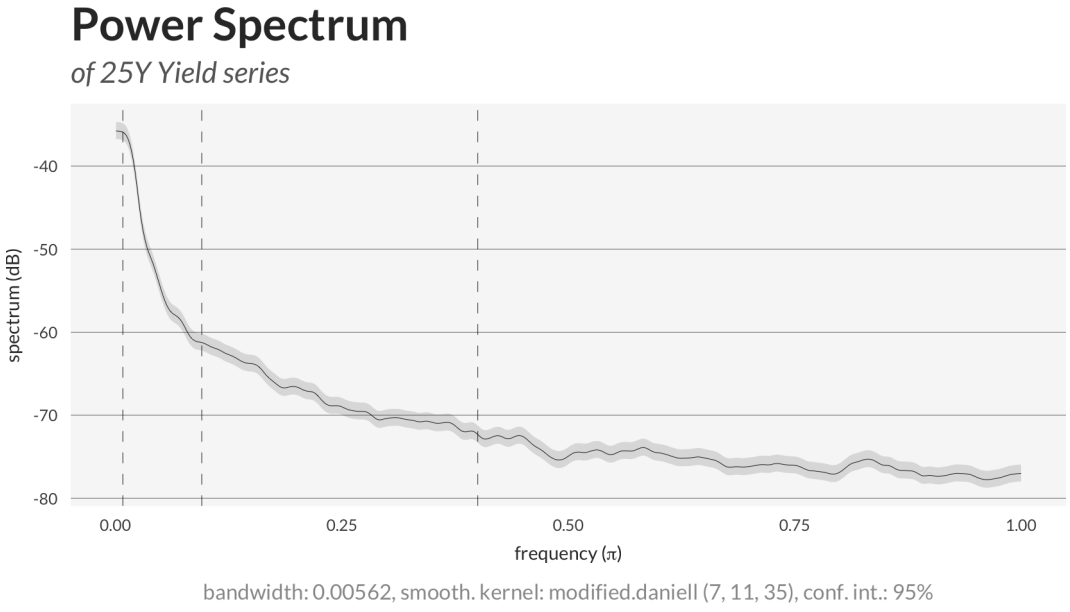

Figure A.16: Spectrum of 25Y yields

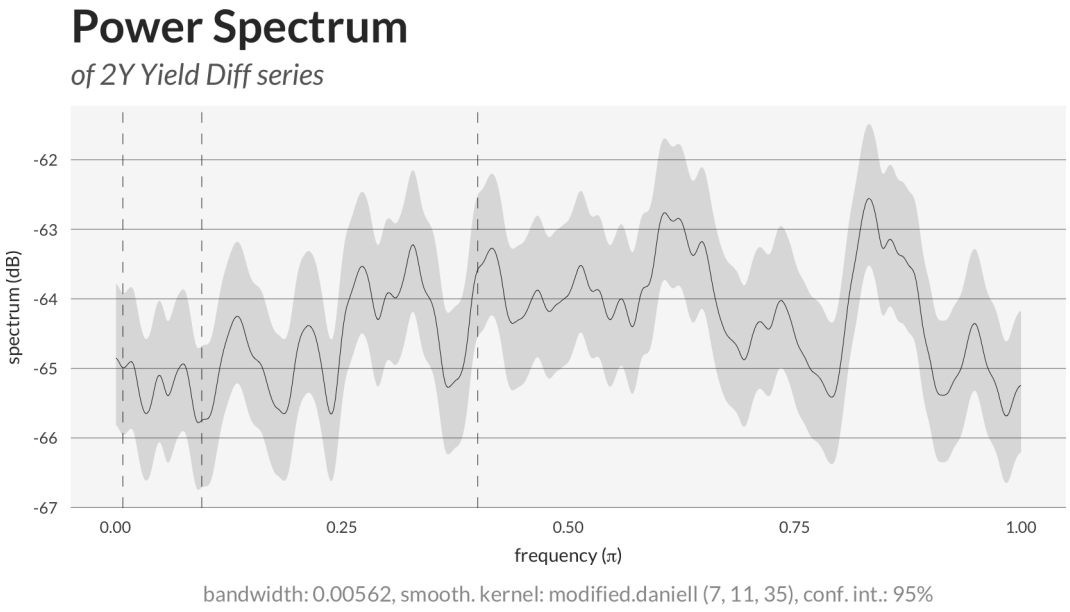

Figure A.17: Spectrum of first-differenced 2Y yields

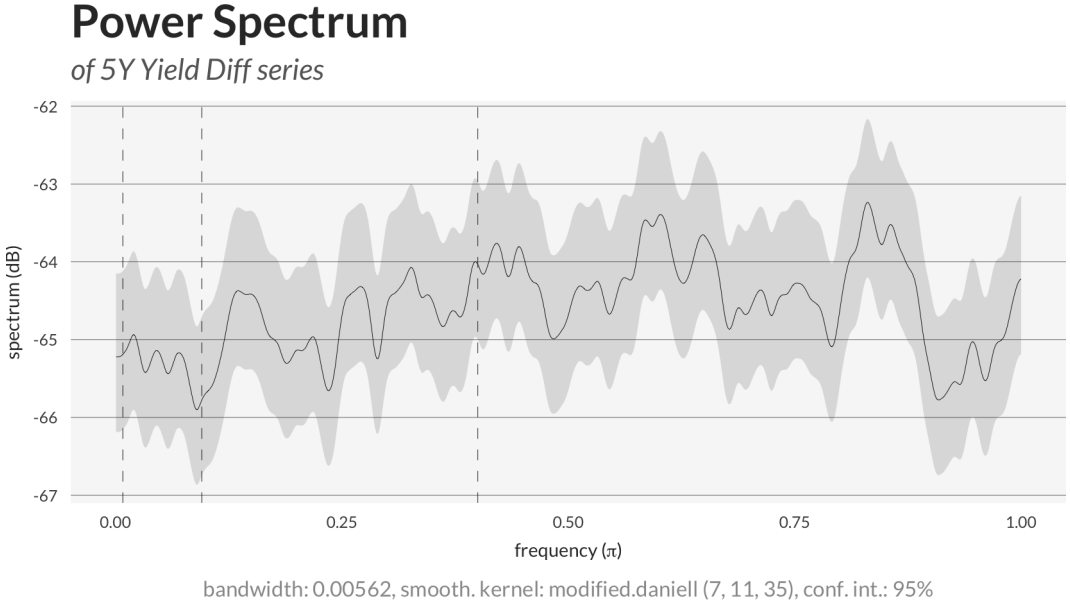

Figure A.18: Spectrum of first-differenced 5Y yields

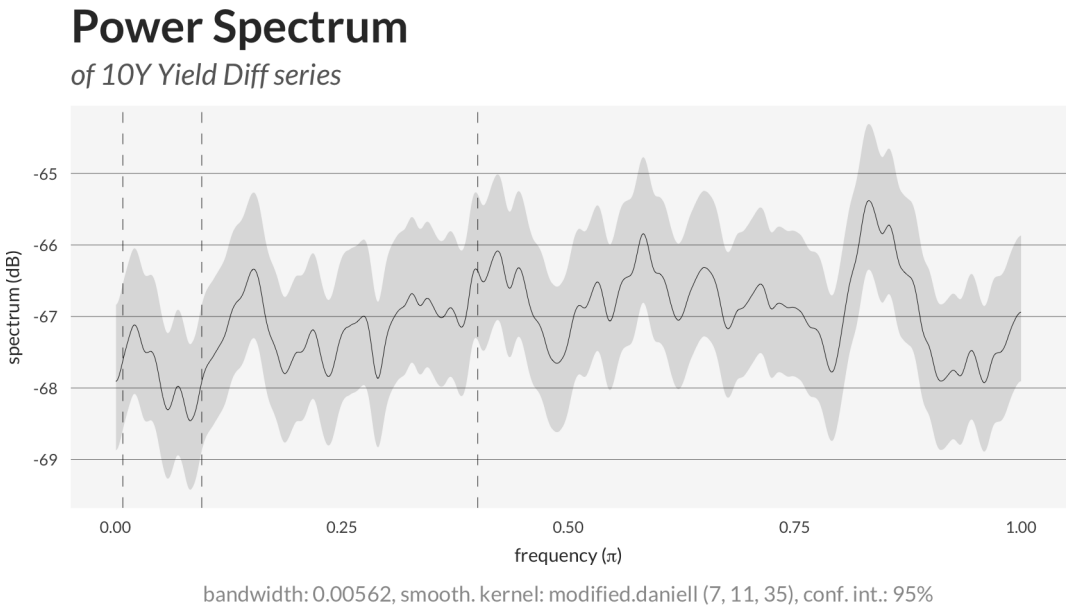

Figure A.19: Spectrum of first-differenced 10Y yields

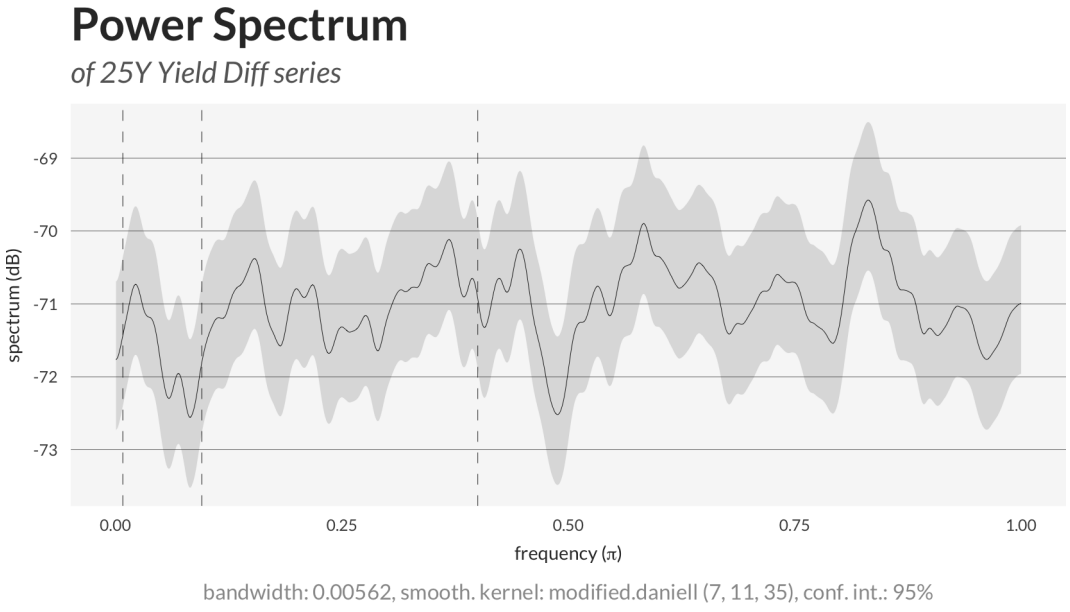

Figure A.20: Spectrum of first-differenced 25Y yields

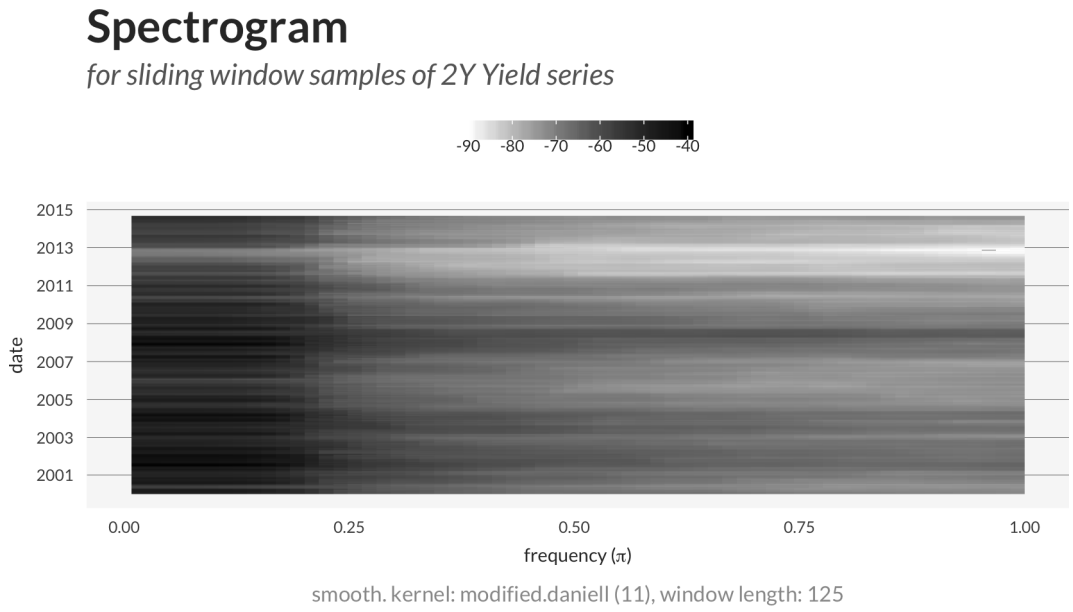

Figure A.21: Spectogram of 2Y yields

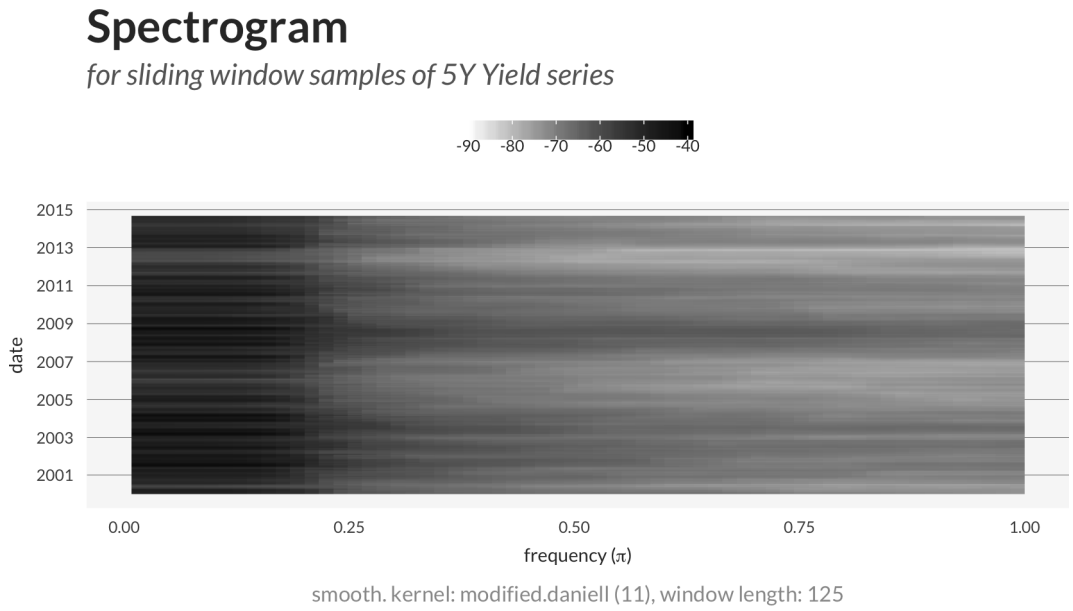

Figure A.22: Spectogram of 5Y yields

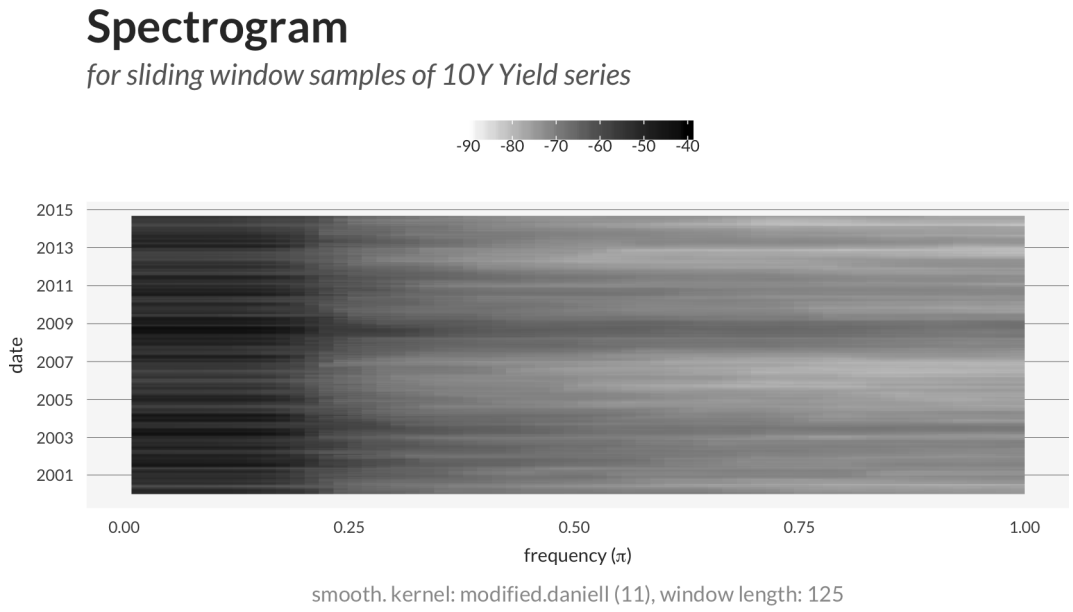

Figure A.23: Spectogram of 10Y yields

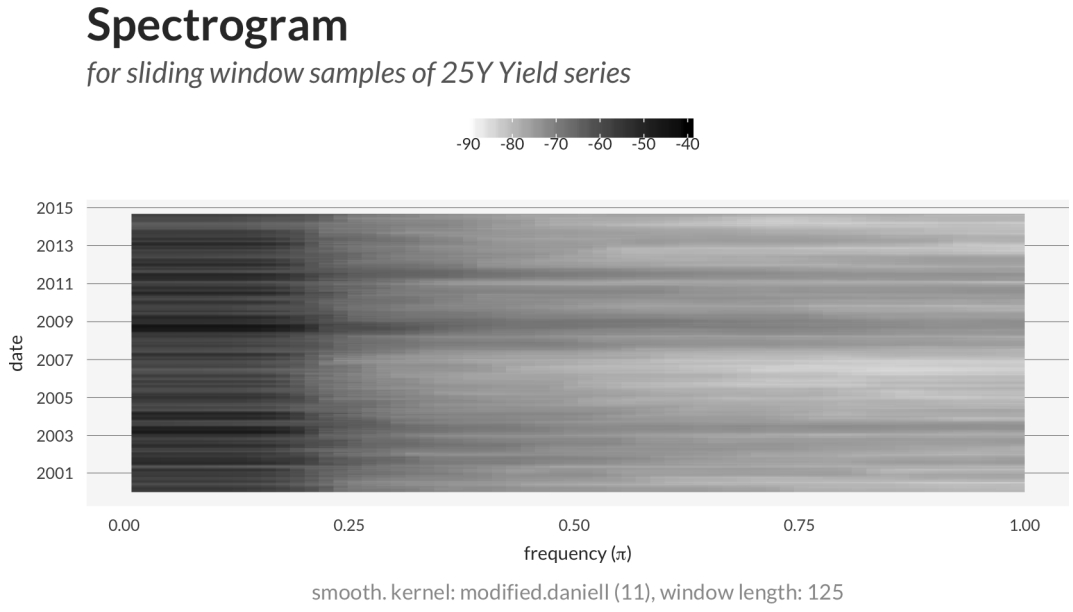

Figure A.24: Spectogram of 25Y yields

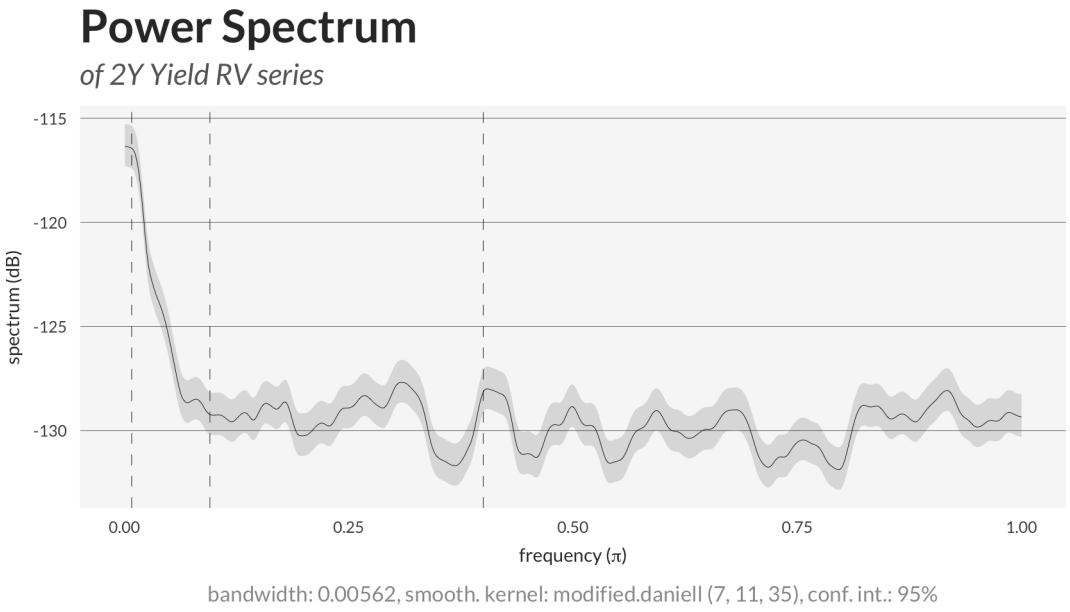

Figure A.25: Spectrum of realised variance of 2Y yields

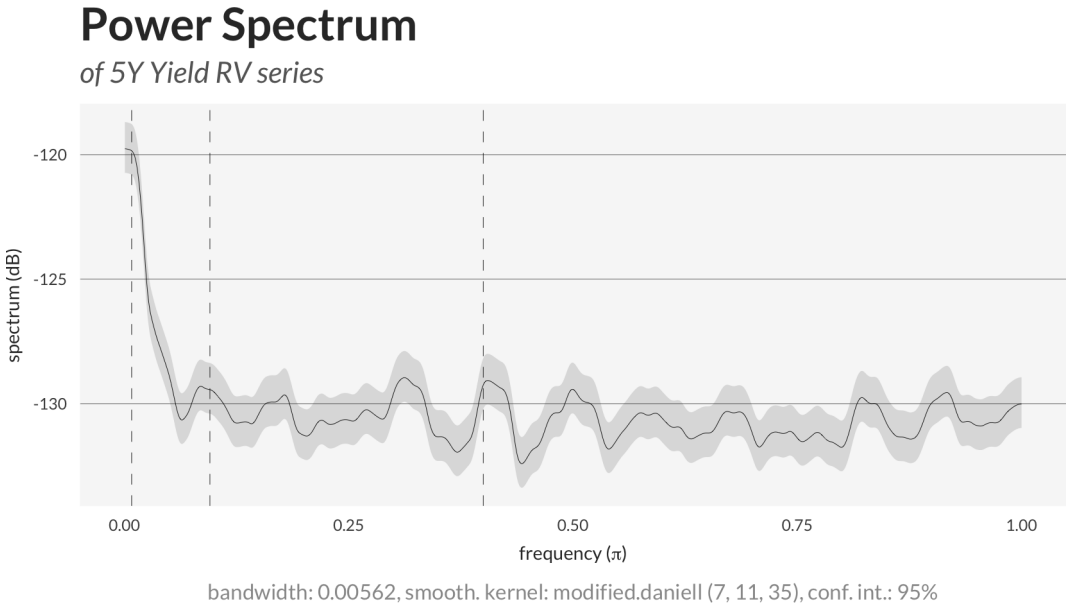

Figure A.26: Spectrum of realised variance of 5Y yields

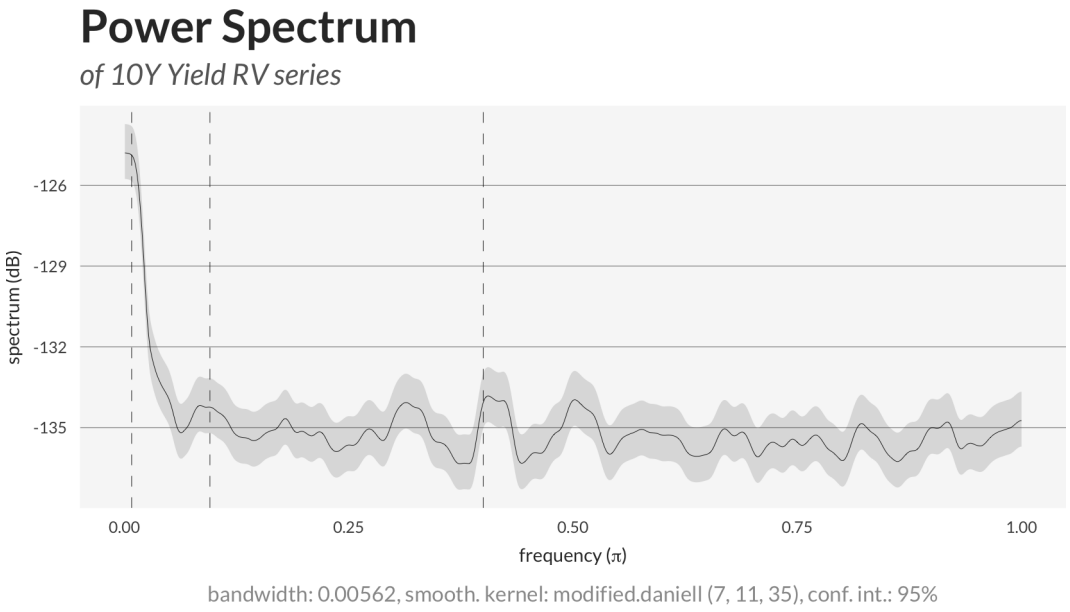

Figure A.27: Spectrum of realised variance of 10Y yields

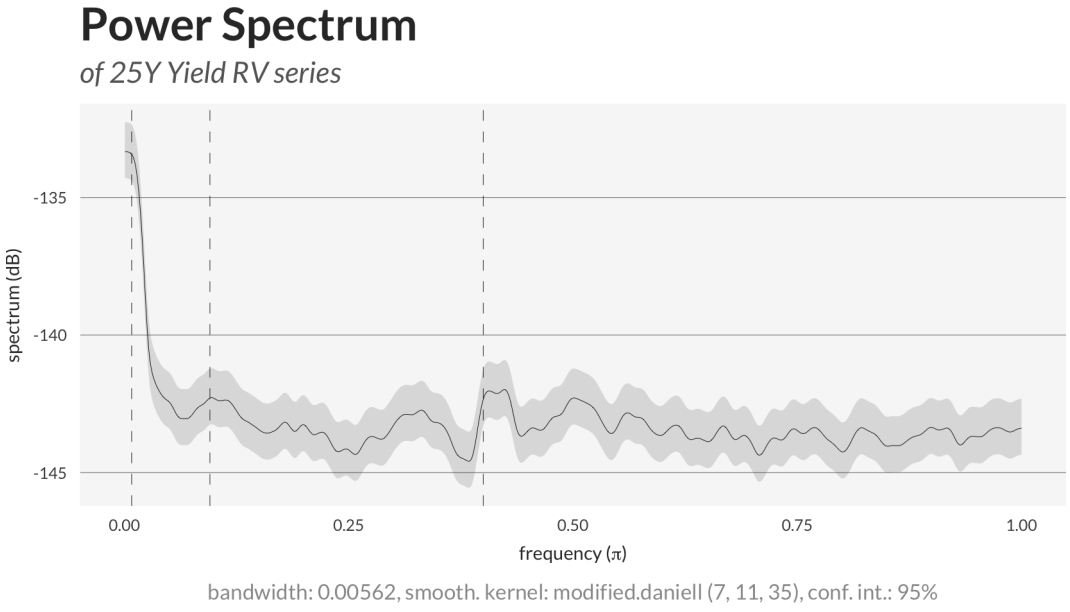

Figure A.28: Spectrum of realised variance of 25Y yields

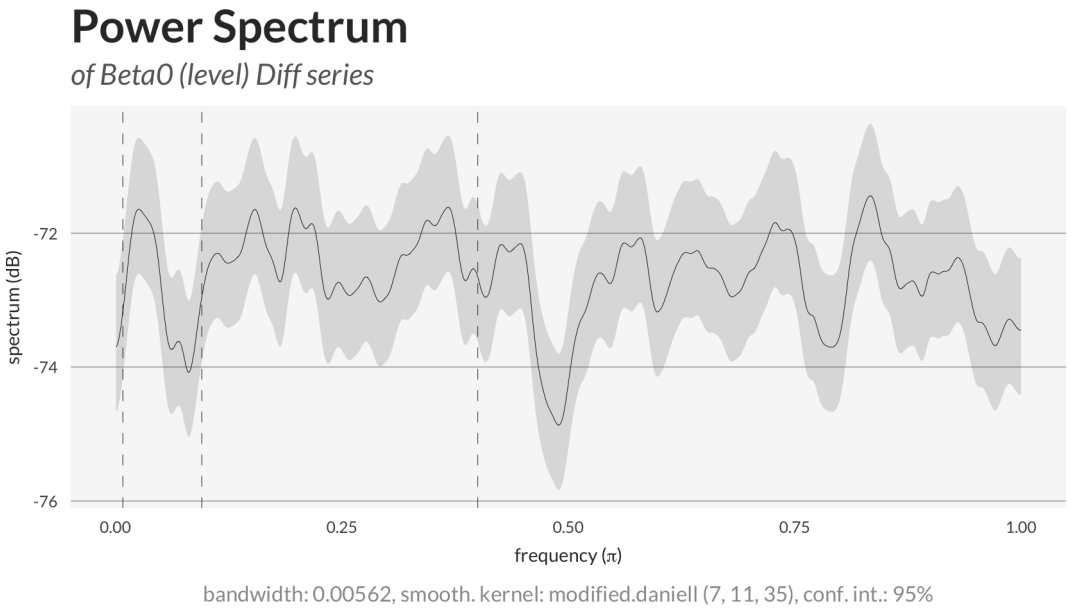

Figure A.29: Spectrum of first-differenced Nelson-Siegel level factor

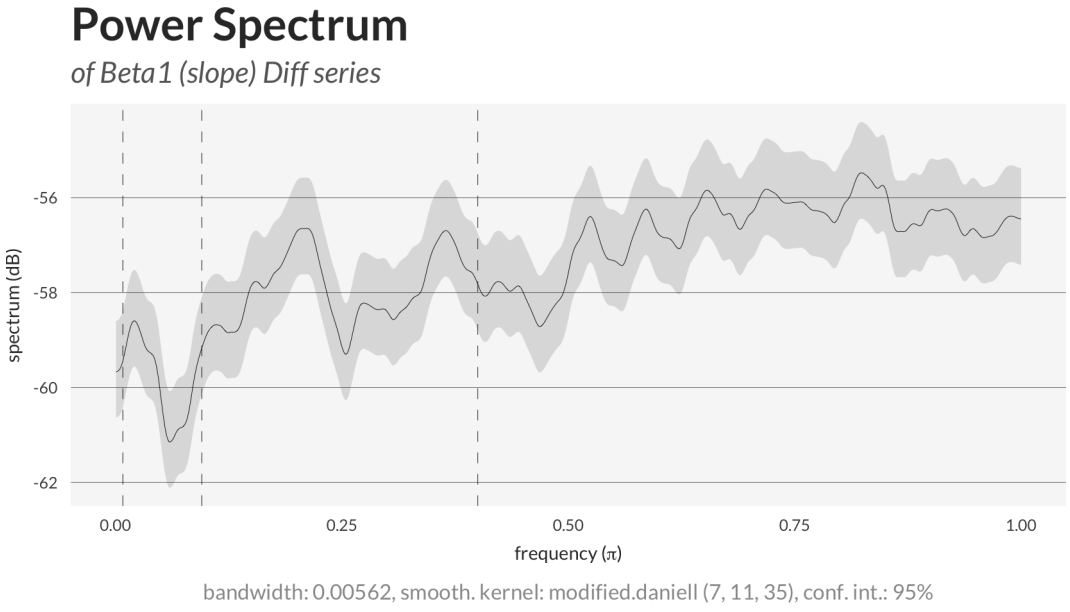

Figure A.30: Spectrum of first-differenced Nelson-Siegel slope factor

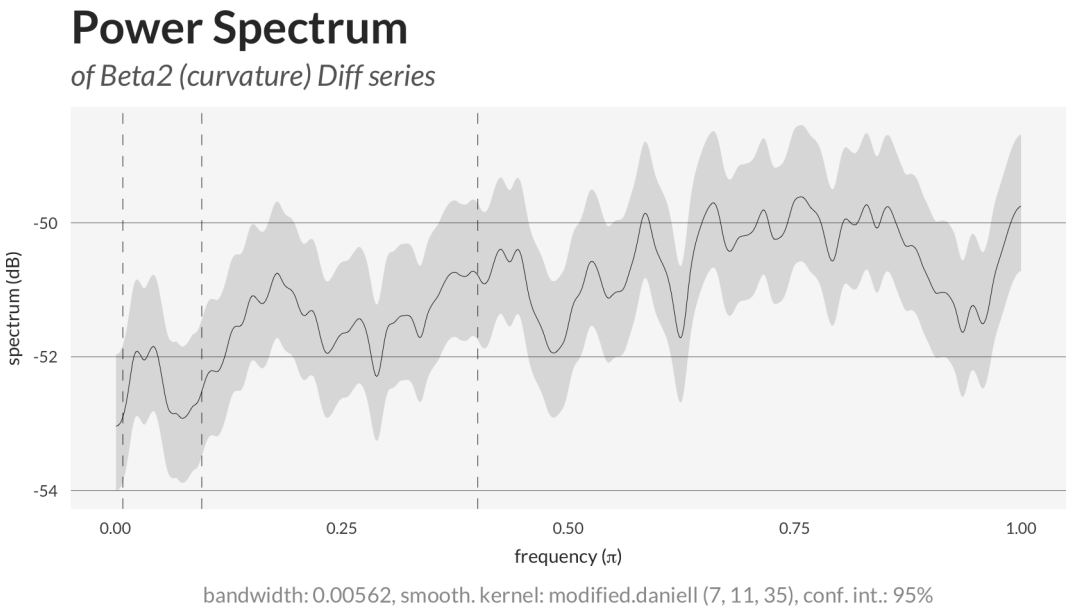

Figure A.31: Spectrum of first-differenced Nelson-Siegel curvature factor

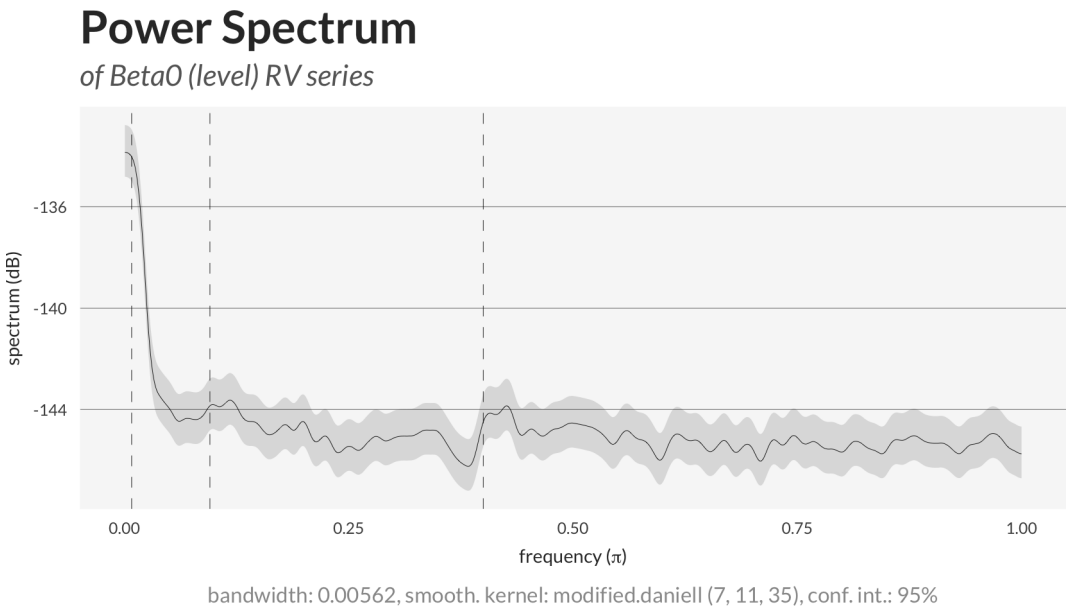

Figure A.32: Spectrum of realised variance of Nelson-Siegel level factor

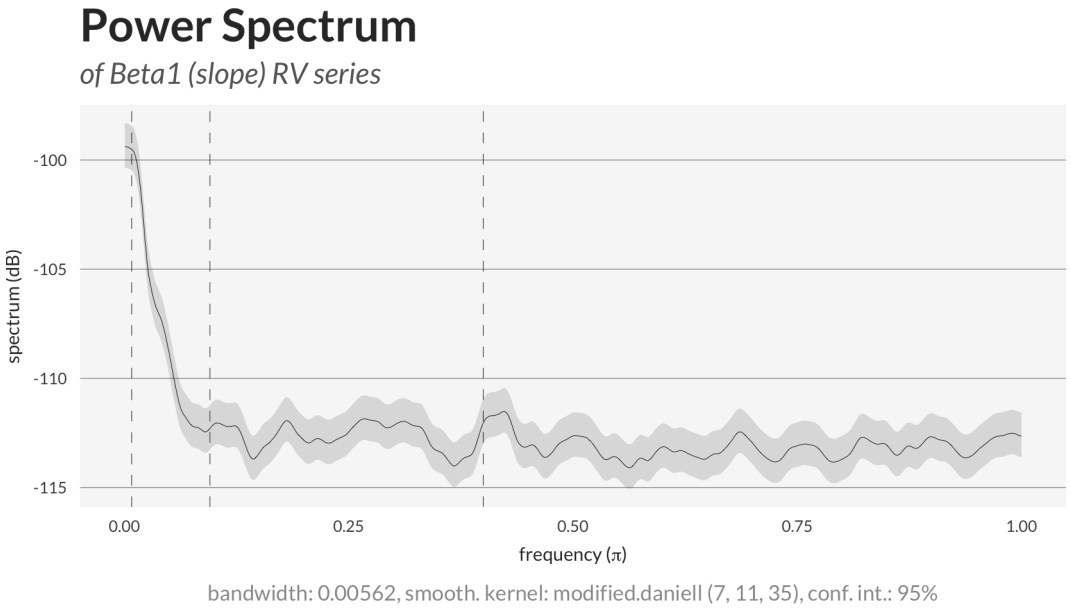

Figure A.33: Spectrum of realised variance of Nelson-Siegel slope factor

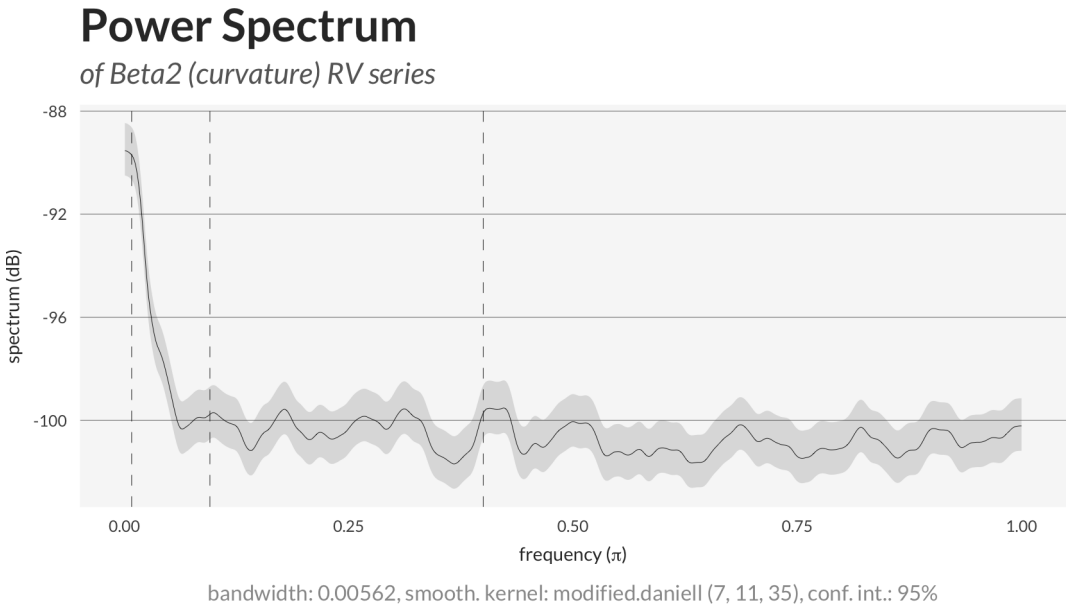

Figure A.34: Spectrum of realised variance of Nelson-Siegel curvature factor

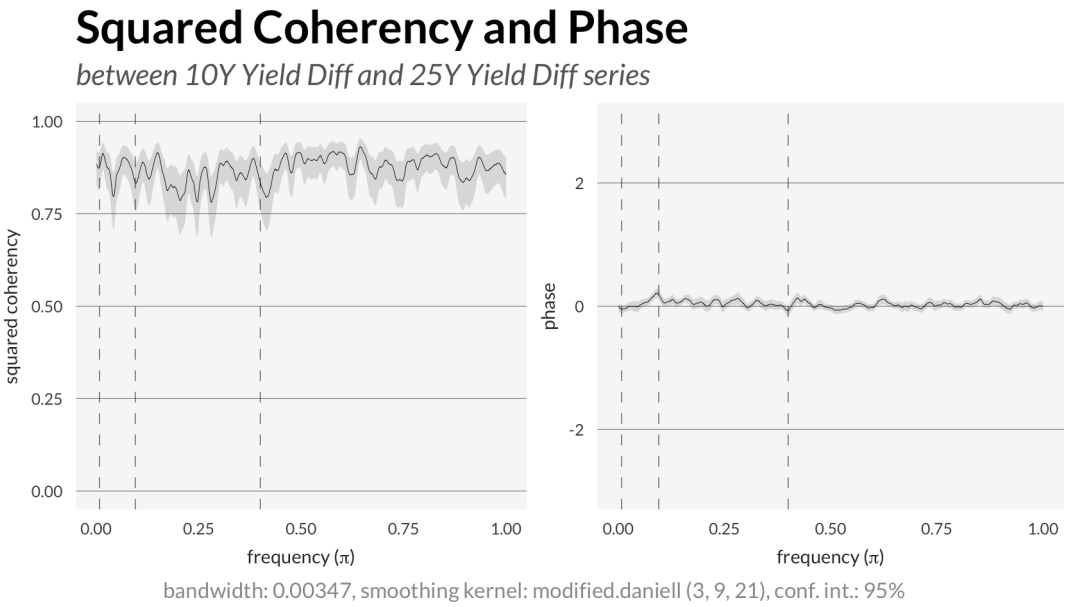

Figure A.35: Coherency and phase between 10Y and 25Y first-differenced yields

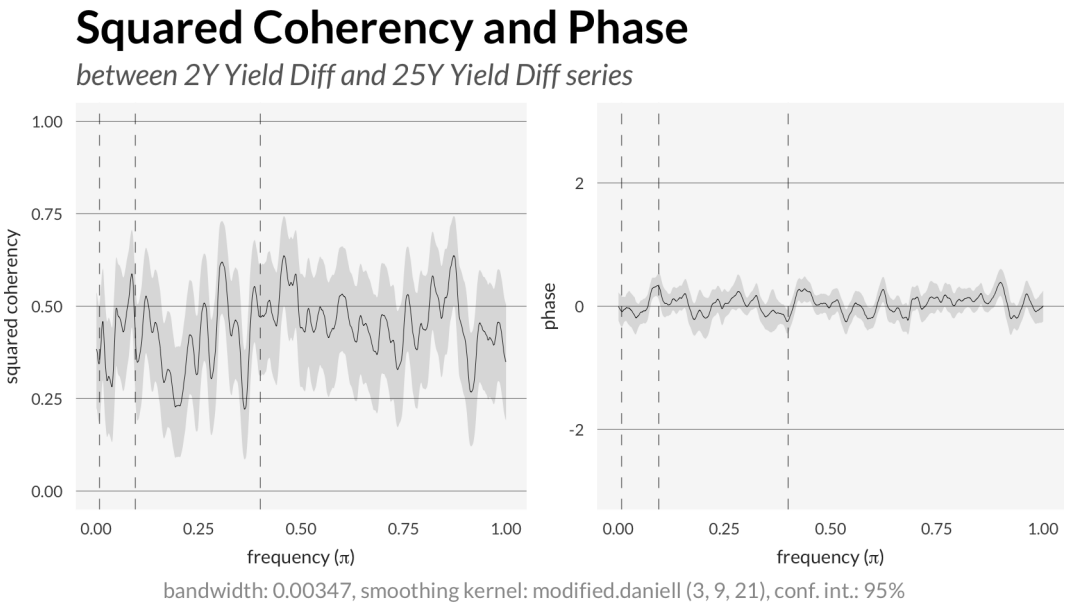

Figure A.36: Coherency and phase between 2Y and 25Y first-differenced yields

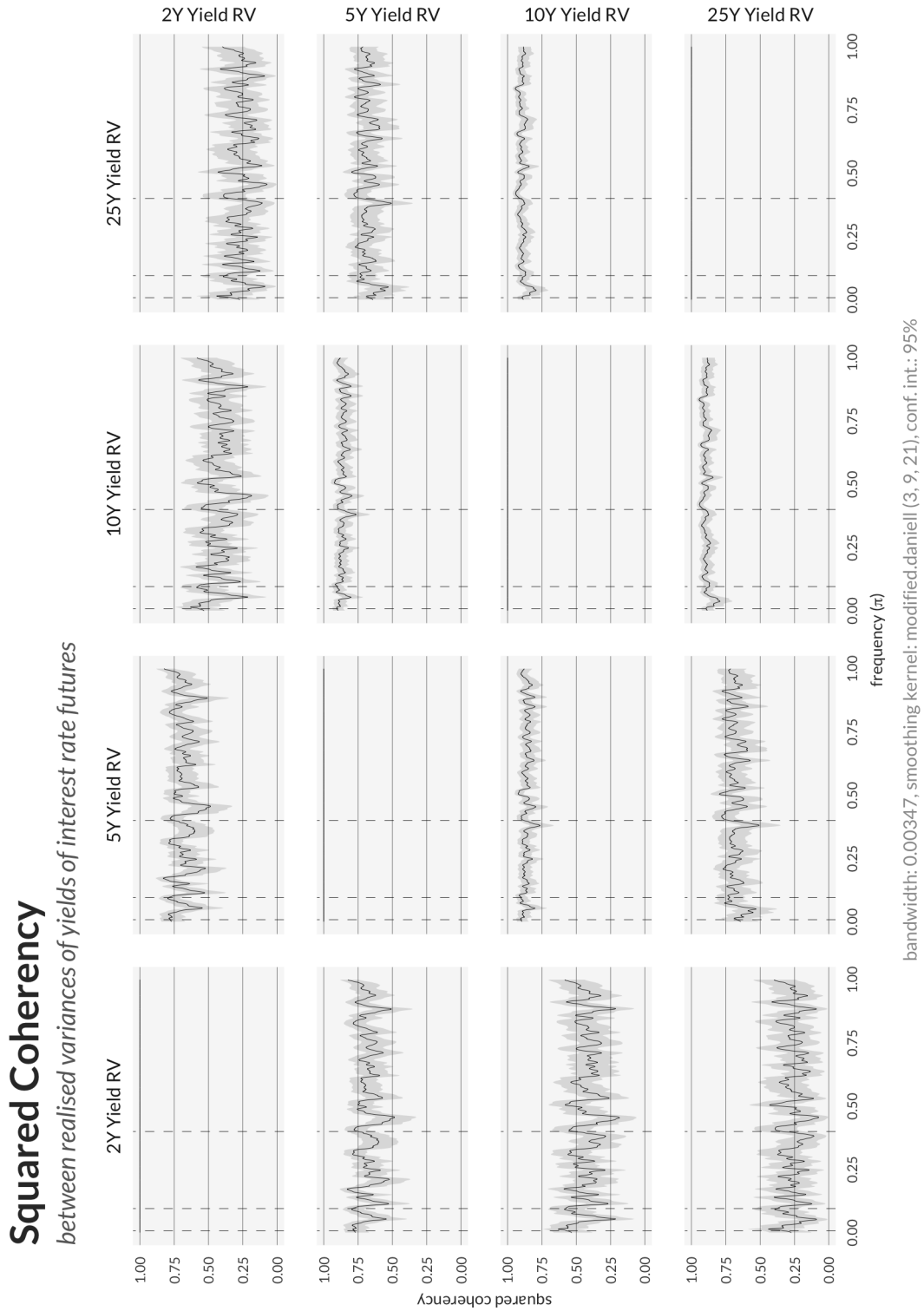

Figure A.37: Coherency between RVs of yields

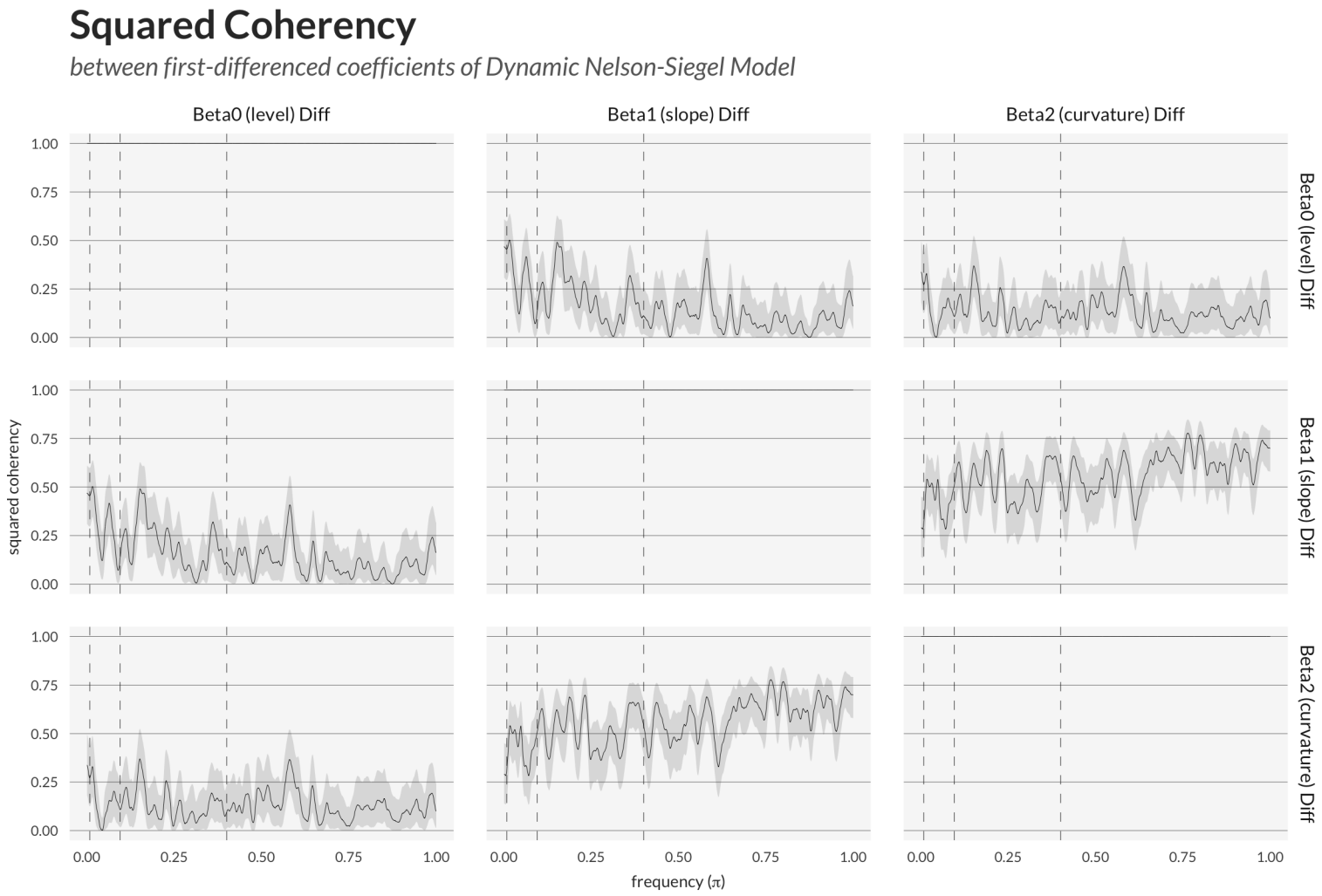

Figure A.38: Coherency between first-differenced DNSM coefficients

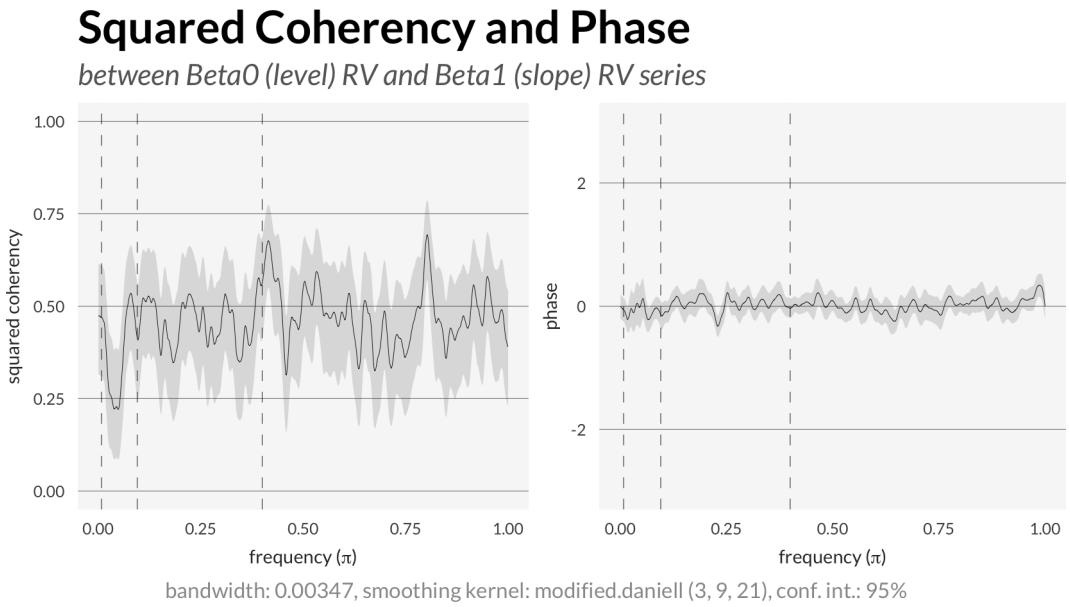

Figure A.39: Coherency and phase between RVs of DNSM level and slope

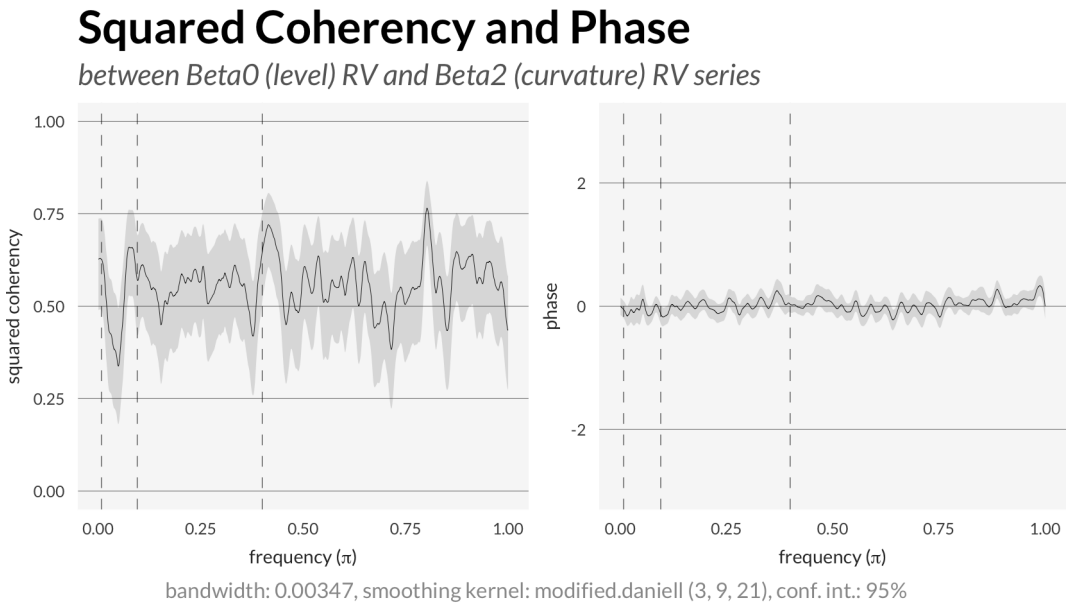

Figure A.40: Coherency and phase between RVs of DNSM level and curvature

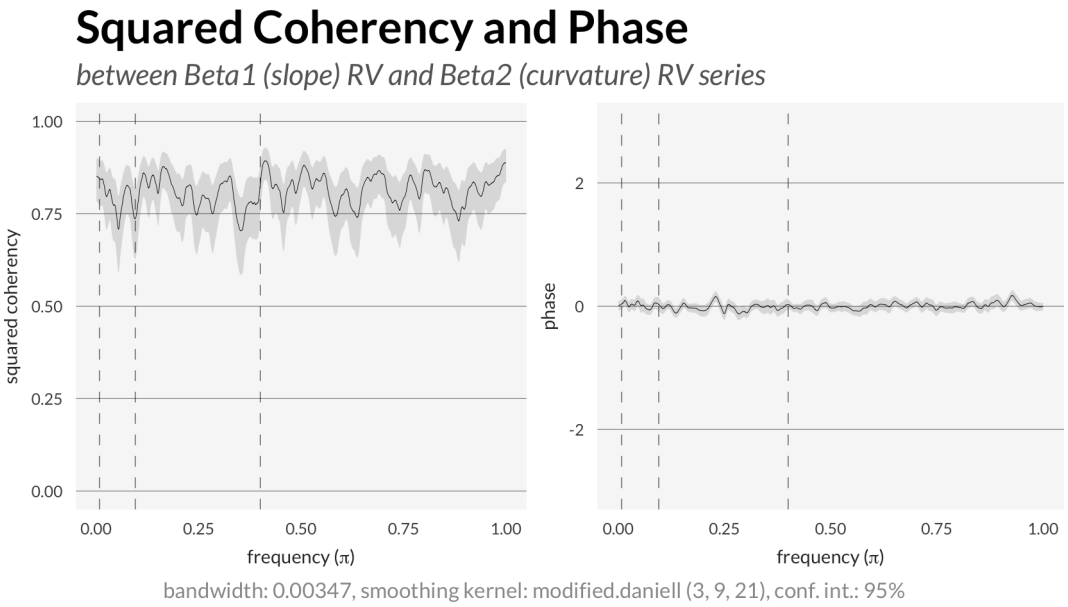

Figure A.41: Coherency and phase between RVs of DNSM slope and curvature

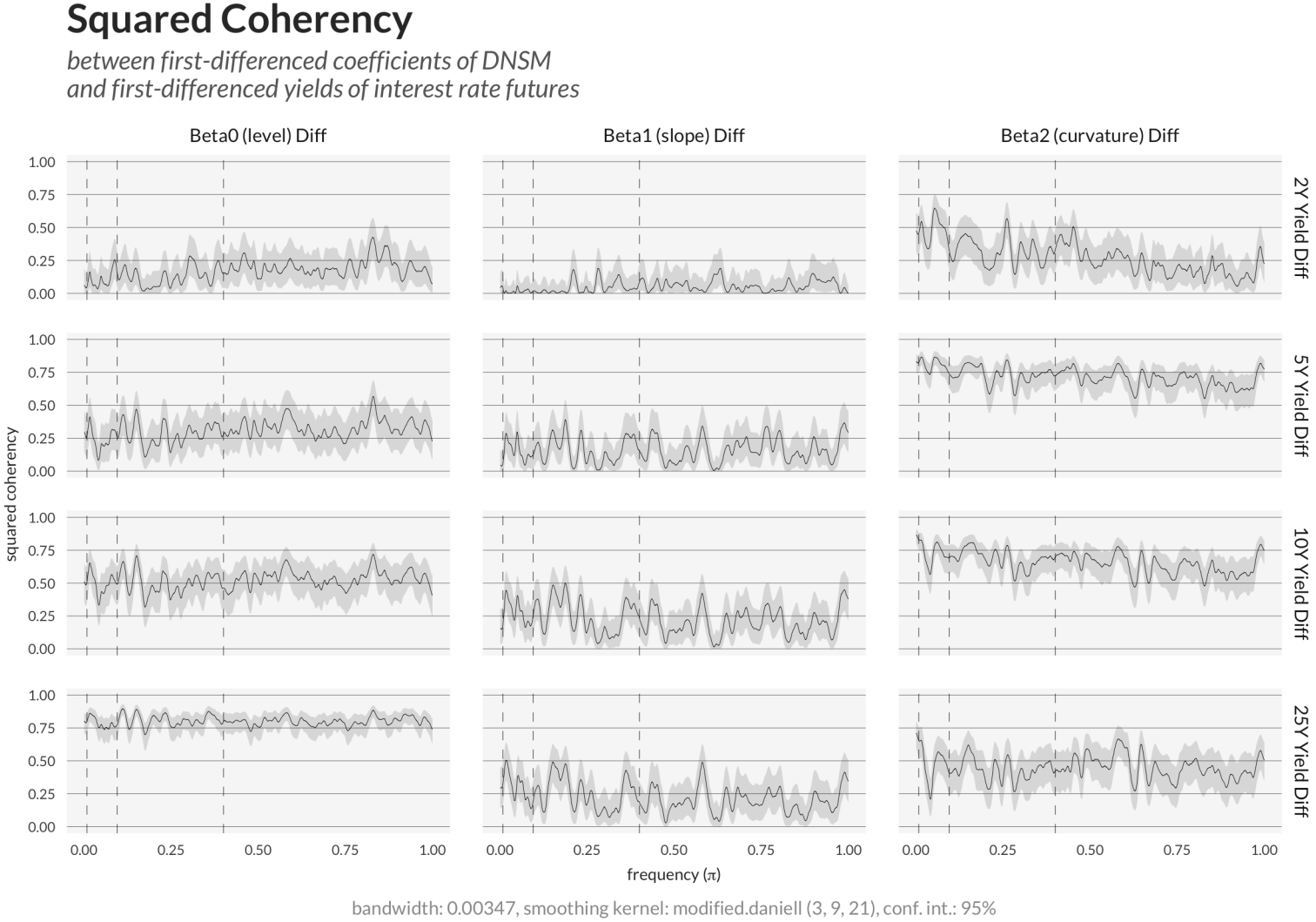

Figure A.42: Coherency between first-differenced DNSM coefficients and first-differenced yields

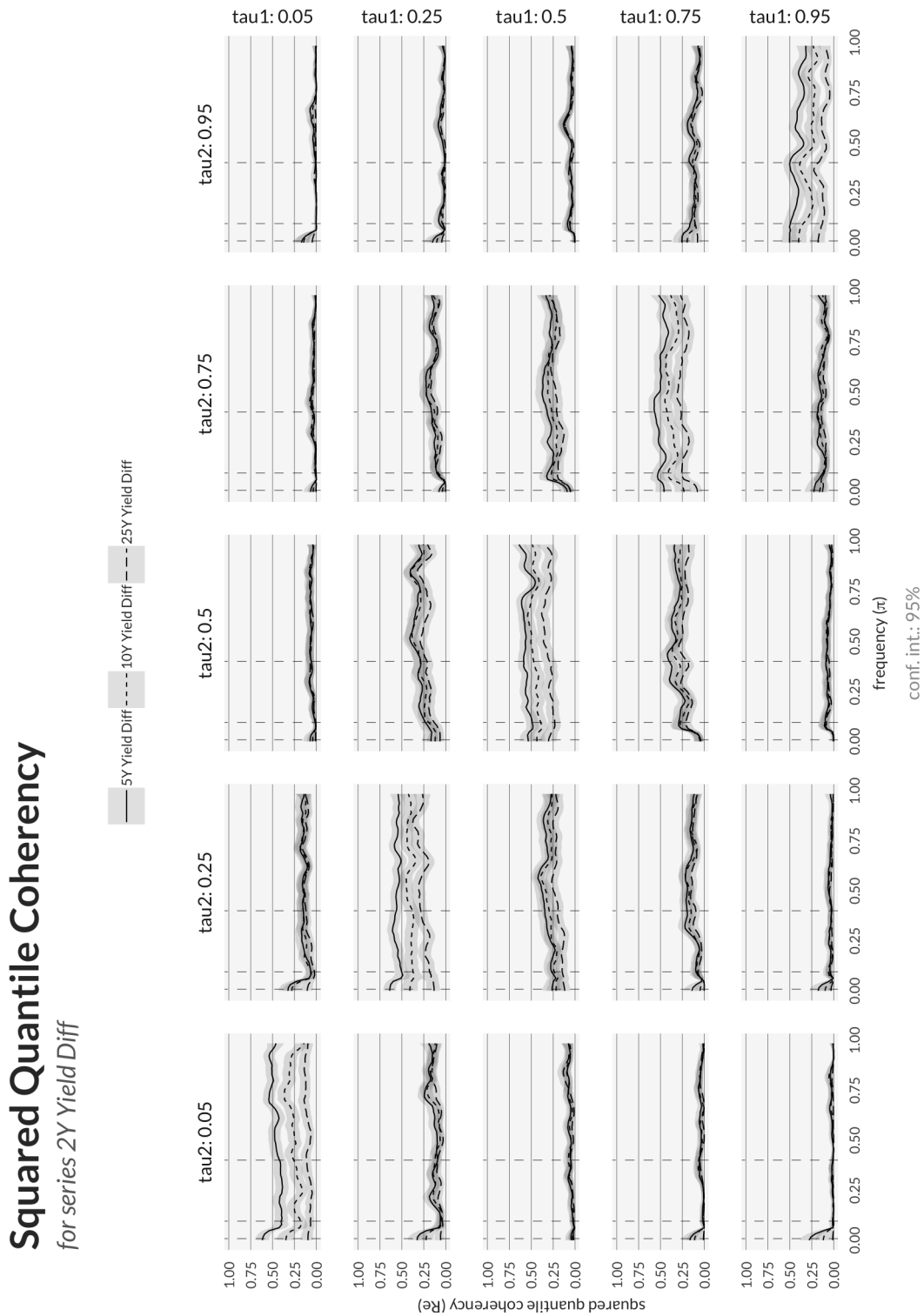

Figure A.43: Quantile coherency of first-differenced 2Y yield

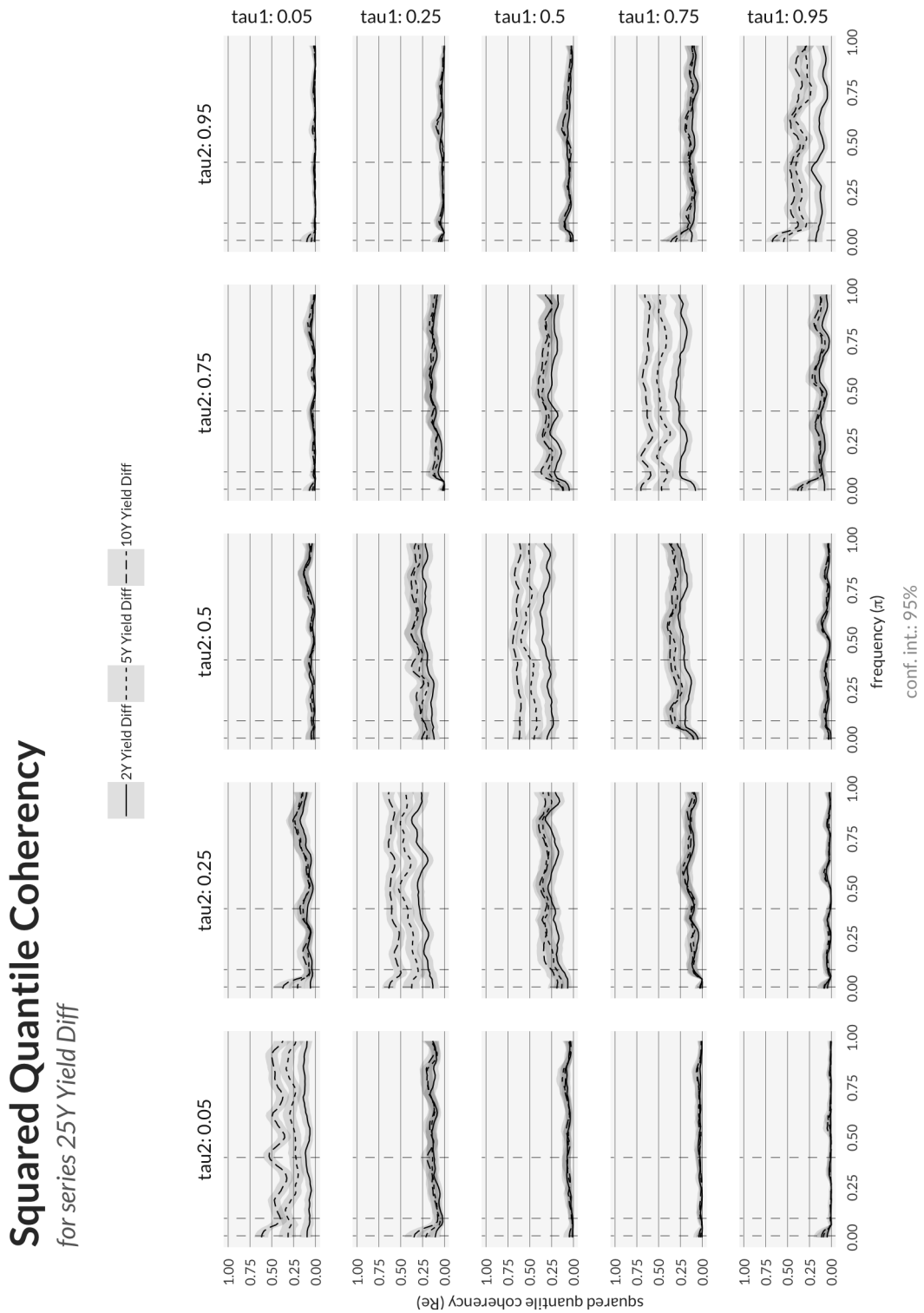

Figure A.44: Quantile coherency of first-differenced 25Y yield

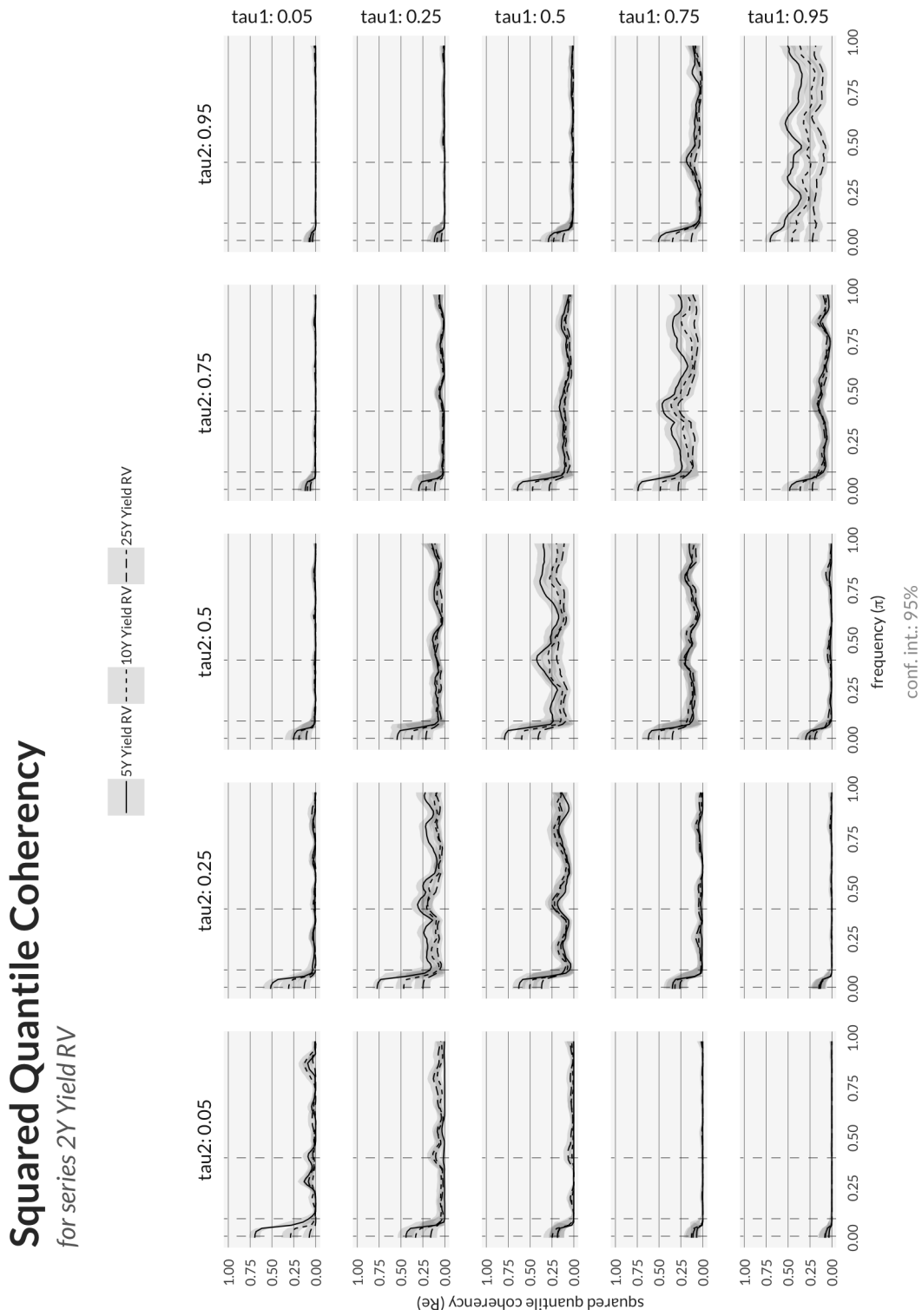

Figure A.45: Quantile coherency of RV of 2Y yield

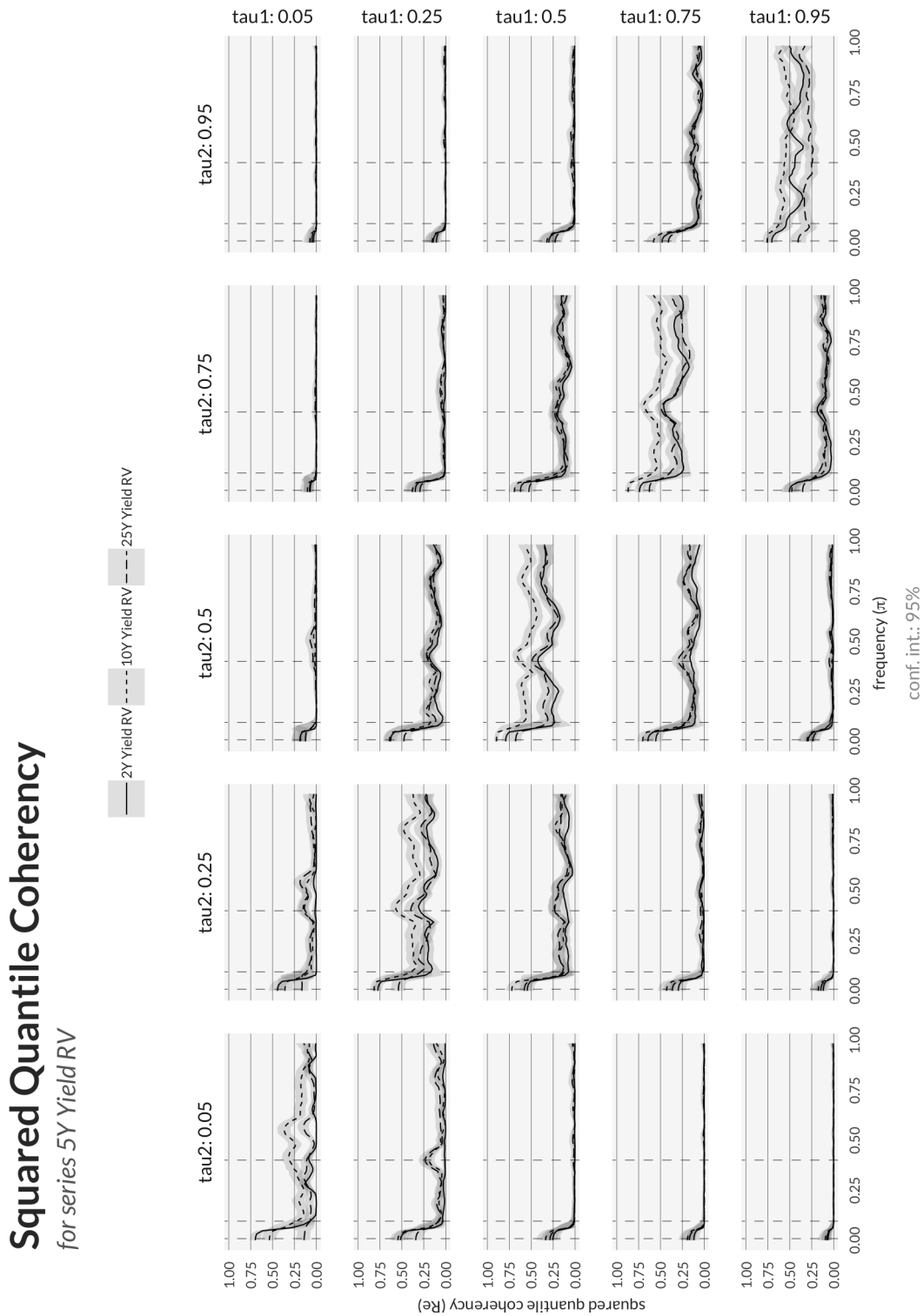

Figure A.46: Quantile coherency of RV of 5Y yield

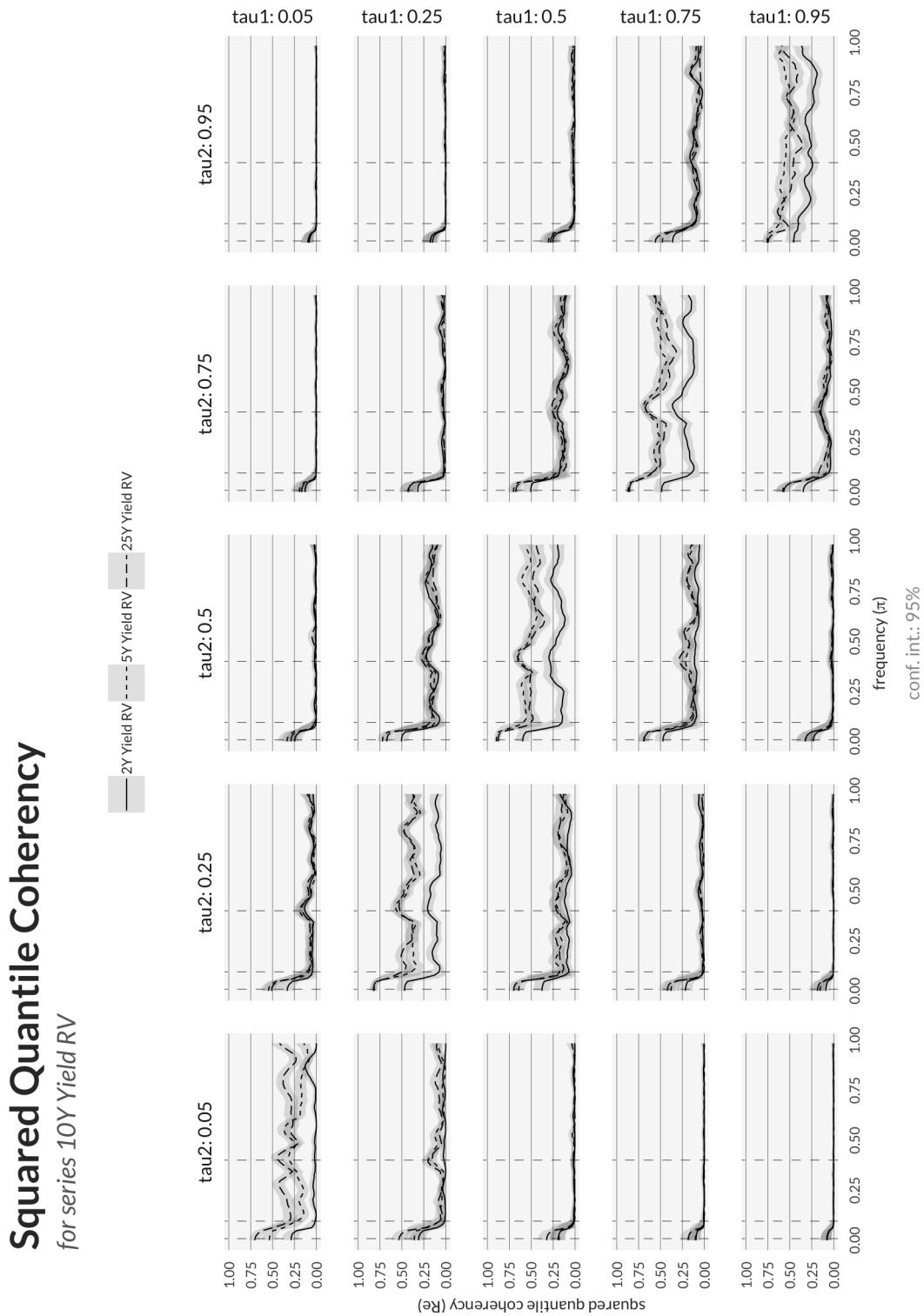

Figure A.47: Quantile coherency of RV of 10Y yield

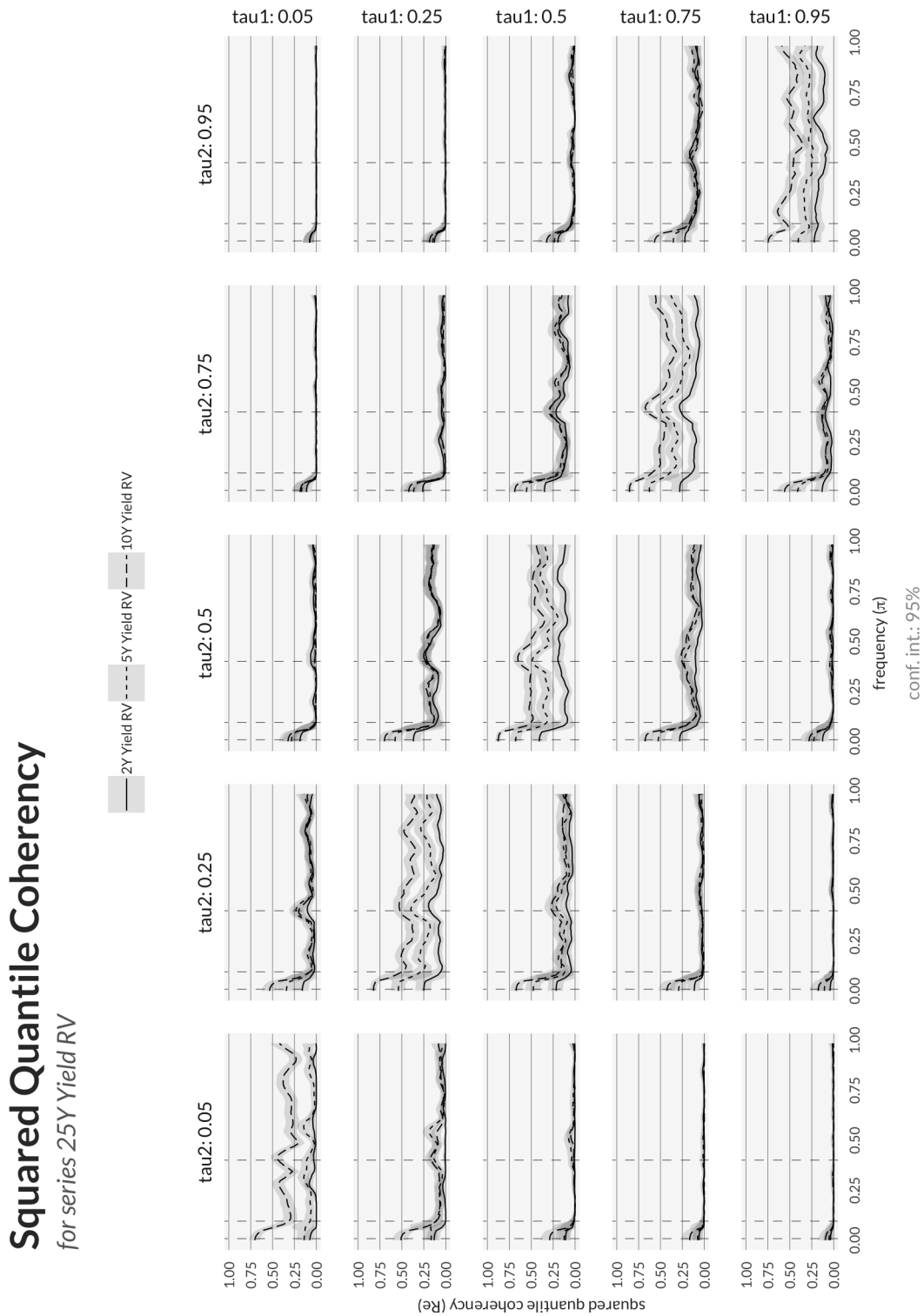

Figure A.48: Quantile coherency of RV of 25Y yield

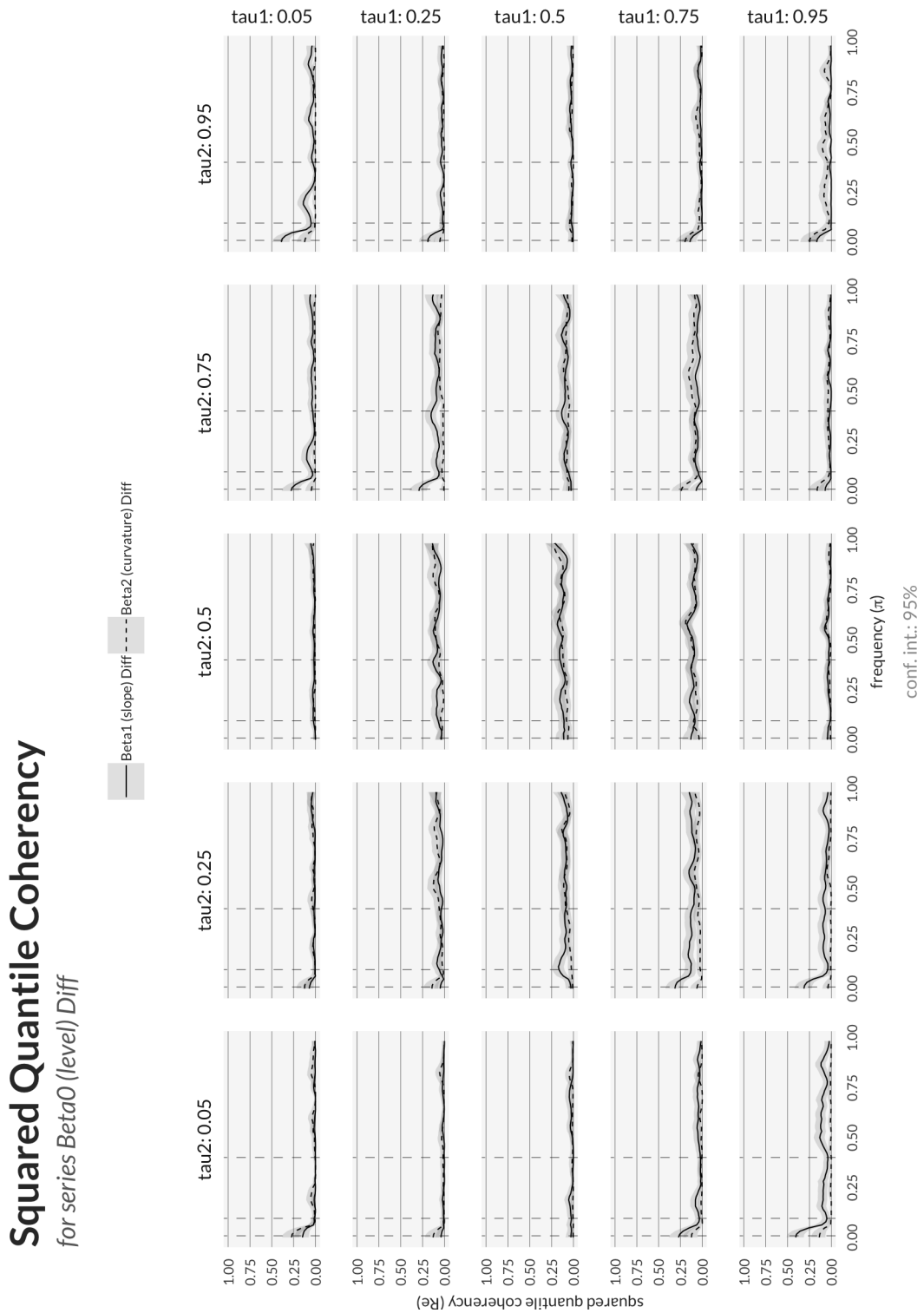

Figure A.49: Quantile coherency of first-differenced DNSM level factor

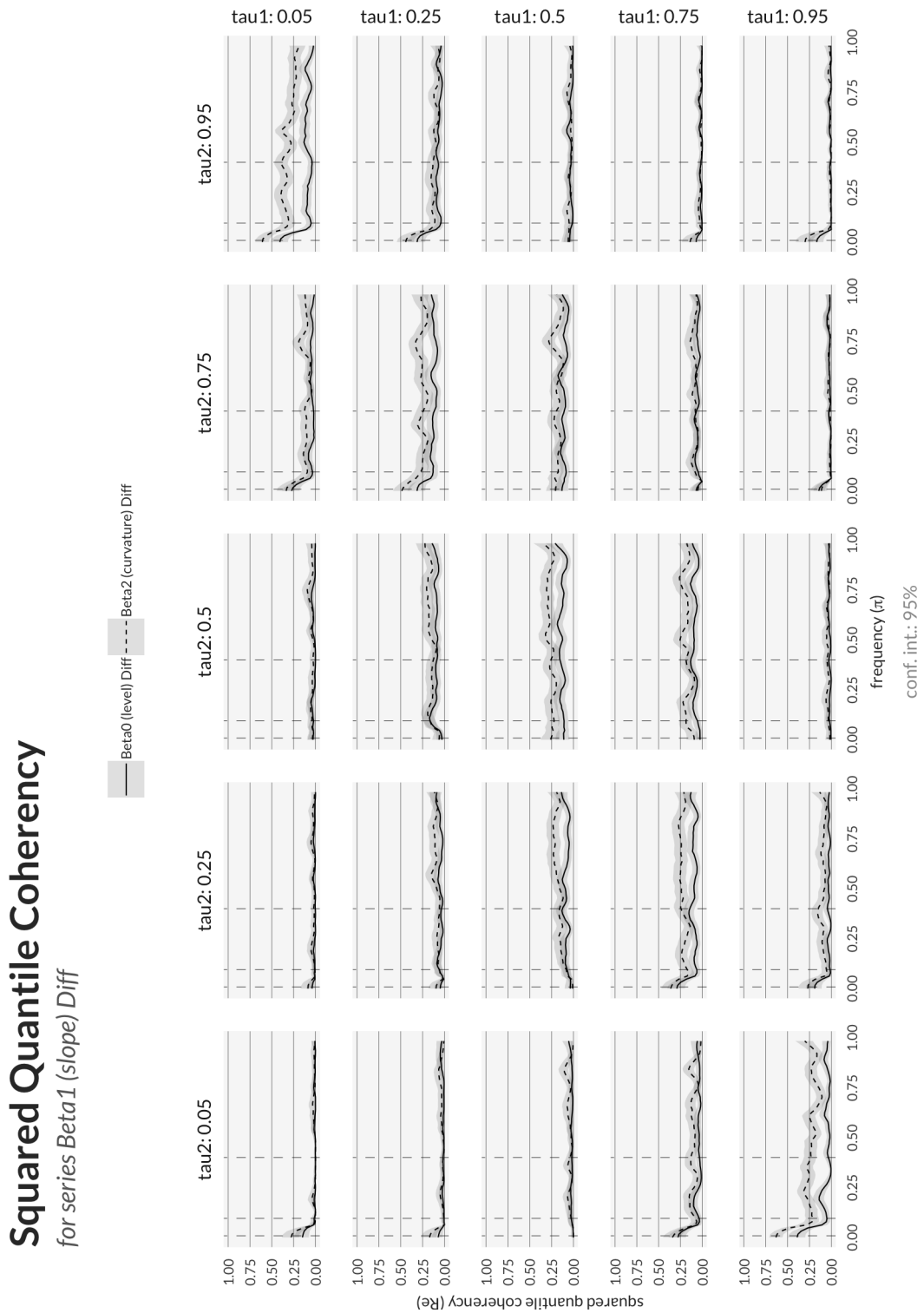

Figure A.50: Quantile coherency of first-differenced DNSM slope factor

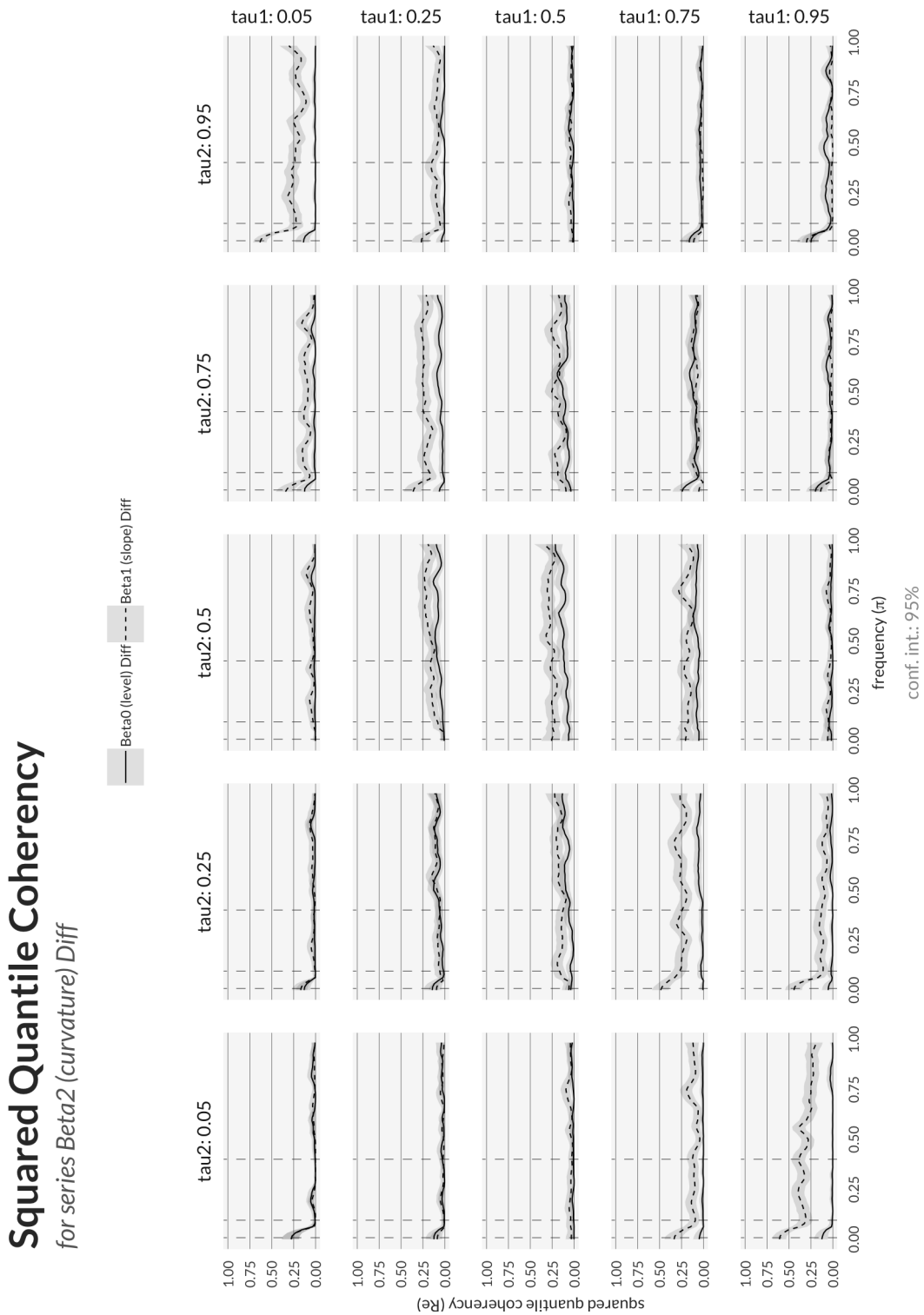

Figure A.51: Quantile coherency of first-differenced DNSM curvature factor

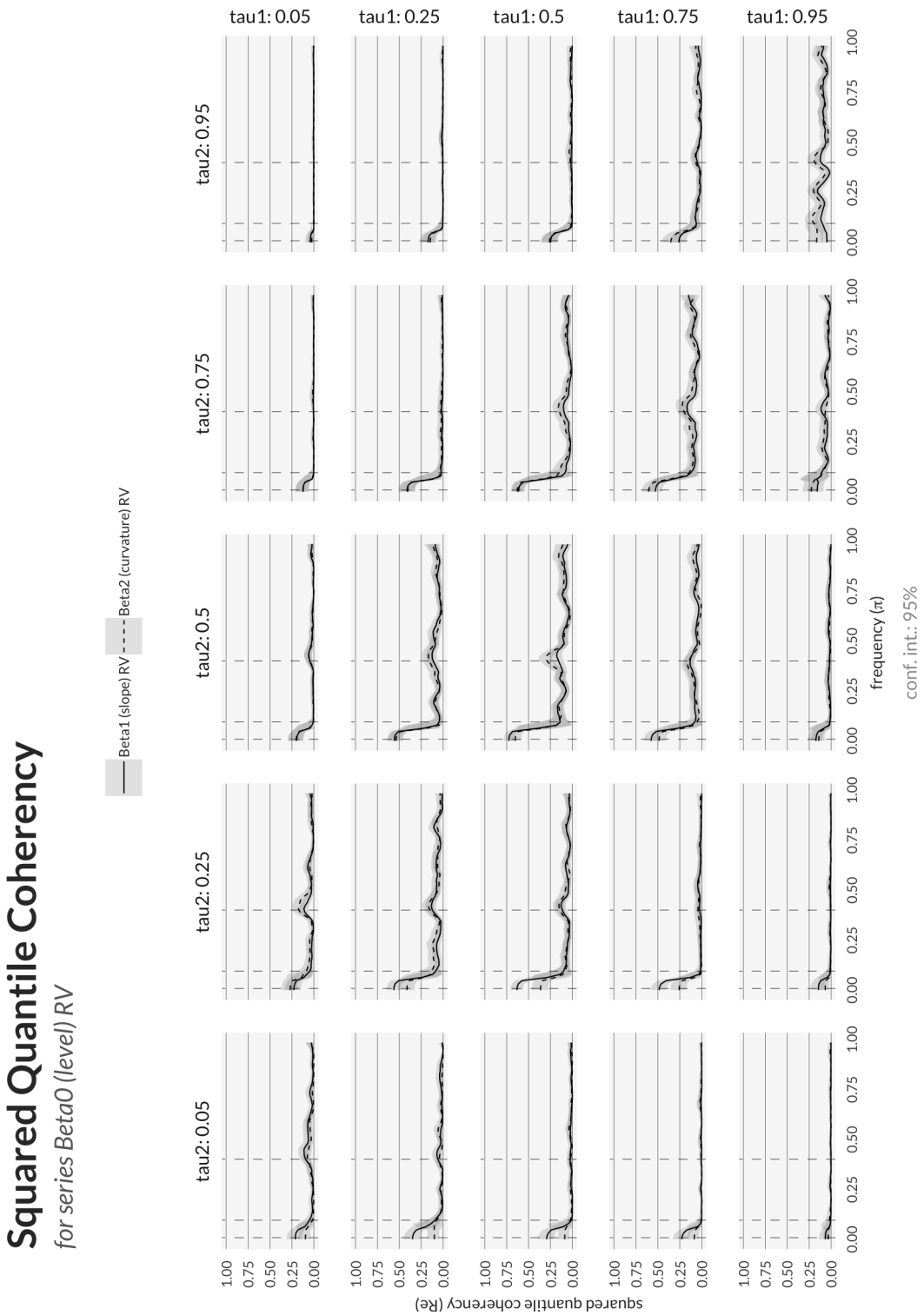

Figure A.52: Quantile coherency of realised variance of DNSM level factor

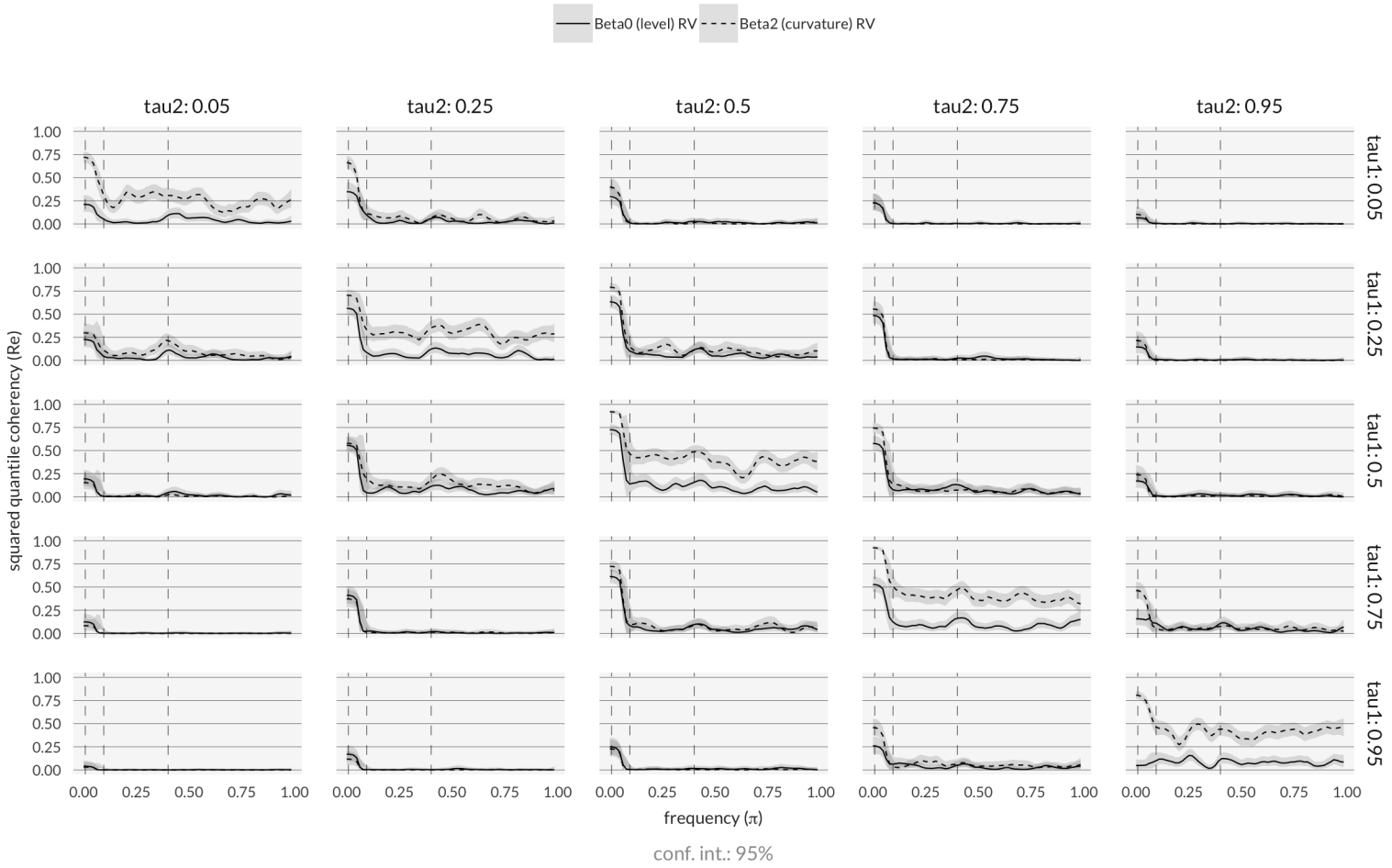

Figure A.53: Quantile coherency of realised variance of DNSM slope factor

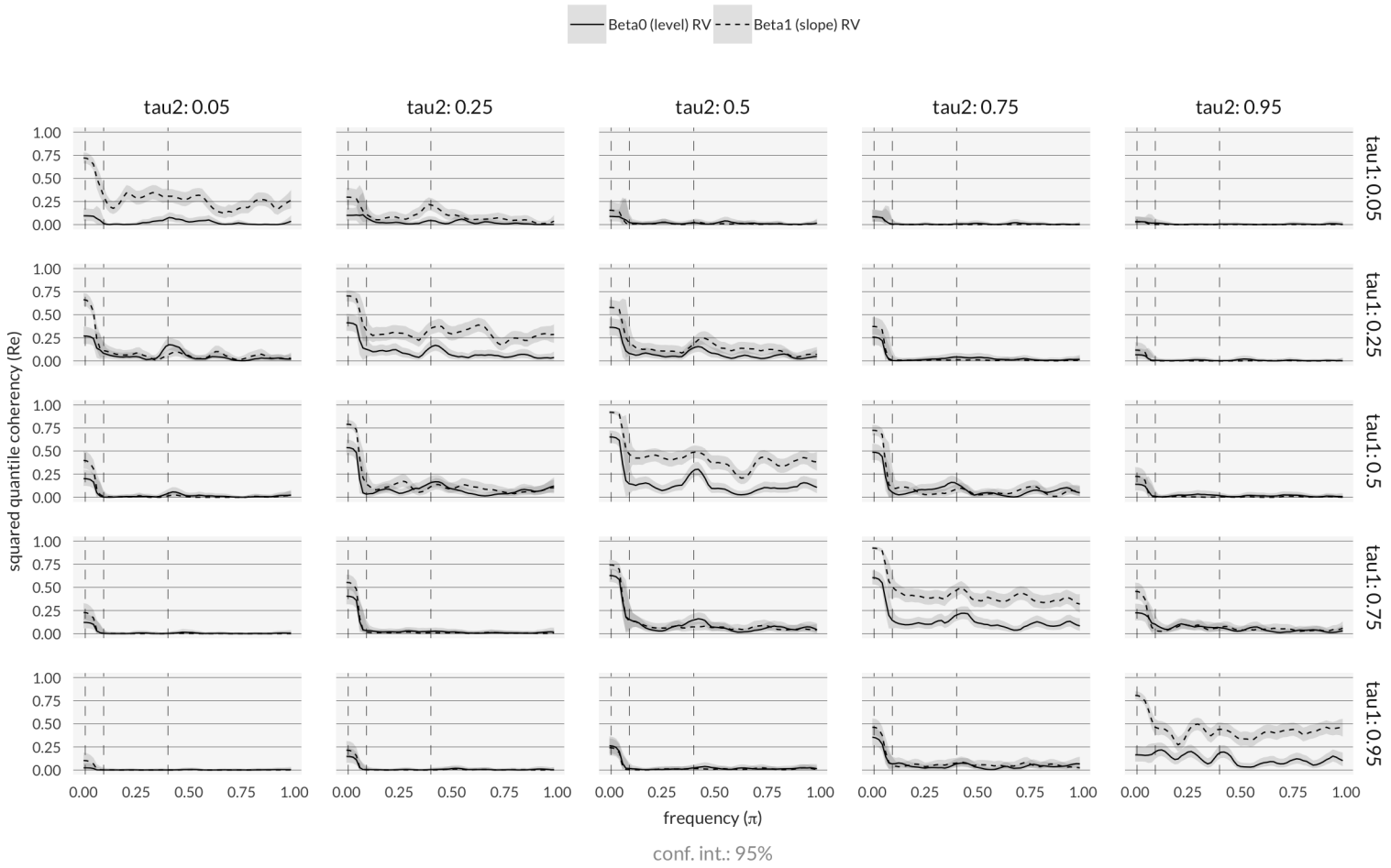

Figure A.54: Quantile coherency of realised variance of DNSM curvature factor

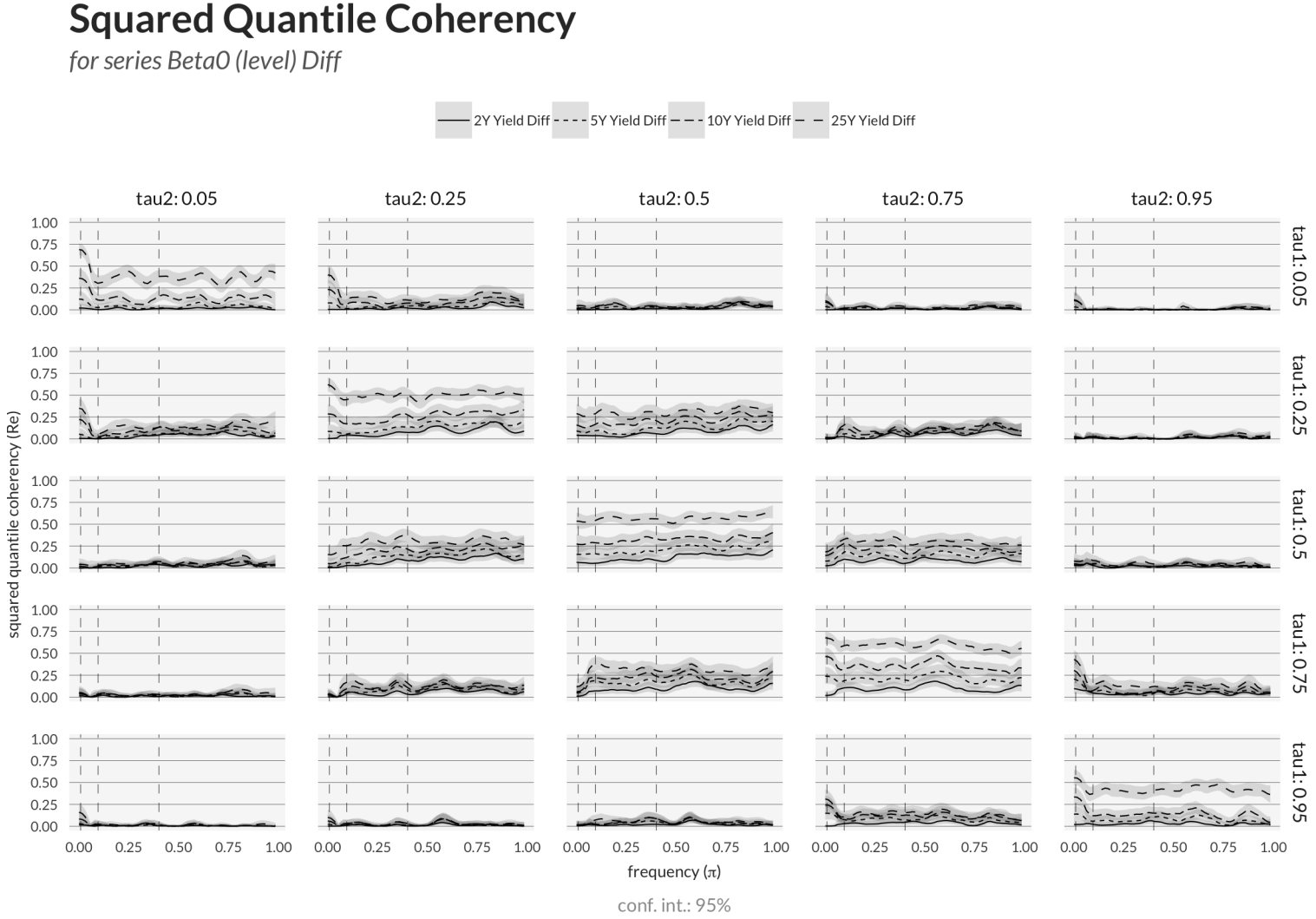

Figure A.55: Quantile coherency between first-differenced DNSM level factor and yields

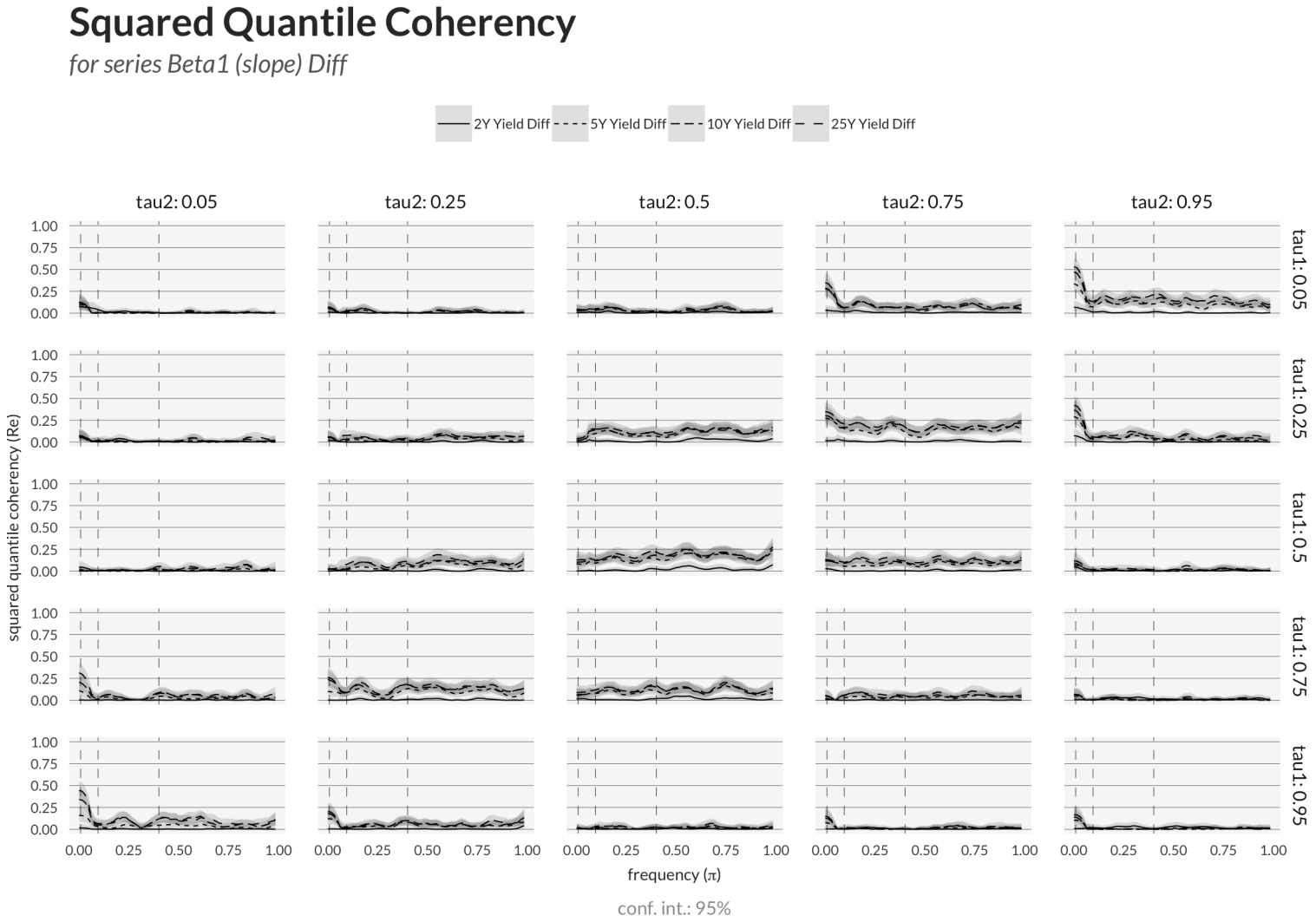

Figure A.56: Quantile coherency between first-differenced DNSM slope factor and yields

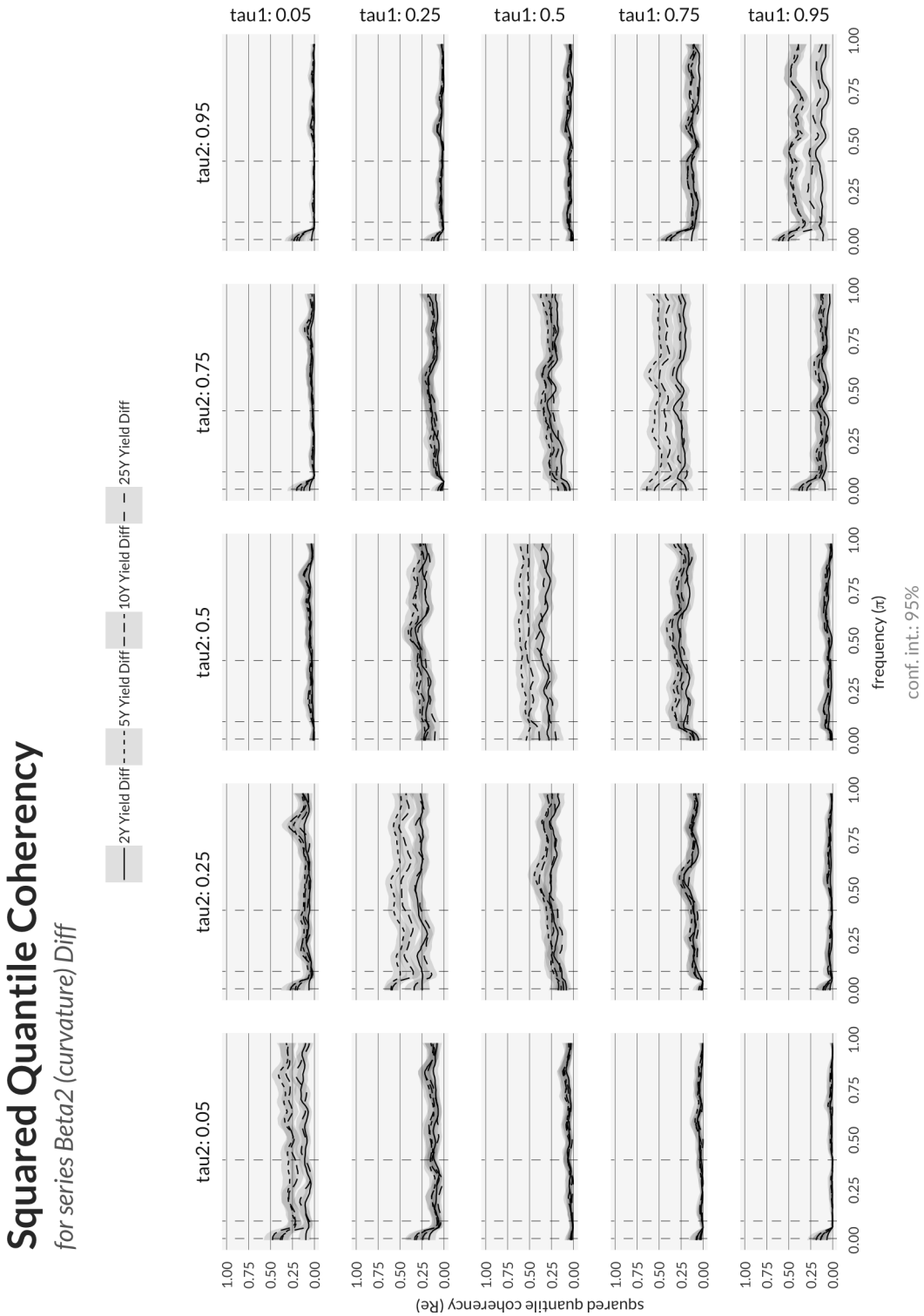

Figure A.57: Quantile coherency between first-differenced DNSM curvature factor and yields

Appendix B

Tables

	2Y Close	5Y Close	10Y Close	25Y Close
Observations	3775.00	3775.00	3775.00	3775.00
Minimum	98.23	96.55	94.00	89.22
Maximum	110.40	124.92	135.25	161.81
1. Quartile	103.38	106.33	108.31	109.11
3. Quartile	109.61	119.19	124.23	130.56
Mean	106.37	112.70	115.77	119.11
Median	107.21	112.53	114.34	115.28
Variance	11.46	53.24	93.35	214.86
Stdev	3.39	7.30	9.66	14.66
Skewness	-0.53	-0.10	0.13	0.56
Kurtosis	-0.91	-1.00	-0.82	-0.61

Table B.1: Summary statistics of daily closing prices

	2Y Yield	5Y Yield	10Y Yield	25Y Yield
Observations	3775.000000	3775.000000	3775.000000	3775.000000
Minimum	0.009694	0.014720	0.029340	0.040674
Maximum	0.070384	0.068381	0.067480	0.065753
1. Quartile	0.013322	0.024301	0.038122	0.049645
3. Quartile	0.043407	0.047959	0.052458	0.057208
Mean	0.029048	0.036350	0.045872	0.053826
Median	0.024586	0.036142	0.046770	0.054884
Variance	0.000276	0.000183	0.000076	0.000026
Stdev	0.016604	0.013525	0.008735	0.005071
Skewness	0.592734	0.218717	0.036747	-0.352482
Kurtosis	-0.803402	-0.897020	-0.726642	-0.701966

Table B.2: Summary statistics of yields

	Series	ADF Stat	P-Value
1	Beta2 (curvature)	-2.71	0.28
2	Beta1 (slope)	-2.09	0.54
3	Beta0 (level)	-3.04	0.14

Table B.3: Augmented Dickey-Fuller Test of Dynamic Nelson-Siegel Model factors (alternative: stationary)

	Series	ADF Stat	P-Value
1	25Y Yield	-3.95	0.01
2	10Y Yield	-3.32	0.07
3	5Y Yield	-2.42	0.40
4	2Y Yield	-1.83	0.65

Table B.4: Augmented Dickey-Fuller Test of yields (alternative: stationary)

		5Y Yield Diff	10Y Yield Diff	25Y Yield Diff
Short-run	2Y Yield Diff	0.8260742	0.6389234	0.3794293
	5Y Yield Diff	-	0.9338904	0.7342682
	10Y Yield Diff	-	-	0.8811431
Medium-run	2Y Yield Diff	0.8182944	0.6186933	0.3519748
	5Y Yield Diff	-	0.9233498	0.7119285
	10Y Yield Diff	-	-	0.8746801
Long-run	2Y Yield Diff	0.8243349	0.6317544	0.4055362
	5Y Yield Diff	-	0.9173409	0.7402397
	10Y Yield Diff	-	-	0.8944193

Table B.5: Average coherency of first-differences of yields by frequency range